Università degli Studi di Ferrara

International Erasmus Mundus Master in
QUATERNARY AND PREHISTORY

Oligocene Primates Facial Morphology: A Reassessment of *Aegyptopithecus zeuxis* through Geometric Morphometrics

Sandra Selene López Balderas

Supervisor: Carlos Lorenzo
Co-supervisor: Julie Arnaud

Academic year 2023/2024

We do not come from nothing; we are the people who lift us up. I look around, and it is always women. I write for them, the ones who have brought me here; I write for those whose voices were denied. No matter what I do, it is always them. Once again... for you.

No venimos de la nada, somos las personas que nos levantan. Miro a todos lados y siempre son mujeres. Escribo por ellas, las que me han traído hasta aquí; escribo por ellas, a quienes se les negó la voz. No importa lo que haga, siempre son ellas. Nuevamente... para ustedes.

ABSTRACT

Despite numerous paleoanthropological studies focused on the analysis of the Hominidae family, gaps persist in understanding their evolutionary history and phylogenetic relationships within the primate order. While attention has primarily been on the relationship between the great apes, due to their proximity to the hominin taxon, the analysis of Oligocene primate fossil taxa has been neglected. These fossils, coming from the Jebel Qatrani formation in Fayum, Egypt, have provided a rich record that has significantly contributed to the understanding of the systematics and phylogeny of catarrhines. Among these fossils, †*Aegyptopithecus zeuxis* stands out, with an estimated age between 35 and 33 million years, positioned as a species prior to the divergence that led to the two current catarrhine superfamilies, Hominoidea and Cercopithecoidea. *†Aegyptopithecus* has a fossil record that includes 4 skulls with the facial region well-preserved, making it an exceptional candidate for morphological analysis. Although studies have been conducted on this fossil, its facial morphology has not been fully updated. Therefore, this study presents a new approach through 3D geometric morphometric analysis, evidencing the primitive and/or derived morphological characteristics of key aspects in the facial shape of this species, and thus reassessing the taxonomic position of †*Aegyptopithecus* relative to the common ancestor of Hominoidea and Cercopithecoidea. By comparing its anatomy with that of different groups of current and extinct primates, this study establishes a crucial link between the fossils of the Oligocene and the Miocene.

RESUMEN

A pesar de los numerosos estudios paleoantropológicos centrados en el análisis de la familia Hominidae, aún persisten lagunas en la comprensión de su historia evolutiva y sus relaciones filogenéticas dentro del orden de los primates. Si bien la atención se ha centrado principalmente en la relación entre los grandes simios, debido a su proximidad al taxón de los homininos, se ha descuidado el análisis de los taxones fósiles de primates del Oligoceno. Estos fósiles, provenientes de la formación Jebel Qatrani del Fayum, Egipto, han proporcionado un rico registro que ha contribuido significativamente al entendimiento de la sistemática y filogenia de los catarrinos. Entre estos fósiles, destaca †*Aegyptopithecus zeuxis*, con una edad estimada entre 35 y 33 millones de años, posicionado como especie anterior a la divergencia que dio lugar a las dos superfamilias de catarrinos actuales, Hominoidea y Cercopithecoidea. †*Aegyptopithecus* cuenta con un registro fósil que incluye 4 cráneos con la región fácil bien conservada, lo que lo vuelve un candidato excepcional para el análisis morfológico. Aunque se han realizado estudios sobre este fósil, su morfología facial aún no se ha actualizado completamente. Por lo tanto, este estudio presenta un nuevo enfoque mediante análisis en 3D de morfometría geométrica, evidenciando las características morfológicas primitivas y/o derivadas de aspectos clave en la forma del rostro de esta especie, y así reevaluar su posición taxonómica de †*Aegyptopithecus* respecto al ancestro común de Hominoidea y Cercopithecoidea. Al comparar su anatomía con la de diferentes grupos de primates actuales y extintos, este estudio establece un enlace crucial entre los fósiles del Oligoceno y Mioceno.

ACKNOWLEDGMENT

This work would not have been possible without the support of so many people who have accompanied me along the way. First and foremost, I would like to thank my supervisors, Carlos Lorenzo and Julie Arnaud, for their time and patience, for every word, correction, and idea, and for instilling in me a passion for paleoanthropology and research.

I also wish to thank Thomas Ingicco and Constantino Buzi for taking the time to read my work and share some of their knowledge with me.

I would like to express my immense gratitude to the IMQP consortium, especially to the coordinator, Marta Arzarello, for providing a platform to develop my skills and for accompanying me in this process. To Sara and Gabro, thank you for the good times and the motivation during every excavation.

I am also deeply grateful to my family and friends, who have supported me from afar. Even though I have often left them a bit behind to pursue my crazy dreams, they have always sustained me and given me their unconditional love.

To my mother, as always, I owe infinite thanks for being my support and inspiration. I hope this achievement serves as a small reflection of the wonderful things you've done in life. None of my successes are a coincidence, and the day you understand that you have been and are the foundation of my entire being, you will realize how much I owe you and how much I love you.

To my father, thank you for your support despite every disagreement and argument. Your teachings have been the foundation of many of my interests; you planted in me many questions and desires. Thank you for being that guiding light and for never giving up on me.

To my brothers and sisters: Claudia, Eduardo, Adriana, and Susana, thank you for always being by my side. Your companionship brightens my path. Regardless of the distance, I always hope you witness my journey, and I will always be there for yours. To my nieces and nephew: Dany, Julieta, Vale, Pame, and Lalito, you are my inspiration to keep growing and to contribute something to this world. I

hope that, in some way, a little piece of all the things I fight for will fill your lives, and that when you think of them, you'll know how much I have loved you.

Thanks to my life partner, Javier. It has been hardest for you to bear my absence, and yet you've been there every step of the way, supporting me. I have dreams and goals along a long road that I hope to walk with you by my side, and I look forward to seeing you shine with me.

Lastly, I thank all my friends and colleagues who shared this passion with me, enduring the longing for home and future plans together. Especially to Andrea, who has always been a pillar and motivation, thank you for being my refuge. To Trishia and Tannishta, the difficult times were so much better with your company.

There are countless people who have given me a part of themselves, so many that it's impossible to name them all. We are each a piece of the essence of those who touch our lives.

AGRADECIMIENTOS

Este trabajo no hubiera sido posible sin el apoyo de tantas personas que han acompañado mi camino. Primero que nada, quisiera agradecer a mis supervisores Carlos Lorenzo y Julie Arnaud por su tiempo y paciencia, por cada palabra, corrección e idea, y por transmitirme la pasión por la paleoantropología y la investigación.

De igual manera, agradezco a Thomas Ingicco y Constantino Buzi por tomarse el tiempo de leer mi trabajo y compartir conmigo parte de sus conocimientos.

Quisiera también expresar mi enorme gratitud al consorcio de IMQP, especialmente a la coordinadora Marta Arzarello, por brindar una plataforma para desarrollar mis habilidades y acompañarme en este proceso. A Sara y Gabro, gracias por los buenos momentos y la motivación en cada excavación.

Agradezco también a mi familia y amigos, quienes me han acompañado desde la distancia. A pesar de que en muchas ocasiones los he dejado un poco de lado para seguir mis sueños locos, me han sostenido y brindado su amor incondicional.

A mi madre, como siempre, le debo infinitas gracias por ser mi soporte e inspiración. Espero que este logro sirva como un pequeño reflejo de las cosas maravillosas que has hecho en la vida. Ninguno de mis éxitos es casualidad, y el día que comprendas que tú has sido y eres la base de todo mi ser, entenderás cuánto te debo y cuánto te amo.

A mi padre, gracias por tu apoyo a pesar de cada desacuerdo y pelea. Tu enseñanza ha sido la base de muchos de mis intereses; sembraste en mí muchas dudas y anhelos. Gracias por ser ese faro y por no desistir en el camino.

A mis hermanos y hermanas: Claudia, Eduardo, Adriana y Susana, por estar siempre a mi lado. Su compañía alegra mi camino. Sin importar la distancia, siempre espero que sean testigos de mi andar, y yo, compañera de sus éxitos. A mis sobrinas y mi sobrino: Dany, Julieta, Vale, Pame y Lalito, ustedes son la inspiración para seguir creciendo, para aportar algo a este mundo. Espero que,

de alguna forma, un pedacito de todas esas cosas por las que lucho llene sus vidas, y que cuando las recuerden, sepan cuánto las he amado.

Gracias a mi compañero de vida, Javier. A ti más que a nadie te ha costado mi partida, y aun así has estado en cada momento apoyando mis pasos. Tengo sueños y metas a lo largo de un camino que espero recorrer a tu lado y verte brillar junto a mí.

Por último, agradezco a todos mis amigos y compañeros que compartieron conmigo esta pasión en común, soportando juntos las añoranzas del hogar y los planes futuros. Especialmente a Andrea, que siempre has sido un pilar y una motivación, gracias por ser mi refugio. A Trishia Y Tannishta, los tiempos difíciles, fueron mucho mejores con su compañía.

Son infinitos las personas que me han brindado una parte de sí, que es imposible nombrarlos a todos. Somos un pedazo de la esencia de cada una de esas personas que toca nuestra vida.

TABLE OF CONTENTS

LIST OF FIGURES

LIST OF TABLES

INTRODUCTION

In the study of human evolution, the phylogenetic relationships of fossil primates that form a crucial link between Eocene fossils and Miocene hominids have often been overlooked or taken for granted, with greater emphasis placed on ape's ancestors. One of the ongoing challenges is the fragmentary nature of the fossil record, with many specimens only partially preserved and often distorted.

The early primates of the Oligocene period (ca. 34-23 million years ago) include primitive fossil catarrhines that existed before the divergence of the two superfamilies: Hominoidea (great apes and humans) and Cercopithecoidea (Old World monkeys). The Fayum deposits in Egypt hold the largest collection of early catarrhines, where early primates have been described for over a century (Harrison 2013; Rasmussen 2002).

These Oligocene primates belong to four genera: †*Aegyptopithecus*, †*Propliopithecus*, †*Parapithecus*, and †*Apidium*. Discovered in the Fayum region of northern Egypt, their fossil record includes a jaw of †*Propliopithecus haeckeli*, the lower dentition of †*Parapithecus fraasi*, an almost complete and slightly distorted skull of †*P. granger* (DPC9867, used in this study), and a partial skull of †*Apidium phiomense*.

The most abundant and well-preserved fossil record belongs to †*Aegyptopithecus*, with only one known species, †*A. zeuxis*. The first skull was discovered in 1966 by Elwyn Simmons, and at least five skulls have since been found, four of which are well-preserved in the facial region, along with various postcranial remains. This has made †*A. zeuxis* one of the best-known and most studied extinct primates. It is considered a common ancestor of both hominoids (great apes) and cercopithecoids (Old World monkeys). Although hypotheses have been proposed regarding the separation of these two groups, little is known about their evolution during the Oligocene period.

Various analyses have been conducted on †*A. zeuxis*, including studies of postcranial bones related to locomotion (Ankel-Simons et al., 1998; Conroy, 1976; J. Fleagle & Simons, 1982), descriptions of facial morphology (J. Fleagle et al., 1980; Kozakowski, 2013; E. Simons, 1987; E. L. Simons et al., 2007), the interorbital septum (E. Simons & Rasmussen, 1989), comparisons of facial morphology with †*Afropithecus (Leakey et al., 1991)*, studies of paranasal sinuses using computed tomography (J. Rossie, 2005), and the use of digital tools for dental topography analysis and use wear (Morse et al., 2023). However, most of these studies were conducted over 20 years ago, focusing on facial morphology through descriptive or metric approaches. These traditional assessments relied heavily on qualitative descriptions and linear measurements, which may overlook subtle shape variations and morphological details. While recent studies using digital tools have primarily focused on dental morphology, a more precise and quantitative analysis of facial morphology is necessary.

Facial morphology is essential for understanding primate evolution, particularly in the separation of catarrhines into Hominoidea and Cercopithecoidea. Variation in cranial and facial structures provide critical evidence for evolutionary divergence, reflecting adaptations to diverse ecological niches and lifestyles. By analyzing these morphological traits, scientists can trace the evolutionary relationships and divergence patterns among early catarrhines. In this context, the facial morphology of †*Aegyptopithecus* plays a vital role, as a stem-taxon that predates the last common ancestor (LCA) of extant catarrhines. Its well-preserved craniofacial fossils allow for detailed comparisons with both extinct and extant primates, offering insights into the evolutionary processes that shaped catarrhine diversification during the Oligocene.

Recent cladistic analyses support the placement of †*Aegyptopithecus* before the split of major catarrhine lineages, making it crucial for reconstructing the evolutionary history of this group and clarifying their phylogenetic relationships. Its well-preserved craniofacial fossils allow for detailed morphological comparisons with both extinct and extant primates, shedding light on the evolutionary processes that shaped the diversification of this group during the Oligocene.

To further elucidate the evolutionary role of †*Aegyptopithecus*, advanced techniques such as micro-CT based virtual reconstructions and geometric morphometrics are employed. These methods allow researchers to correct for fossil distortions and quantitatively assess morphological affinities within a broad comparative framework.

In this complex context, this research aims to enhance the specificity of facial morphology reconstructions using 3D morphometrics, providing greater insight into how the facial shape varies among the fossils of †*Aegyptopithecus zeuxis* discovered to date. Compared to traditional descriptive observations and linear measurements, geometric morphometric analyses offer more detailed information about shape, examining size and spatial relationships between different anatomical features (Adams & Otárola-Castillo, 2013; Slice, 2007; Zelditch & Swiderski, 2023).

Geometric morphometrics is a widely used method for studying facial morphology such as the analyze orbit shapes for classifying populations and sex differentiation (S. Xing et al., 2013) .However, earlier studies using orbit shape as a linear or non-metric trait lacked conclusive quantitative data. Additionally, analysis of sexual dimorphism in this sample of primates can provide insights into the role of sexual selection and its effects on the variability of facial morphology.

By achieving these objectives, this study aims to significantly advance the field of paleoanthropology and primate evolution, offering new perspectives on the morphological diversity and evolutionary history of early primates.

Aims and objectives

In the specific, the present research can be declined into one main objective and several specific objectives:

General objective

Describe and analyze the facial morphology of Oligocene catarrhines, specifically †*Aegyptopithecus zeuxis,* using geometric morphometric techniques to formulate a facial reconstruction of the last common ancestor of Hominoidea and Cercopithecoidea.

Specific objectives

- Compare the facial morphology of fossil and extant primate species
- Distinguish the repercussions of sexual dimorphism in the facial morphology in primates
- Identify the degree of morphological variability within the facial structure of †*Aegyptopithecus zeuxis*.
- Corroborate the phylogenetic position of the facial morphology of Aegyptopithecus Zeuxis between linear metric and geometric morphometrics
- Summarize the evolutionary significance of †*Aegyptopithecus zeuxis* within the broader framework of Oligocene primate evolution, particularly in relation to the divergence of Hominoidea and Cercopithecoidea.

Hypotheses

The facial morphology of †*Aegyptopithecus zeuxis*, as revealed through geometric morphometrics, is consistent with the morphology of Catarrhini, implying that †*Aegyptopithecus* as a stem-catarrhine exhibits key features that align with the evolutionary traits shared by both Hominoidea and Cercopithecoidea.

Chapter overviews

This thesis is composed of four chapters, in addition to the introductory chapter, which outlines the study's aims, objectives, and overview. It also discusses the research hypothesis, its significance, and its limitations.

Chapter I establishes the theoretical framework or state of the art, by exploring key concepts and the background of research that has been done from paleoanthropology and primatology, on the anatomy, biology, evolution and phylogeny of the primate order. To provide an overview and a summary that highlights the importance of focusing on other non-human primates to understand and compare in a more holistic and complete way the evolution of our own species.

The chapter also analyzes previous research, methodologies, and findings related to facial anatomy and its ontogeny, with a focus on how facial features develop and vary among primates. Additionally, it introduces the background and applications of geometric morphometrics for analyzing facial morphology. In a current effort to reevaluate the morphology with new techniques that provide more information and can be the basis for corroborating or disconfirming the data that linear metrics have provided in other times.

The second chapter describes the methodologies used in this research, detailing the digital repository sources and types of data, with a description of the sample of extant and fossil primates, covering aspects of conservation, aging and sex determination. The nest part explains the preparation of the digital material to obtain the 3D facial model of each specimen, the software’s use and the posterior configuration of landmarks for geometric morphometrics. Providing a list of the 61 landmarks stablish, their importance, and the base of other methodologies to choose this configuration.

Describes the specific techniques used to do the geometric morphometric, such as General Procrustes Analysis (GPA) to homogenize the data and permit the comparison between each species in a Principal Components Analysis (PCA) and Multivariate Regression. Also is describe the realization of graphic representation in each value of the principal components, to create visualization

of the change in the facial morphology. The last part addresses potential errors in the analysis and methods for validating the results.

The chapter III present the results, including the outcomes of geometric morphometric and statistical analyses. It provides detailed findings on the facial morphology of the studied primates, including comparisons between species, the sex and the position of each fossil compared with the extant primates. Results that were analyzed and contrast within the context of the theoretical framework and research objectives in the last chapter.

It explores the implications of the findings for understanding primate evolution, particularly regarding the facial morphology of catarrhines and the role of †*Aegyptopithecus*.

Finally, the thesis concludes by summarizing the key findings, reflecting on the research objectives, and discussing the significance of the results. It provides concluding thoughts on the implications for the field of primate evolution and suggests directions for future research.

CHAPTER I: THEORICAL FRAMEWORK, STATE OF THE ART

1.1. Definition of the Primate Order

Primates represent a diverse group of mammals belonging to the superorder Euarchontoglires, alongside four other orders: Rodentia (rodents), Lagomorpha (rabbits), Scandentia (tree shrews) and Dermoptera (flying lemurs) (J. G. Fleagle, 2013; J. Fleagle & Kay, 1994; Kozakowski, 2013).

This order is one of the more diverse of living mammals, in their body size, covering a range between 100 g of the mouse lemurs or pygmy marmoset, and to 200 kg of the gorillas. It is distinguished by their developed brains, advanced cognitive abilities, grasping hands, forward-facing eyes with binocular vision, and normally complex social structures. Additionally, most primates possess opposable thumbs and/or big toes, which allow precise manipulation of objects and agile movement through their environments (Ankel-Simons, 2007; Preuss, 2007).

1.1.1. Classification of living primates

The order Primates includes 61 extant genera with 252 species, as well as between 200 and 218 fossil genera containing 405 species. Although for some authors the extant species reach at least 450 (Springer et al., 2012). Primates are divided into two suborders: Prosimii and Anthropoidea. The latter, also known as higher primates, includes Old and New World monkeys, apes, and humans, while the Prosimii contains three infraorders, including four extant families from Madagascar: Cheirogaleidae, Lemuridae, Indriidae, and Daubentoniidae and two families from Africa and Asia: Lorisidae and Tarsiidae, although the last one is often classified within Anthropoidea (Ankel-Simons, 2007; R. F. Kay et al., 1997).

Compared to non-primates, members of Prosimii possess unique traits such as a petrosal bulla, a higher degree of orbital frontality, and at least one digit with flat nails (More details: Table1). They differ from Anthropoidea by having a postorbital bar instead of full postorbital closure, and they lack the fusion of the metopic suture between the frontal bones.

In lemurs and lorises, olfactory nerves pass between the orbits from the internal cavity to the brain, within, numerous turbinate's attached to the nasal cavity. However, in tarsiers, monkeys, apes, and humans, this region is simplified, with olfactory nerves passing over the interorbital septum and turbinate's reduced, having a dry nose, a continuous upper lip, and often a hairy region between the lip and the base of the nasal opening (Asher, 1998; J. G. Fleagle, 2013).

Figure 1. Composition of the bony elements in the orbital region of an Old-World monkey (above) and a lemur (below). *(Ankel-Simons, 2007)*

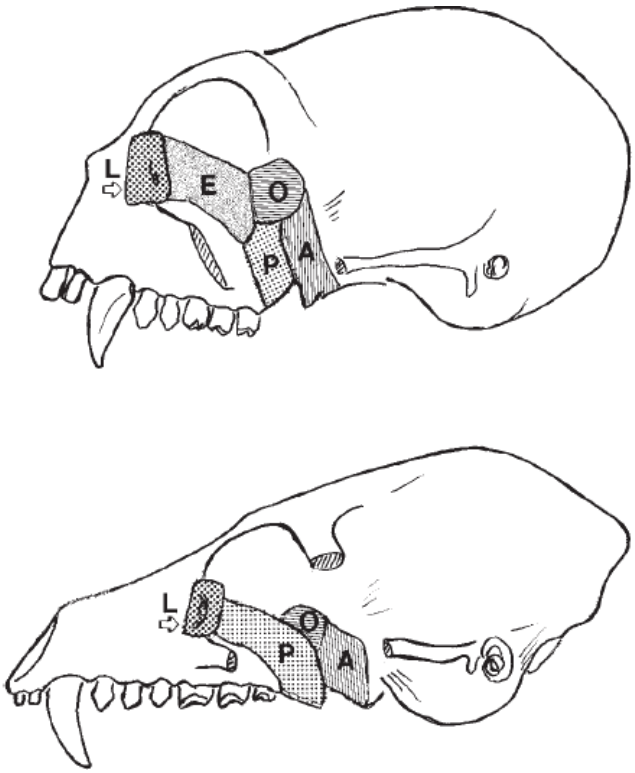

A=alsphenoid; E=ethmoid; L=lacrimal; O=orbitosphenoid; P=palatine.

Associated with the moist rhinarium of strepsirrhines is the nasolacrimal duct, which transmits tears from the orbit to the nasal cavity (Fig.1). The length and orientation of the duct vary between the two suborders of primates (J. B. Rossie & Smith, 2007). In strepsirrhines, like in fossils such as adapiforms and omomyiforms, the lower end of the duct extends anteriorly to direct moisture towards the external nose been oblique rostroventrally, while in haplorrhines, this anterior portion is absent, resulting in a vertical duct and oriented perpendicular to the infraorbital canal (J. G. Fleagle, 2013; Tabuce et al., 2009).

Despite differences in relative sensitivity to frequencies, all primate ears function similarly. The inferior surface of the middle ear is covered by a thin bone sheet called the auditory bulla, derived from the petrous part of the temporal bone. However, the bulla varies, it can be inflated or balloon-like, divided into compartments, or flatter. In lemurs, the tympanic ring lies within the cavity formed by the bulla; in lorises, it is attached to the inside wall and in New World monkeys, it is attached to the outside wall. In tarsiers and catarrhines, the ring is also attached to the bulla's wall but extends laterally to form a bony tube, the external auditory meatus(J. G. Fleagle, 2013).

Prosimii have procumbent lower incisors (known as a tooth comb) and at least one grooming claw on the hind foot. Their eye sockets are rotated forward, with an angle between the visual axes of both eyes of 60 to 70 degrees (Ankel-Simons, 2007; R. F. Kay et al., 1997).

The suborder Anthropoidea, also known as Haplorhini, comprises the higher primates, which include New World monkeys, Old World monkeys, apes, and humans. These primates are characterized by closed eye sockets, a fused mandible and frontal bone, and an auditory region where the stapedial artery[1] is replaced by a large promontory artery.

Platyrrhini, commonly known as New World monkeys are found in Central and South America. The name "Platyrrhini" comes from the Greek words "platy," meaning flat, and "rhin," meaning nose, referring to their broad and outward-facing nostrils. This nasal structure is one of the most distinctive features of this group.

Many Platyrrhines possess prehensile tails, that acts as a fifth limb, especially useful for arboreal (tree-dwelling) life. They tend to be smaller in size compared to their Old-World counterparts, range in body size from the 100 g pygmy marmoset to the 10 kg of the largest species, the woolly spider monkey, and typically have three premolar teeth instead of two in each toothrow, constituting a dental formula of 2.1.3.3. The dental formula and the absence of a

[1] A Branch of the carotid artery supplying blood to the brain

complete bony tube enclosing their ear canal distinguish them from other living monkeys. These characteristics are thought to be primitive retentions.

Table 1. Classification of the suborder Strepsirhini and their principal characteristics. (Ankel-Simons, 2007)

Infraorder	**Family**	**Genera**	**Locality**	**Activity Pattern**	**Principal features**
Lemuriformes	Lemuridae	*Lemur, Eulemur, Varecia, Hapalemur*	Madagascar	Diurnal/ Nocturnal	Large, social, diverse diets, some species with complex vocalizations
	Cheirogaleidae	*Cheirogaleus (dwarf lemur), Microcebus, Mirza, Allocebus, Phaner*	Madagascar	Nocturnal	Small, arboreal, large eyes, primarily insectivorous/ frugivorous
	Lepilemuridae	*Lepilemur*	Madagascar	Nocturnal	Vertical clingers and leapers, florivorous, solitary
	Indriidae	*Indri, Propithecus, Avahi*	Madagascar	Diurnal/ Nocturnal	Vertical clingers and leapers, florivorous, loid calls
	Daubentoni	*Daubentonia (Aye-aye)*	Madagascar	Nocturnal	Unique elongated finger for extracting insects, rodents-like incisors
Lorisiformes	Lorisidae	*Loris, Nycticebus, Perodicticus, Arctocebus*	Southeast Asia, Africa	Nocturnal	Slow, toxic bites, specialized grip
	Galagidae	*Galago, Otolemur, Euotis*	Sub-Saharan Africa	Nocturnal	Agile leapers, large eyes, known as bush babies
Tarsiiformes	Tarsiidae	*Tarsius, Carlito, Cephalophachus*	Southeast Asia	Nocturnal	Huge eyes, vertical clinger and leapers, entirely carnivorous

They are classified into 16 genera and approximately 75 species, which can be grouped into four major subfamily radiations as indicated in the table below (Table 2). This subfamily classification is widely accepted, except for two genera, *Aotus* and *Callicebus*, for whom morphological and molecular signals of relatedness are not as clear. Studies that supported the close affinities of genera within the *Atelinae*, *Pitheciinae* and *Callitrichinae*, and the unity of *Cebinae* with callitrichines (Hartwig & Rosenberger, 2006).

Figure 2. Craniofacial differences between the suborders Strepsirhini and Haplorrhine

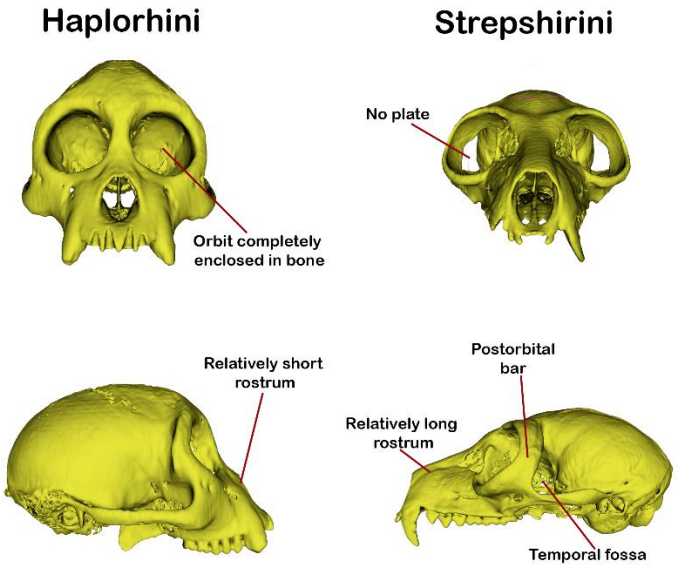

In contrast, Old World monkeys or Catarrhini are distributed across a variety of habitats in Africa and Asia, from rainforests to savannas to mountainous regions, except for Homo sapiens, which have a wider distribution. They lack prehensile tails and are often more terrestrial, with many species exhibiting significant sexual dimorphism. Beside the dental formula of 2.1.2.3, with two incisors, one canine, two premolars, and three molars on each side of both jaws. The term "Catarrhini" derives from the Greek "kata," meaning downward, indicating their downward-facing nostrils. The image above shows some of the principal craniofacial differences of each group (Figure2).

Table 2. Classification of the suborder Haplorhini and their principal characteristics. (Ankel-Simons, 2007; J. Fleagle & Kay, 1994)

Infraorder	**Family**	**Subfamily**	**Principal Features**	**Size**	**Diet**	**Social Organization**
Platyrrhini	Cebidae	Cebinae (Capuchins)	Highly intelligent, prehensile tails, tool use	Medium; 30-60 cm (body); 2-4 kg	Omnivorous (fruits, insects, small animals)	Social groups, often with complex hierarchies
		Saimiriinae (Squirrel Monkeys)	Agile, small, large social groups	Small; 25-35 cm (body); 0.7-1.1 kg	Omnivorous (fruits, insects)	Large, multi-male/multi-female groups
	Aotidae	None	Nocturnal, large eyes, monogamous	Small; 24-37 cm (body); 0.5-1.2 kg	Frugivorous, some insects	Monogamous pairs, small family groups
	Pitheciidae	Pitheciinae (Sakis, Uakaris)	Strong jaws for seed eating, robust bodies	Medium; 30-60 cm (body); 2-3 kg	Frugivorous, seed-eating	Small social groups, sometimes monogamous
		Callicebinae (Titis)	Pair bonding, territorial, duetting vocalizations	Small; 30-45 cm (body); 0.8-1.5 kg	Frugivorous, some insects	Monogamous pairs, small family groups
	Atelidae	Alouattinae (Howler Monkeys)	Loud vocalizations, prehensile tails	Large; 40-70 cm (body); 4-10 kg	Folivorous, some fruits	Social groups, territorial, multi-male/multi-female
		Atelinae (Spider Monkeys, Woolly Monkeys)	Prehensile tails, long limbs	Large; 40-70 cm (body); 6-11 kg	Frugivorous, some leaves	Fission-fusion groups, multi-male/multi-female
Catarrhini	Cercopithecidae	Cercopithecinae	Cheek pouches,	Medium to	Omnivorous (fruits,	Large, complex social groups

	(Macaques, Baboons)	ischial callosities	large; 40-70 cm (body); 5-30 kg	seeds, small animals)	with strong hierarchies
	Colobinae (Colobus Monkeys, Langurs)	Leaf-eating, specialized stomachs	Medium; 45-75 cm (body); 5-15 kg	Folivorous (leaves, seeds)	Multi-male/multi-female, with some all-male groups
Hylobatidae	None	Brachiation (arm swinging), loud calls	Medium; 45-90 cm (body); 5-12 kg	Frugivorous, some leaves	Monogamous pairs, small family groups
Hominidae	Ponginae (Orangutans)	Large, arboreal, solitary males	Large; 1.2-1.5 m (body); 30-100 kg	Frugivorous, some leaves	Semi-solitary, females with offspring

Within the infraorder Catarrhini, the superfamily Hominoidea includes apes and humans. These species are generally larger, lack tails, and have a more upright posture compared to other primates. They possess larger brains relative to body size and demonstrate high levels of social complexity and cognitive abilities. The family Hominidae, within Hominoidea, comprises modern humans, their ancestors, and great apes (chimpanzees, bonobos, gorillas, and orangutans). We can see the division of each group and some of their species, in the time-tree that springer and collaborators (Springer et al., 2012),based on the molecular data (Figure3).

1.1.2. Ecology

Primates occupy a wide range of ecological niches across the globe, thriving in diverse habitats such as tropical rainforests, temperate forests, savannas, and mountainous regions. Their dietary flexibility, include fruits, leaves, insects, seeds, and occasionally small vertebrates, that enabled primates to adapt to numerous environmental conditions (Andrews, 1992; Ankel-Simons, 2007; J. Fleagle & Kay, 1994).

Most nonhuman primates are distributed across Africa, Asia, South America, and their adjacent islands, primarily inhabiting tropical climates. However, a few exceptional species can be found in temperate regions with cold winters, such as macaques in Nepal and Japan. Within these geographic regions, primates occupy a diverse array of habitats, ranging from deserts to tropical rainforests, with some species adapted to drier or less vegetated areas, such as chimpanzees, baboons, and Senegal bushbabies. Adapted to different niches, like the tropical primary and secondary forests. The primary one, with tall trees forming a relatively continuous canopy, while secondary is denser with an abundance of vines and shorter trees (J. G. Fleagle, 2013).

Socially, primates typically live in complex social groups, which can range from small family units to large multi-male, multi-female communities. These social structures serve various purposes, including protection against predators, cooperative hunting, and the sharing of resources. (Kozakowski, 2013).

Sexual dimorphism is prominent in many primate species, where males and females exhibit distinct differences in size, morphology, or coloration, related some time with complex polygynous groups. For example, the largest males of gorillas with a pronounced sagittal crest, baboons with larger canine, or male orangutans with large cheek pads and throat sacs (Fleagan, Kay y Simon 1980).

In prosimians and New World monkeys, dimorphism is generally less pronounced. Like howler monkeys that exhibit differences in vocal anatomy, with males possessing larger vocal sacs, to produce territorial louder calls. Evolution and phylogeny of primates.

1.1.3. Principal hypothesis for the origin of the primates

As we have seen previously, the Primate Order lacks a single defining characteristic, making it difficult to understand the origin and diversification of each of its traits. This complexity has led to the development of various hypotheses over the years regarding how this group may have emerged. In this section, we will revisit three of the main hypotheses.

The first is the Arboreal Hypothesis proposed by Frederic Wood Jones, which suggests that many primate characteristics evolved to enhance tree-dwelling locomotion. For instance, the anatomy of hands and feet, which facilitates gripping branches, is thought to be an adaptation to life in the trees. This hypothesis also posits that the reduced olfactory system, acute vision, and forward-facing eyes are adaptations for making precise leaps and movements within a complex, three-dimensional canopy (Cartmill, 2018; Ross & Martin, 2007).

Later, in the late 1960s, Matt Cartmill criticized this theory by pointing out that animals outside the primate order, such as squirrels, have specialized anatomy for arboreal locomotion, and that other non-primate animals, like felines, share certain traits with primates, such as forward-facing eyes. Consequently, Cartmill proposed that the unique set of characteristics in primates is an adaptation for detecting prey and guiding the hands and/or feet to capture it (Bloch & Boyer, 2003; Cartmill, 2018), but not all the primates have a predatory conduct.

The most accepted hypothesis: Angiosperm-Primate Coevolution, proposed by ecologist Robert Sussman, sustain that during the Eocene epoch (56-33.9 M), a significant coevolutionary relationship settled between Euprimates and flowering plants.

Contrary to the theory that primates developed enhanced vision primarily for hunting, many predators rely more on sound or smell. The forward-facing eyes of primates are instead linked to the "X-ray vision" hypothesis, which suggests that stereoscopic vision provides superior depth perception and the ability to see through dense foliage in thick forests. Other distinct primate traits, such as opposable thumbs, evolved to aid in maneuvering at the tips of branches, where fruits are typically found, thus facilitating efficient foraging. Primates also contributed to the dispersal of angiosperm seeds by consuming and excreting fruits, developing a mutualistic relationship (Sussman, 1991; Sussman et al., 2013).

Figure 3. Timetree for 70 primate genera. *(Springer et al., 2012)*

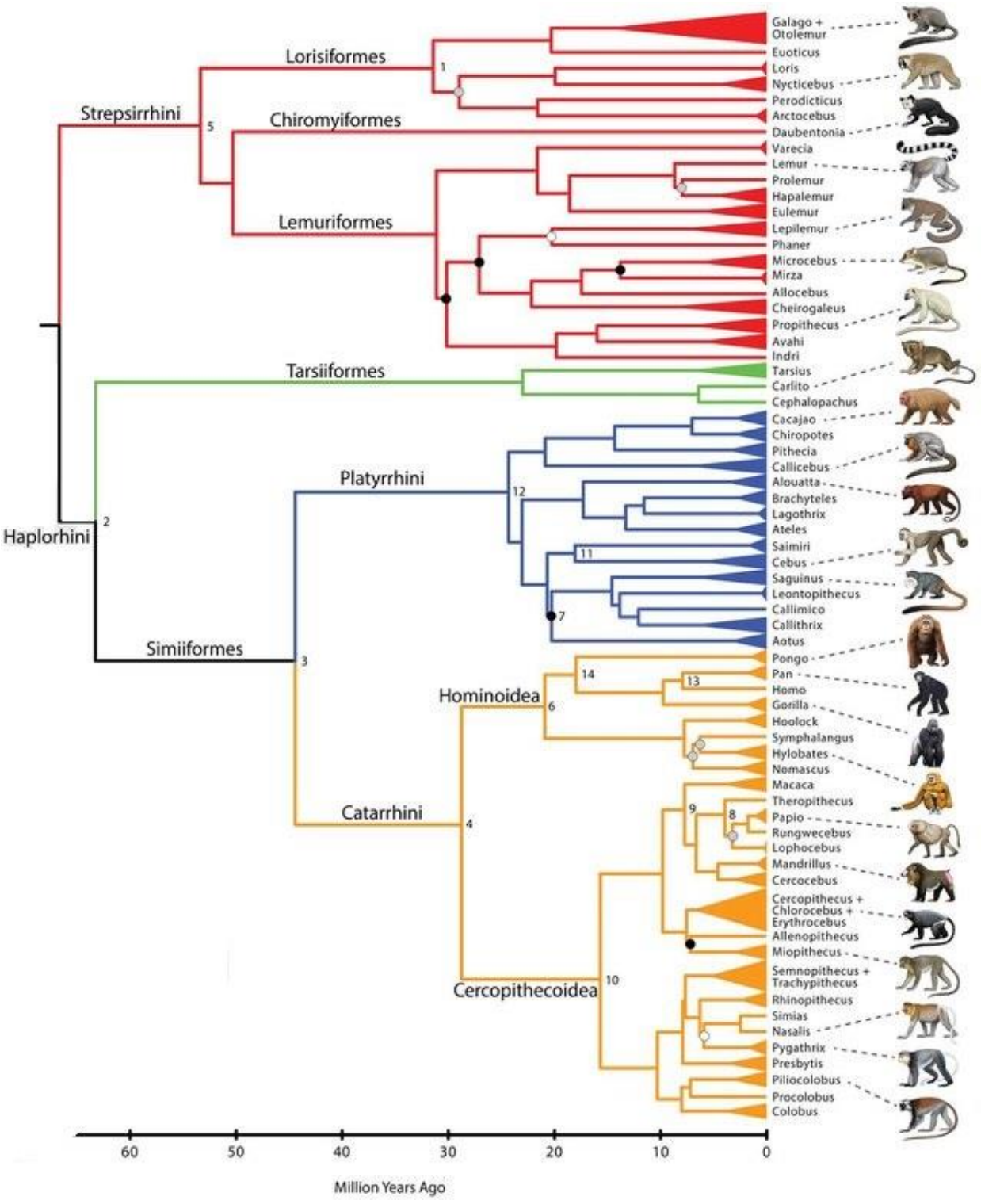

1.1.4. A new era: the origin of adapiforms

Placental mammals, including primates, first appeared during the Mesozoic Era (252 to 66 Mya). These early mammals were generally small and likely nocturnal.

However, after the extinction of the dinosaurs at the end of the Cretaceous Period, they diversified, dispersed, and increased in size as new ecological niches became available.

The oldest stem primates, called Plesiadapiformes (Figure4), appeared around 65 million years ago during the Paleocene epoch. While these early mammals were not true primates, they shared some features, such as grasping hands.

True primates, or Euprimates, emerged in the Eocene epoch, around 55 million years ago. †*Purgatorius* is generally considered the earliest primate with an arboreal lifestyle, though it is often regarded as a basal plesiadapiform, with little evidence linking it directly to Euprimates (Chester et al., 2015; Silcox, 2001).

Plesiadapiforms were numerous and diverse during the Paleocene, particularly in Western North America, Western Europe, and Asia. Most were small, with the largest species reaching about 3 kg. They had small brains, relatively large snouts, and variable eye sizes, generally faced more laterally compared to those of Euprimates. Typically had large incisors relative to their molars, and in some species, the lower incisors were elongated like daggers or spears. Many species also exhibited a reduction or loss of canines and anterior premolars, resulting in a rodent-like diastema, indicator of an herbivorous diet.

One of the plesiadapiform families, Carpolestidae of the Middle to Late Paleocene, with molars resemble those of other plesiadapiforms, but their lower posterior premolars (P_4) are laterally compressed, leaf-shaped, and bear vertical striations topped with small cusps (plagiaulacoid), similar in some living and fossil marsupials (Simpson, 1933). Most species had sharp claws on most or all digits, except for the species †*Carpolestes simpsoni* that have a distal thumb with a nail (Ankel-Simons, 2007; J. Fleagle & Kay, 1994).

The first universally accepted primates in the fossil record belong to two superfamiles Adapoidea and Omomyoidea. Both groups appeared at the beginning of the Eocene and are found in western North America, Western Europe, and India. Over time, these groups became quite distinct, occupying

mutually exclusive niches, achieved considerable diversity during the Middle Eocene(Shook et al., 2024).

Adapoids were primarily diurnal and herbivorous, with some species reaching size up to 10 kg. Divided into six families, they exhibit key Euprimate characteristics, such as a postorbital bar, flattened nails, grasping limbs, and a petrosal bulla. Additionally, some adapoids retain the primitive dental formula: 2.1.4.3. Generally, their incisors are small compared to their molars, but the canines are relatively large, with sexual dimorphism in some species. The snouts are long, and cranial evidence suggests variability in the carotid artery.

The family Adapidae was exclusive to Europe and includes some of the most robust cranial and postcranial primates of the Eocene, distinguish the species †*Adapis*. Other family was Notharctidae from western North America, with some species also found in Europe, described as lemur-like, based on their postcranial adaptations for clinging and leaping, as well their crania (Bernardi & Couette, 2017; Godinot, 1998). And most of the primitive adapoids are include in de Cercamoniidae with several genera with short snout, robust jaw, loss of some premolar teeth, and adaptations for leaping. This family was likely widely dispersed across North America, with representatives in the Eocene of Europe, Africa, and Asia (Lewis et al., 2023).

In contrast of adapidiforms, omomyoids were mainly nocturnal, insectivorous, and frugivorous, and small. Both barely survived the Eocene-Oligocene extinctions when cooler temperatures increased, retreated of tropical forests to lower latitudes. In North America, a genus originally considered omomyoid but recently reclassified within the Adapoidea persisted into the Miocene: †*Ekgmowechashala* (Hartwig & Rosenberger, 2006).

1.1.5. Origin of Strepsirrhines

Early primates are divided into two main suborders: Strepsirrhini and Haplorhini, which diverged from other primates between 64 and 58 Ma during the Paleocene. Strepsirrhines likely originated in the Afro-Arabian region, and the split between lemuriforms and lorisiforms is believed to have occurred on the African continent.

Figure 4. Phylogenetic tree of the major fossil forms of primates. (Jones and Pelbeam (Ed.) , 1992)

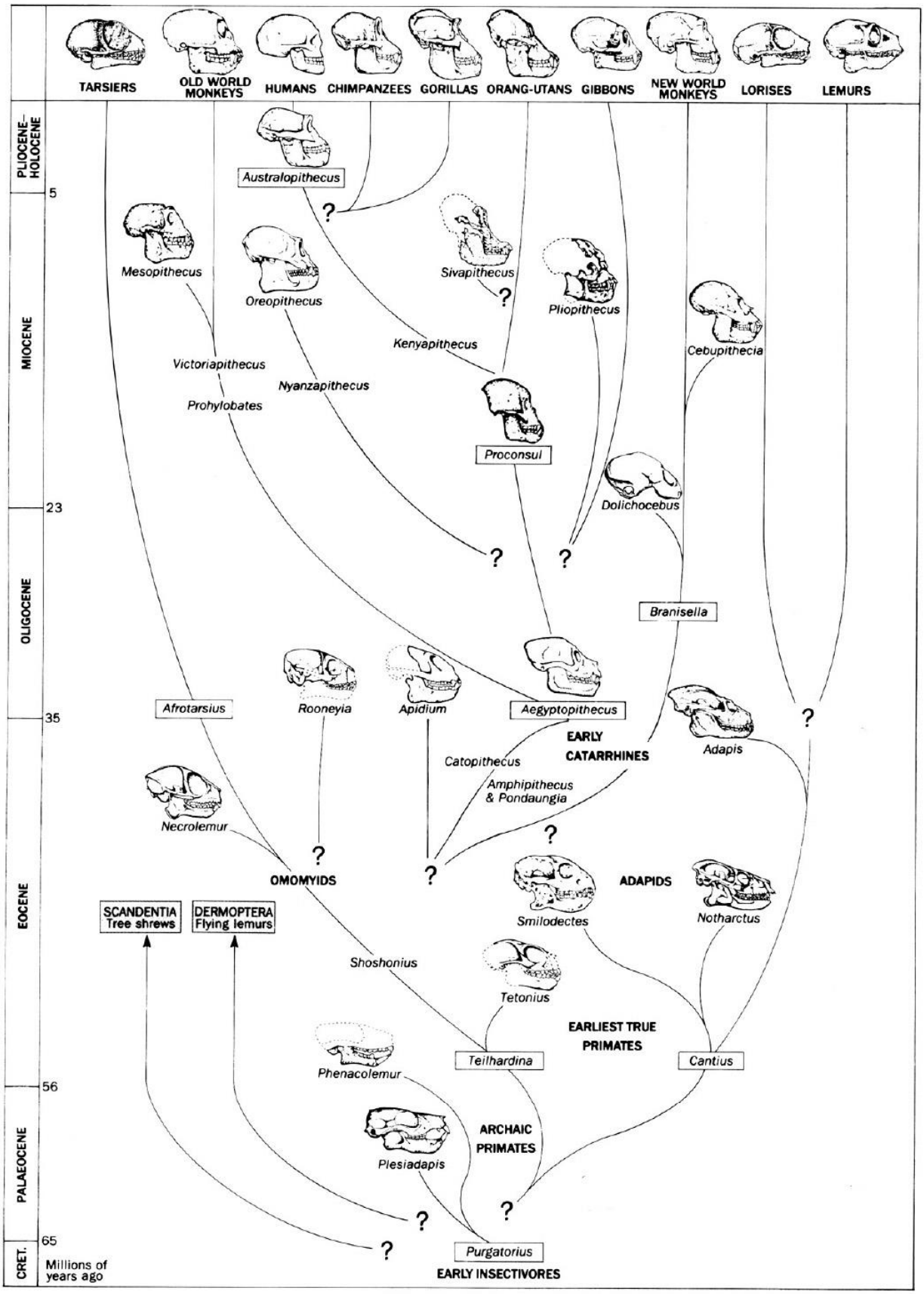

Following this split around 50 M ago, lemur ancestors dispersed to Madagascar (Springer et al., 2012), more related with the gruop of fossils know like Adapids, while omomyids are linked to tarsiers and anthropoids (J. Fleagle & Kay, 1994).

1.1.6. Origin of Haplorhines

The firsts anthropoids were small, nocturnal, and arboreal, primarily consuming insects and fruits. Over time, they transitioned to a diurnal lifestyle and a more herbivorous diet, which was pivotal in their evolution (J. Fleagle & Kay, 1994; R. F. Kay et al., 1997).

Tarsiers, a distinct lineage within the Haplorhini suborder, diverged from the ancestors of monkeys and apes around 55 Mya. Fossil records for tarsiers are scarce, but we can mencioned the Eocene species †*Xanthorhysis,* †*Archicebus achilles* (considered the most basal tarsiiform) and †*Tarsius eocaenus*, that present already the moder features (J. G. Fleagle, 2013; Shook et al., 2024)

The other major group within Haplorhini, Anthropoidea, split into Platyrrhini in South America and Catarrhini in Africa and Asia about 40 million years ago (R. F. Kay et al., 1997; Sussman, 1991).

A) New World monkeys

The Platyrrhini infraorder, representing the diverse primates of South and Central America, includes approximately two dozen extinct genera spanning nearly 30 million years (Hartwig & Rosenberger, 2006). Primates likely colonized South America during the Eocene, originating from Africa (R. F. Kay et al., 1997). The most plausible scenario suggests that primates were stranded on vegetation rafts carried across the ocean (Hartwig & Rosenberger, 2006). Once on land, platyrrhines spread across South America relatively quickly, as the earliest known primates from the continent are from Perú (M. Tejedor & Novo, 2016).

Other fossils have been discovered in Bolivia, Argentina, Chile, Colombia, Brazil, and the Caribbean, suggesting that the past biodiversity of New World monkeys was greater than that of living species. The evolution of feeding niches played a key role in the diversification of New World monkeys. An early

phylogenetic split likely occurred between frugivore-faunivores (e.g., Cebinae and Callitrichinae) and frugivore-folivores (e.g., Atelinae, Pitheciinae, Aotinae) (Arnal et al., 2020; M. Tejedor & Novo, 2016).

These adaptive radiations led to distinct groups, including atelines, pitheciines, and callitrichines, with Platyrrhines remaining highly forest-dependent and not evolving terrestrial forms like Old World anthropoids. Some extinct fossils, such as those in Brazil, indicate that primates once reached sizes up to 25 kg (Novo et al., 2021; M. F. Tejedor & Bosco, 2016; M. Tejedor & Novo, 2016).

B) Old World monkeys

The richest deposits of early anthropoid fossils from the Late Eocene and Early Oligocene are found in Egypt's Fayum Basin, specifically in the Jebel Qatrani and Birket Qarun Formations. These wet, swampy conditions (Bonnefille, 2010) preserved numerous fossils exhibiting key anthropoid features, such as postorbital closure, fused mandibular symphyses, and specific dental formulas (2.1.3.3 or 2.1.2.3) (E. Simons & Kay, 1983).

Figure 5. A sample of Fayum Anthropoid fossils. (Shook et.al. 2024)

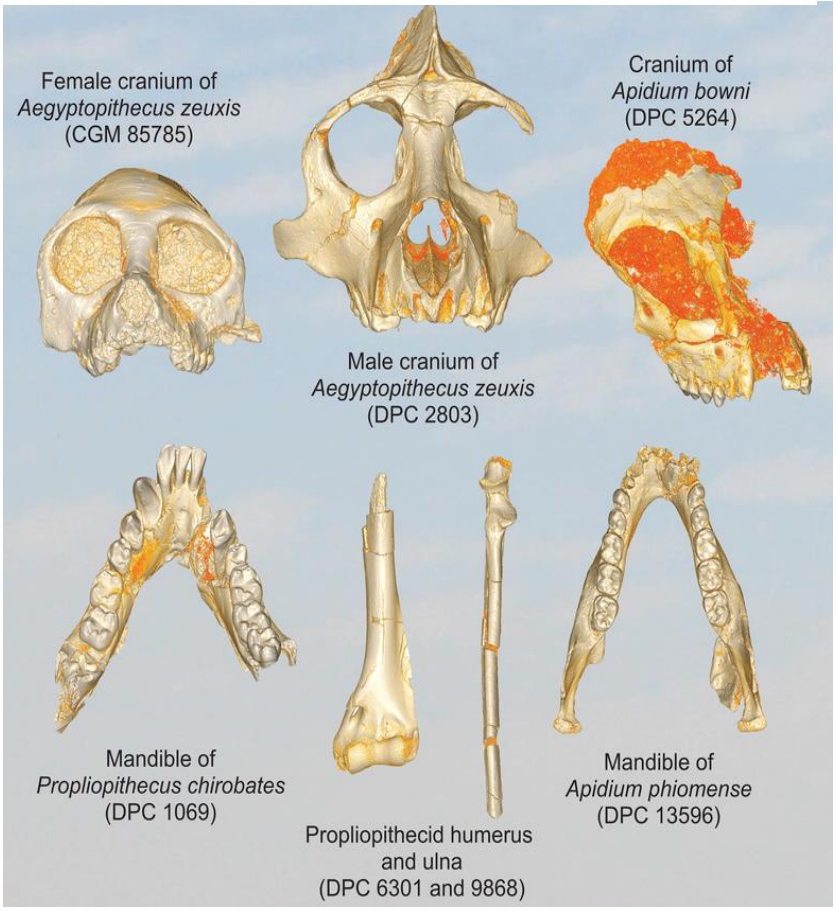

Fossils range from small species like †*Qatrania* and †*Biretia* (under 500 g) to larger ones like †*Aegyptopithecus*

(about 7 kg), which were likely diurnal quadrupeds. Some, like †*Apidium* (Figure5), were adept leapers(Shook et al., 2024).

The Propliopithecoidea superfamily, including genera like †*Aegyptopithecus* and †*Oligopithecus*, are considered stem-catarrhines that diverged around 25 million years ago during the Oligocene. †*Aegyptopithecus* is a well-known propliopithecid, characterized by the catarrhine dental formula and canine honing complex (E. Simons & Rasmussen, 1989). The Parapithecoidea superfamily, including †*Apidium* and †*Parapithecus*, exhibits a more primitive anthropoid dental formula and features suggesting a frugivorous diet and adept leaping abilities (Ankel-Simons et al., 1998). The phylogenetic position of †*Apidium* within Parapithecidae are generally accepted as a stem anthropoid clade (Beard et al., 2016).

The genus †*Parapithecus* shows an extreme reduction of the incisors, including the complete absence of lower incisors in †*P. grangeri* (E. Simons, 2001; E. L. Simons et al., 2007), a trait unique among primates.

While initially thought to be ancestral to platyrrhines, parapithecids are now considered a primitive anthropoid clade. The catarrhine fossil record after propliopithecoids is sparse, but fossils like †*Kamoyapithecus* from Kenya suggest a possible split between hominoids and cercopithecoids between 29 and 24 million years ago (Zalmout et al., 2010). The Miocene period saw some diversification of Cercopithecoidea, with †*Victoriapithecus*, found in the middle Miocene deposits from Maboko Island, Kenya, dated to 14.7 M. This small-bodied monkey had a small brain, a long-narrow sloping face and round eye sockets. It shares some cranial features with †*Aegyptopithecus*, such as a deep zygomatic bone region and a well-developed sagittal crest but is reconstructed as more frugivorous and with terrestrial locomotion (B. Benefit & McCrossin, 1997; J. Fleagle et al., 1980; J. Fleagle & Kay, 1994).

Near the Oligocene–Miocene boundary, the collision between the Afro-Arabian and Eurasian landmasses initiated periodic faunal interchange, contributing to the eventual replacement of many resident species by immigrant species. Fossils from the Rukwa Rift, such as †*Nsungwepithecus gunelli* and

†*Rukwapithecus fleaglei*, both from the 25.2 M. old, or †*Noropithecus* provide a vison of the Paleogene catarrhine diversity during this period (Stevens & Heesy, 2006).

Old World monkeys, divided into the cercopithecines and colobines, first appeared clearly at the end of the Miocene, around 15 million years ago, with some representants like †*Microcolobus* or †*Pliopapio*. This period coincided with the closure of the Tethys Sea and the formation of the Gomphotherium Landbridge, which, along with global warming, led to a significant mammalian migration from Africa to Eurasia. Some of these species eventually re-entered Africa and contributed to the ancestors of modern apes, including hominids (Arenson et al., 2022; B. Benefit & McCrossin, 1997).

The Hominoidea superfamily, consisting of lesser and great apes, shares a common ancestor from around 14 million years ago (Springer et al., 2012). Differing in body size and craniodental morphology, but sharing postcranial features related to orthograde behaviors (D. M. Alba et al., 2024). Early Miocene Africa was home to 14 genera of early apes, primarily arboreal quadrupeds with frugivorous diets (R. F. Kay et al., 1997). Late Miocene hominoids like †*Nakalipithecus* (9.9 M) and †*Chororapithecus* (10.7 M) suggest that African hominoid diversity persisted throughout this period, possibly leading to the last common ancestor of modern African apes (Neaux et al., 2013; Pugh, 2020).

†*Proconsul*, an early ape genus from East Africa, lived between 22 and 17 million years ago and exhibited features linking it to the Hominoidea, such as a short face and above-branch locomotion. Proconsul likely lived in dense, closed-canopy forests and was a tailless monkey, a trait distinguishing apes from Old World monkeys (Andrews, 1992; Gingerich, 1977; E. Simons & Rasmussen, 1989).

Eurasian hominoids adapted to their environments with diverse dietary strategies, ranging from soft fruit consumption to hard object feeding, influenced by seasonal changes and the availability of fallback foods, while other fossils show adaptations for tougher diets (deMenocal, 2004).

For example, †*Oreopithecus bambolii* had features suggesting a highly folivorous diet (D. M. Alba et al., 2024) (Andrews, 1992; Susanna et al., 2014). †*Gigantopithecus*, one of the largest known apes, possibly weighed up to 270 kg and was a bamboo specialist (D. M. Alba et al., 2024; Bocherens et al., 2015). Smaller †*Pliobates* (family Pliobatidae), dating to 11.6 Mya were frugivores with unique locomotion, including palm-down walking and flexible wrists (D. M. Alba et al., 2024). †*Pierolapithecus* from Spain had an orthograde body plan similar to modern apes but lacked adaptations for suspensory locomotion (J. Fleagle & Simons, 1982; R. Kay et al., 1981; R. F. Kay et al., 1997), while †*Anoiapithecus* had a flat face and less specialized teeth (D. Alba et al., 2024; Moyà-Solà et al., 2009; Pugh et al., 2023a).

The Vallesian Crisis in the Late Miocene led to the extinction of most Eurasian hominoids, with *Oreopithecus* and *Gigantopithecus* among the last survivors (Bocherens et al., 2015). Lesser apes like *Laccopithecus* share features with modern gibbons, including a generally small body size and a short face, but are more primitive. The history of Hylobatidae becomes clearer in the Pleistocene with †*Yuanmoupithecus xiaoyuan* taxon from China (Shook et al., 2024).

Today, orangutans are found only on the islands of Borneo and Sumatra, but in Pleistocene-aged have a vast range of distribution in Cambodia, China, Laos, Peninsular Malaysia, and Vietnam. †*Sivapithecus*, a Miocene ape from India and Pakistan, closely resembles ancestral orangutans but had a more generalized locomotion (Andrews, 1992).

The earliest fossil evidence of chimpanzee's dates to 545 Kya years ago (McBrearty & Jablonski, 2005), and the basal member of gorillas are representing by †*Chororapithecus* and †*Nakalipithecus* (Geology & Program, 2005; Kunimatsu et al., 2007).

1.1.7. Stem-catarrhines: the case of †*Aegyptopithecus zeuxis*

Fossil primates from the Egyptian Oligocene, specifically in the Jebel el Qatrani Formation, include the notable "Dawn Ape," containing a single species, †*Aegyptopithecus zeuxis*, a slow-moving, arboreal quadruped that lived around 33 Mya (Oligocene) (J. G. Fleagle, 2013).

Propliopithecids are considered stem-catarrhines, predating the divergence of modern catarrhines. They share key cranial features with living catarrhines, such as complete post-orbital closure, absence of the metopic suture, a 2.1.2.3 dental formula, increasing molar size from M1 to M3, and ape-like lower molars with five cusps. However, their heteromorphic premolars and molars resemble those of Cercopithecoidea, underscoring their ancestral status as early catarrhines (Mccabe, 2017).

†*A*. Zeuxis, part of the Propliopithecidae family, exhibited high sexual dimorphism (Figure6), particularly in canine size. Studies of its teeth suggest an average body weight between 4.5 to 7.5 kg, and an encephalization quotient of 0.85, indicating a brain size smaller compared with modern anthropoids. The fossils are found in channel and over bank deposits, capped by a basalt layer dated to 27 million years ago (Gingerich, 1977).

Females have sharp, conical lower canines and sectorial lower anterior premolars, comparable to males but smaller. The second molar (M2) is much larger than the first molar (M1), with lower molar crowns compressed buccal-lingually and their crown margins flaring outward, giving them a bulbous appearance. Lower premolars have greater breadth buccal-lingually than mesial-distally, and upper premolars and molars have strongly developed lingual cingula (R. Kay et al., 1981; E. L. Simons et al., 2007).

Leonard Radinsky (1973) analysis of †*Aegyptopithecus* braincase fragments revealed that its brain was more advanced than most modern prosimians, resembling that of †*Dryopithecus* with a larger visual cortex and smaller olfactory bulbs, but less advanced than anthropoids due to a smaller frontal lobe (Table3).

Displayed a mix of primitive and derived features, indicating mosaic evolution, with a skull that reseamble the Eocene adapids, including a large facial structure, small braincase, pronounced sagittal crest, marked postorbital constriction and dorsally facing orbits (plesiomorphies). The frontal lobes are smaller than in anthropoids but larger than in most prosimians, with a well-developed visual cortex and smaller olfactory lobes and compared to extant

cercopithecoids the orbits are smaller and the palate widens posteriorly (R. Kay et al., 1981).

Figure 6. Comparison of the sexual dimorphism between the female CGM 85785 (left) and the male CGM 40237 (right) of *Aegyptopithecus zeuxis*. (Ankel-Simons, 2007)

Radinsky suggested that †*Aegyptopithecus* might have been a giant relative to its derived group, with brain shape affected by allometric factors. In fact, these species show several anthropoid characteristics, such as a fused mandibular symphysis with both superior and inferior transverse tori. The foramen magnum's position and the unique structure of the ectotympanic bone also distinguished it from other Old-World anthropoids, the jaw has a V shape in occlusal view, with very narrow and high-crowned incisors (E. Simons, 1987; E. L. Simons et al., 2007).

In postcranial skeleton, the humeri possess an entepicondylar foramen, present in about half of the genera of platyrrhines. Primitive characters include a wide trochlea, large medial epicondyle, and a shallow supracapitular depth. The ulna is like *Alouatta*, and the first basal metatarsal provides evidence for an opposable grasping hallux. Phalanges and caudal are like those of other arboreal anthropoids (J. Fleagle & Simons, 1982; R. Kay et al., 1981).

Table 3. Comparison of the cranial anatomy of *Aegyptopithecus zeuxis*, *Pliopithecus vindobonensis* and *Dryopithecus africanus. (R. Kay et al., 1981)*

	Aegyptopithecus	***Pliopithecus***	***Dryopithecus***
Premaxilla	Large with smooth infraorbital surface	Small with projecting lip-like infraorbital surface	Small with smooth infraorbital surface
Root of zygomatic arch	Above M_2	Above M_2	Above M_2
Nasals	Long, projecting	Short, projecting	Short, not projecting
Interorbital breadth	Large	Extremely large	Large
Orbits	Small face slightly laterally and dorsally	Large, face forward	Intermediate
Brain size	Small compared to modern Anthropoidea	Possibly moder sized	Modern Anthropoidea size-range
Post-orbital constriction	Marked	Little	Little
Mandibular tooth rows	Diverge posteriorly	Diverge posteriorly	Diverge posteriorly
Mandibular corp	Deep, under molars	Shallower, under molars	Generally shallower ma

CHAPTER II: MATERIALS AND METHODS

2.1. Data collection

The study used a sample of 68 primates (58 extant and 10 extinct) of which 56 are hominid crania, including 6 species of the parvorder Platyrrhini (n=12), 15 species of the superfamily Cercopithecoidea (n=30), and 7 species of the superfamily Hominoidea (n=14). For the primate fossil sample 10 species were used: †*Aegyptopithecus zeuxis* (n=4), †*Parapithecus grangeri* (n=1), †Afropithecus turkanensis (n=1), †*Turkanapithecus kalakolensis* (n=1), †*Pierolapithecus catalaunicus* (n=1), †Rhinocolobus turkanensis (n=1) and †Theropithecus oswaldi (n=1). *A. zeuxis* fossils were the focus of this project, so their sample sizes are larger than the other comparison taxa.

In this study, only specimens with at least 80% of the face preserved were selected. This criterion was chosen to ensure that the specimens had sufficient facial preservation, prioritizing those with complete crania. For specimens with damaged calvariae, preference was given to those where most of the frontal bone was intact, even if the calvaria was partially missing due to cuts made for study purposes. This allowed for accurate identification of key landmarks, such as the temporal lines.

Additionally, specimens with minimal deformation were preferred. Among these, only one specimen was missing the inferolateral part of the orbit and the zygomatic bone. The zygomatic arch was often incomplete or missing in the fossils, so only two landmarks on the zygomatic were included to ensure all specimens could be analyzed.

2.1.1. Extant non-human primates

From the 56 specimens (Not couting the outgrop: two lemurs) corresponding to extant primates 39 were obtained from the digital repositories: Primate Research Institute at Kyoto University, Japón (*Digital Morphology Museum, Kupri*[2]*)* *(Table4)*. When one species of interest is not available or only is available a male

[2] http://dmm.pri.kyoto-u.ac.jp/dmm/WebGallery/index.html

Table 4. Extant primates' comparative sample

Genus	Species	n	Specimens ID*	Sex	Holding institution	Conservation
Platyrrines						
Alouatta	*A. caraya* *A. seniculus*	4	Ac_959 Ac_961 As_963 As_T965	F M M F	KUPRI	All specimens present use-wear on incisors and diastema between incisors and canines. 2. Postmortem loss of the right P2 3.Lateral-superior deformation in the right orbit 4.Postmortem loss of left I2, C, and right P4, antemortem loss of I2
Ateles	*A. geoffroyi*	2	Ag_540 Ag_551	F M	KUPRI	1.Postmortem loss of all teeth except M1 2.M3 right not emerged
Cacajao	*C. calvus rubicundus*	2	Cc_302626 Cc_302627	M F	NMNH	Diastema I-C 1.right C broken
Cebus	*C. apela*	2	Ca_957 Ca_1067	M F	KUPRI	1.Postmortem loss of incisors and M3 2.Diastema I-C and temporal lines close to each other
Lagothrix	*L. lagotricha*	2	Ll_349 Ll_542	M F	KUPRI	1.Three holes present in the frontal bone 2.Postmortem loss M3
Cercopitheoids						
Cercocebus	*C. torquatus*	2	Ct_507 Ct_735	M F	KUPRI	Medial-superior notch in the orbits 1.M3 not erupted 2.Right I1 broke, M3 visible but not completely emerged
Cercopithecus	*C. campbelli*	2	Cca_1070 Cca_1073	F M	KUPRI	Medial-superior notch in the orbits 1.Cusp of M2 and M3 well developed
Colobus	*C. guereza*	2	Cg_938 Cg_939	M F	KUPRI	1.Postmortem loss of I1 and C 2.Postmortem loss of I1, I2 and C
Erythrocebus	*E.patas*	2	Ep_924 Ep_967	M F	KUPRI	1.Cusp very marked, slices of the 2D not at the same distance 2.Postmortem loss of right I2, cusp very marked in molars
Macaca	*M. fasciculari s* *M. fuscata* *M. mulatta*	6	Mf_1157 Mf_1455 Mfu_1182 Mfu_1184 Mm_1160 Mm_1463	M F M F M F	KUPRI	Medial-superior notch in the orbits 1.Browridge large and squared 2.Right zygomatic fracture, estimation of zygomaticofacial foramen
Mandrillus	*M. sphinx*	2	Ms_070 Ms_1021	F M	KUPRI	Medial-superior notch in the orbits 1.Postmortem loss of I1, I2, C and P3 2.Postmortem loss of right I2, C and P3, left I1, I2 and C
Miopithecus	*M. ogouensis*	2	Mo_8519 Mo_8534	M F	NMNH	1.Little medial-superior notch in the orbits 2.Without orbital notch
Nasalis	*N. larvatus*	2	Nl_1422 Nl_3734	M F	NMNH/ MS	Present of three holes in the infraorbital foramen 2.Postmortem loss of left C
Papio	*P. hamadryas*	2	Ph_402 Ph_424	M F	KUPRI	Medial-superior notch in the orbits 1.Postmortem loss of left I1, Right I1, I2 and P3

Pliocolobus	*P. badius*	2	Pb_941 Pb_946	F M	KUPRI	1.Use-wear on incisors and postmortem loss of left C 2.Left P4 lingually deviated
Presbytis	*P. melalophos*	2	Pm_1055 Pm_1057	F M	KUPRI	Well-developed cusps of P and M 1.Extreme use-wear in left I2
Theropithecus	*T. gelada*	2	Tg_447 Tg_1028	M F	KUPRI	1. Use-wear in left I2 2.Extrem use-wear in C and P and unclear zygomaticofacial foramen
Trachypithecus	*T. germaini germaini*	2	Tgr_2366 Tgr_3077	F M	NMNH	1.Well-developed cusps in P and M 2.Left I1 broken
Hominoids						
Gorilla	G. gorilla	2	Gg_1345 Gg_2525	M F	KUPRI/ NMNH	Postmortem loss of left I1 and C, affected alveolar plane with possible antemortem loss of right I1, I2, and C and unclear zygomaticofacial foramen 2. M2 broken and use-wear in incisors
Hoolock	H. hoolock hoolock	2	Hh_1126 Hh_8342	M F	MS	Zygomaticofacial foramen divided in two 1.Little damage to the upper part of the nasal aperture 2.Little notch in the upper ridge of the left orbit by fracture or unfused
Hylobates	H. lar carpenteri	2	Hl_7752 Hl_7755	M F	NMNH	Notch in inferior ridge of the orbit (union between maxilla and zygomatic) and zygomaticofacial foramen divided in two
Nomascus	N. concolor	2	Nc_4649 Nc_5422	F M	NMNH	Zygomaticofacial foramen divided in three
Pan	P. troglodytes	2	Pt_12 Pt_T515	F M	KUPRI	Zygomaticofacial foramen divided in two 1.Use-wear in the alveolar part of incisors, possible antemortem loss of central I (prosthion and orale estimated) 2.Medial-superior notch in the orbits
Pongo	P. abelii	2	Pa_796 Pa_1343	M F	KUPRI	1.Alveolar plane deteriorated (exposure of the roots), postmortem loss of right P4 and M, left C and M3 and infraorbital foramen divided in three 2.Antemortem loss of right P3 and M2, displacement of the P and M and exposure of the root
Symphalangus	S. syndactylus	2	Ss_2710 Ss_1719	F M	NMNH	1.Notch in the inferior ridge of the orbit and ramus of zygomatic fractured 2.Postmortem loss of left P4 and little displacement between the right and left side of the cranium (for a midsagittal cut)
Total		56				

*The ID of each specimen was created based on the abbreviatures of the species plus the number of file that each repository gives to each one. This IDs are the ones that we used in the posterior analysis.

or a female specimen, we complete the data with the 3D Digitization collection of National Park Service Paleobiology of the Smithsonian Institute[3] (14 specimens) and f Morphosource (3 specimens).

2.1.2 Primate fossils

In total the 5 fossils cast were recovered from 3D data repository MorphoSource[4], as part of a contribution of Duke Lemur Center Museum of Natural History. In the case of the †*Aegyptopithecus zeuxis* and *Parapithecus grangeri* sample in format of volumetric Computed tomography scans (CT) and the rest in surface mode (Table5).

The only criteria for excluding some fossil species were poor preservation, incomplete descriptions, or low-quality CT scans. However, in this study, the material was exceptionally well-preserved, so no fossils were eliminated, which, together with extant primates, allowed us to draw a first phase to mostly cover the facial morphology, resulting in a dataset with 61 landmarks.

The main issue was the limited diversity and number of available and accessible fossils. We focused on the face because †*Aegyptopithecus* and other fossils in the sample have exceptionally well-preserved facial structures, whereas the cranium is often less complete. Previous studies have used facial morphology as a key indicator of evolutionary changes in primate fossils, offering a strong methodological basis for our work. The face provides a more reliable reference for understanding species differences and evolutionary changes than the calvaria or cranium.

Other criteria for selection included prioritizing the preservation of *Aegyptopithecus* and maximizing the inclusion of other fossils in the sample, due to missing parts and the preservation state a reduced dataset of 48 landmarks was used for the 3D geometric morphometric analysis. This focused more on the upper part of the face, as the fossils were minimally reconstructed for this analysis. The asymmetrical deformation in the zygomatic and lower facial

[3] https://3d.si.edu/
[4] https://www.morphosource.org/?locale=en

regions, particularly in the alveolar area, could not be corrected through simple mirroring. Consequently, landmarks such as zygomaxillare, zygion, jugale, canine jugum, alveolar I2, and the single points incisive foramen, orale, and prosthion were excluded.

As a result, two separate analyses were conducted: 1) on extant primates using the complete set of 61 landmarks, and 2) on the entire collection, using only the landmarks present in all specimens.

2.1.2. Outgroup

The method of outgroup analysis is used to determine which characters are apomorphic or plesiomorphic to reconstruct the phylogeny that determines to which group *Aegyptopithecus* is closest and which characters it shares that make it a monophyletic group. The outgroup helps us to guarantee that the ingroup cladogram and the related groups are parsimonious, because their states and interrelationship with the ingroup show the ancestral character states (Maddison et al., 1984).

To select the out groups, it is helpful to include extant taxa because most or all the characters have been sampled before. Using the definition of an outgroup as the clade that attaches to the stem coming down from the ingroup, ideally the most closely related sister taxa are chosen (Post et al., 2023). In this study our principal species of analysis is a stem catarrhine.

To test this hypothesis, we also analyze different species of the sister taxon of Catarrhini, the Platyrrhini. Both pavorders belongs to the Haplorrhini suborder, which is why we consider the Strepsirrhinni suborder the best outgroup.

This suborder is constituted by lemuriforms, galagos and pottos, among this the infraorden Lemuriformes include all the living strepsirhines, the Malagary Lemuroidea and the Asian and Africa Lorisoidea, distinguish from the infraorder Adapiformes, that includes most of the fossil strepsirhines that do not possess the tooth comb, for what them are considered a sister taxon group of the Lemuriformes(Godinot, 2006).

Table 5. Fossil primates' comparative sample

Genus	Species	n	Specimens ID	Temporality	Age interval	Position	Holding institution	Conservation
Propliopithecoidea								
Aegyptopithecus	*zeuxis*	4	Az_8578 Az_2803 Az_3161 Az_8794	Oligocene	38-34 M	Stem catarrhine	Morphosource	M3 visible but not emerged, alveolar planum damage affecting the location of right zygomaxillary, zygion and both jugales; Postmortem loss of I, C and P3 and canine jugum calculated; Postmortem loss of I, C and left P4, rhinion, nasospinale, prosthion, left alare and alveolar I2 not located; Missing part of the alveolar planum in the incisors area and not located nasospinale, prosthion, alveolars I2, left canine jugum, maxilla tuberosities and approximated infraorbital foramen
Parapithecidea								
Parapithecus	*grangeri*	1	Pg_18651	Eocene-Oligocene	40-33 M	Steam anthropoideans	Morphosource	Right orbit distorted, left canine jugum not located
Proconsulidae								
Afropithecus	*turkanensis*	1	At_16999	Miocene	18-17 M	Hominidae	Africanfossils	Left orbit ridge, lower nasal aperture and alveolar plane of incisors missing
Turkanapithecus	*kalakolensis*	1	Tk_16950	Miocene	17.7-16,6 M	Proconsulidae	Africanfossils	Nasospinale, prosthion, orale, incisive foramen, lomi, left zygion, left maxilla inflection not located and approximated rhinion
Hominidae								
Pierolapithecus	*catalaunicus*	1	Pg_25250	Miocene	13 M	Stem hominine	Morphosource	Temporal lines, zygomaxillary, zygion, jugale and incisive foramen not located
Cercopithecidae								
Rhinocolobus	*turkanensis*	1	Rt_1485	Pleistocene	1.5-3 M	Cercopithecidae	Africanfossils	Poor quality of the 3D model, slight deformation of the right orbit, and difficulty in delineating the teeth
Theropithecus	*oswaldi*	1	To_60609	Pleistocene	2.5 M-500 Kyr	Cercopithecidae	Africanfossils	Infraorbital foramen not located due to poor resolution; prosthion, I, C and P not located because the alveolar part is damaged
Total		10						

*The ID of each specimen was created based on the abbreviatures of the species plus the number of file that each repository gives to each one. This IDs are the ones that we used in the posterior analysis.

The Strepsirrhini suborder includes lemuriforms, galagos, and pottos. Among these, the infraorder Lemuriformes includes all living strepsirrhines, the Malagasy Lemuroidea, and the Asian and African Lorisoidea. This group is distinguished from the infraorder Adapiformes, which includes most of the fossil strepsirrhines that do not possess the tooth comb, making them a sister taxon group to the Lemuriformes (Godinot, 2006).

For this group, we chose *Lemur catta* (Lc_035 and Lc_1040) due to specimen availability in the Kupri repository, having one specimen of each sex, and because, contrary to the lorisiforms, it has a diurnal behavior like all the other specimens in this sample.

2.1.4. Aging and sex

Each specimen had a sex designation included in the inventory list of the different repositories. From this list, one male and one female of each species were chosen. Although it was prioritized to include the greatest number of species, rather than focusing solely on a statistical representation of sexual difference, unassigned specimens would severely limit the analysis. It was considered important to assess whether sex played a role in shape variation of the face between and within species.

Similarly, the age of the specimens was showed on the inventory, either in years or by developmental stage. For this research, adult crania were selected. To corroborate the information provided by the repositories, we saw the eruption of the third molar, which is indicative of dental development. Age was figured out based on the eruption of permanent dentition, as published for various primates (Table 6).

For the primates without specific study, we assumed that their dental development falls within the species that previously were analyzed, exhibiting dental eruption and life stage pattern, albeit towards the variation range, assuming the adulthood stage associated with the partial or total emergence of the third molar.

In this case only 3 specimens do not present the complete emergence of M3: the two *C. torquate* (Ct_507 and Ct_735) and one †*A. Zeuxis* (Az_3161).

Table 6. Age of emergence of permanent teeth of chimpanzees. *(Kuykendall et al., 1992; Smith & Boesch,* 2011)

Maxillary tooth	**Age of emergence in year from Kuykendall *et.al.* (1992)**	**Age of emergence in year from Zihlman *et.al.* (2004)**	**Age of emergence in year from Smith and Boesch (2011)**	**Stage**
M^1	3.18	>3.75	4.1	Juvenil
I^1	5.55	6.24	6.3-8.4	Juvenil
I^2	6.21	6.63	7.4-8.6	Juvenil
M^2	6.74	7.16	8.2-8.4	Juvenil
C	8.08	10.04	10.1-10.8	Adolescent
M^3	-	12.63	12.4	Adulthood

The observation of the total emergence of M2 was considered, because is only after of this completion that the allometric trajectories in males and female diverge significantly (Collard & O'higgins, 2001; Paddock et al., 2020). But also, previous studies show indicated a later emergence in males for all teeth except the left maxillary M1 (Kuykendall et al., 1992).

2.2. Sample preparation.

Sixty-eight Computerized Tomography's (CT) scans of the face from various extant and extinct primates have been processed using the 3D slicer ®v5.2.2(Fedorov et al., 2012a) an open-source software for visualization and analysis image computing datasets. The software was chosen for the acquisition of the data due to its ability to quickly collecting, the flexibility of the output, and their accessibility without cost.

The information collection involved CT-scans, where individual slices were combined to form a complete three-dimensional surface model using a segmentation process. The data obtaining was filtered and selected based on head scans, with no need to crop the focus area, which was the face.

The general procedure for segmentation to obtain the 3D model involved selecting the correct density of the bone material, extracted from the virtual volume using automatic density thresholding, with the mean density of each specimen variable between -399 to 6368 Hounsfield Units (HU) for extant primates and between 1587 and 19349 for the fossils.

According to their condition minor manual corrections were made to the automatic segmentation for a complete extraction of the bone information, because different densities present in various sections of a bone, as the details of some spongy or thinner bone were not necessary for this analysis. Working with the most superficial parts and due to the good quality of the CT scans, choosing the range of grayscale was simplified.

The crop tool was only used when the CT data present other elements beside bone material, such as metal used for positioning the craniums during the scanning, and this was solely for aesthetic purposes.

Subsequently, a *.stl* file (which maintains the same quality as the *.ply* format, but reduce the size) was generated and exported to create a complete 3D model of the cranium, removing the tissue and leaving only the bones. If necessary, parts like the mandible that might obstruct the location of landmarks such as the orale or infradental were cut. The other data of the specimens, provided as a 3D model already, were adjusted. Later, we positioned the landmarks using the same software.

All specimens were identically fixed in a standard plane so that osseous orbits were seen in planarity on the anterior aspect of the face and landmark, to best represent the facial skeletal shape. The rendered surfaces could be edited and re-landmarked with ease, thereby reducing user error. In the case of the 3D model previously made, we did not have the opportunity to explore the 2D slices to help in the location of the landmarks.

2.2.1. Landmarks configuration

The analytical approaches used in this study are from the field of geometric morphometrics (GM), used evaluating biological variation and the covariation of shape with other variables, based on the analysis of shape with Cartesian geometric coordinates or landmarks that are relative arrangement to one another to represent a shape (Pugh, 2020).

Landmarks as loci delimit our explanation of effects upon form. These points can be two-dimensional or three-dimensional and can be placed in the position of a particular feature, defined as loci both on a biologically or geometrically. They should be homologous or correspond well from one sample to another; and can be found repeatedly and reliably (Bookstein, 1991; Pugh, 2020; Von Cramon-Taubadel et al., 2007) .

For the analysis have been considered a series of three-dimensional coordinates, four landmarks from the midline and 28 pairs of lateral landmarks, establishing a total of 60 boundary points (Table7, Figure7), according to their typology, type I when the landmark represents a unique and easily identifiable entity, usually related to anatomical point, and types II and III as a position in space that is determined by other factors (Bookstein, 1991):

1) Type I: meeting points or intersections of features that represent a discrete juxtaposition.
2) Type II: points of maxima curvature that can be tips, bulges or dips of a feature.
3) Type III: extremal points or constructed landmarks of single coordinates, found on an outline or surface but not to a specific location, such as maximal diameters or curvature endpoints.

The choice of landmarks was based on a combination of methodologies followed by Pugh *et.al.* (2023), Neaux *et.al.* (2013) and Collard and O´Higgins (2001). This template is optimized to capture the maximum amount of morphological

information by recording data from every region of the face surface, representing the location of sutural junctions, maxima of curvature, and other anatomical features that give precise data on facial elongation, facial width, proportion and structure organization such as orbital or nasal aperture locations, as in other studies (Lieberman, et.al., 2007).

Occasional difficulties were met with the identification and localization of the landmarks, there were approximated as best as possible, with the aid of viewing the 3D models in a texture/color mesh or comparing against the slice in 2D, when there were available.

Identifying specific points is crucial for accurately locating landmarks. For instance, the medio-inferior orbital landmarks are placed at the lower edge of the lacrimal canal, as this structure influences the shape of this orbital region. This anatomical feature also assists in distinguishing species variations. Additionally, the lacrimal canal helps in identifying the dacryon landmark, located at the canal's superior border, which is particularly useful when the junction between the maxillary, lacrimal, and frontal bones is unclear.

In external groups, the dacryon cannot be directly identified. Instead, the reference point is taken where the maxilla ends at the orbital ring, which is formed by the jugal (or zygomatic) and frontal bones.

A special case involves the foramens, landmark are generally located at the center of the foramen. However, when the foramen is too large, such as the infraorbital foramen in some species, is placed at the most lateral edge. When a foramen is divided into two or three parts, the landmark is positioned at the center of the foramens. The incisive foramen landmark is located at the most posterior part.

Finally, due to the frequent occurrence of tooth loss, the alveoli are consistently used as reference points.

Table 7. Definition of the face landmarks used in 3D geometric morphometric analysis

Number	Landmark	Abbreviation	Type	Definition
1	Glabella	g	II	Most anterior midline point on the frontal bone
2	Nasion	n	I	Midline point where nasals bones and the frontal bone intersect
3	Rhinion	rhi	II	Midline point at the inferior free end of the internasal suture
4	Nasospinale	ns	II	Midline point on the inferior nasal aperture margin
5-6	R-L alare	Ral-Lal	II	Most lateral point on the margin of the anterior nasal aperture
7-8	R-L nasal aperture	Rna-Lna	III	Point of intersection between the maxilla and nasal bones in the nasal aperture
9-10	R-L Minimum Nasal Width	Rmn-Lmn	III	Point on the lateral edge of the nasal bone closest to the midline
11-12	R-L mid-supraorbitale	Rmso-Lmso	II	Point in the anterior-superior margin of the orbit, a line that cut vertically the orbit
13-14	R-L orbitale	Ror-Lor	II	Inferior-most point on the orbital margin
15-16	R-L ectoconchion	Rec-Lec	II	Lateral-most point on the orbital margin
17-18	R-L dacryon	Rd-Ld	I	Point where the maxillo-lacrimal suture meets the frontal bone
19-20	R-L orbitale latero-inferior	Roli-Loli	III	Point of greatest inflection of orbital margin between the lateral-most and inferior-most points on the orbit
21-22	R-L orbitale medio-superior	Roms-Loms	III	Point of greatest inflection of orbital margin between the medial-most and superior most points on the orbit
23-24	R-L orbitale medio-inferior	Romi-Lomi	III	Point of greatest inflection of orbital margin between the inferior-most and medial-most points on the orbit
25-26	R-L orbitale latero-superior	Rols-Lols	III	Point of greatest inflection of orbital margin between the lateral-most and superior-most points on the orbit
27-28	R-L brownridge	Rbr-Lbr	III	Most superior point of the brown ridge
29-30	R-L temporal line	Rtl-Ltl	III	Point of greatest inflection of temporal line in post-orbital region

31-32	R-L zygoorbitale	Rzo-Lzo	II	Point where the orbital rim intersects the zygomaticomaxillary suture
33-34	R-L zygomaxillare	Rzm-Lzm	II	Inferior-most point on the zygomaticomaxillary suture
35-36	R-L zygion	Rz-Lz	II	Point of maximum lateral extent of the lateral surface of the zygion arch
37-38	R-L jugale	Rj-Lj	II	Point in the depth of the notch between the temporal and frontal processes of the zygomatic
39-40	R-L maxilla inflection	Rm-Lm	III	Point of greatest inflection at root of zygomatic process of maxilla
41-42	R-L Infraorbital foramen	Ri-Li	I	Foramen of the maxillary bone, below the infraorbital rim
43-44	R-L Zygomaticofacil foramen	Rfz-Lfz	I	Foramen of the Zygomatic bone, below the infraorbital rim
45	Prosthion	pr	II	Midline most anterior point on the alveolar process of the maxilla
46-47	R-L canine fossa	Rcf-Lcf	III	Deepest point within canine fossa
48-49	R-L canine jugum	Rc-Lc	III	Most anterolaterally protruding point on canine jugum
50-51	R-L alveolar I2	Rai-Lai	III	Point on the buccal alveolar margin of I2 alveolus
52-53	R-L alveolar C	Rac-Lac	III	Point on the buccal alveolar margin of C alveolus
54-55	R-L alveolar P3	Rap-Lap	III	Point on the buccal alveolar margin of P3 alveolus
56-57	R-L ectomolare	Recm-Lecm	III	Point most lateral in the buccal alveolar margin in the center of M2
58-59	R-L maxillary tuberosity	Rmt-Lmt	II	Most posterior point of the maxillary alveolus
60	Orale	o	II	Midline point on the hard palate where a line at the level of the posterior margins of the central incisor alveoli crosses the midline
61	Incisive foramen	if	II	Most anterior and inferior midline point of incisive canal on the hard palate

Figure 7. Face landmarks used in the present study

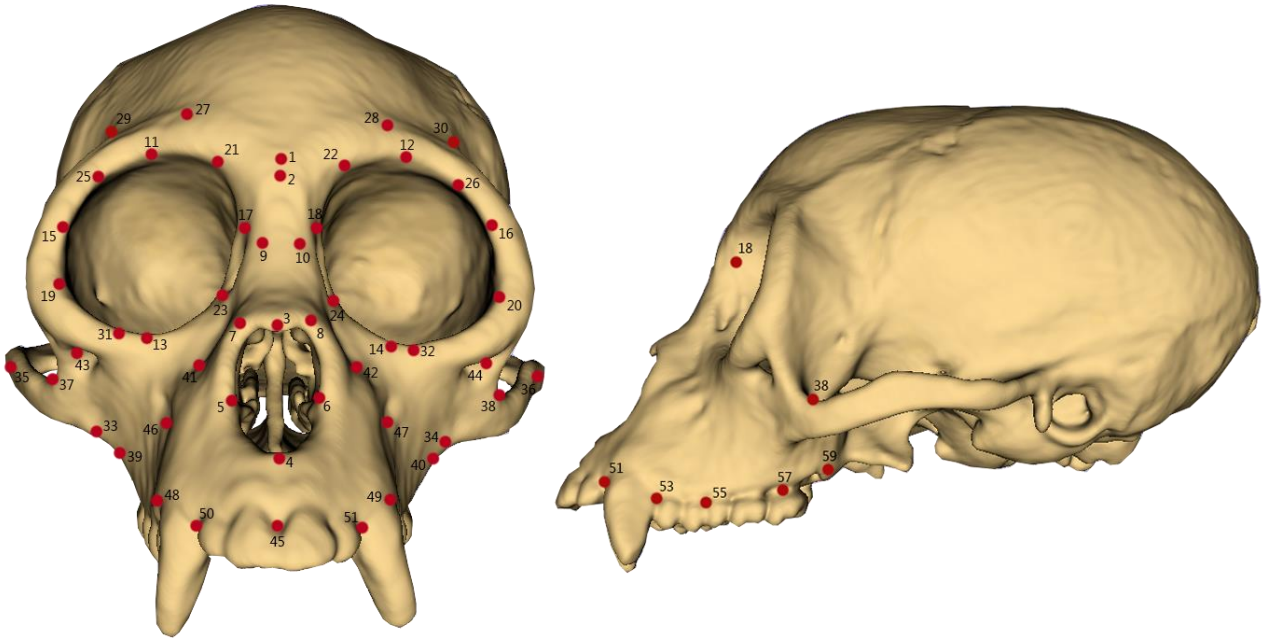

2.3. Geometric Morphometric analysis

The collected landmarks 3D coordinates were then processes with a series of analysis which has been performed using the extension of SlicerMorph package available in 3Dslicer ®v.5.6.2 (*3D Slicer Image Computing Platform* | *3D Slicer*, n.d.; Fedorov et al., 2012b), and Rstudio ®v.4.3.2 software (Posit team, 2024).

2.3.1. General Procrustes Analysis (GPA)

The Procrustes superimposition method used for this research is the Generalized Procrustes Analysis (GPA) that analyzes the shape, which refers to the geometric properties, independent of the position, scale and position of an object (Figure8), contrary to the form that contains information of shape and size. Converts landmark data into shape coordinates, addresses alignment issues by scaled each specimen to a unit Centroid Size, defined as the square root of the sum of squared distances from the landmarks to their average location (Bookstein, 1991; Gower, 1975; Mitteroecker & Gunz, 2009; Slice, 2007).

This scaling standardizes all landmark configurations into a common coordinate system, where differences in coordinates reflect shape differences. These variables can be used for multivariate testing to analyze covariance structure, group differences, and functional relationships.

Figure 8. Step of the Procrustes superimposition

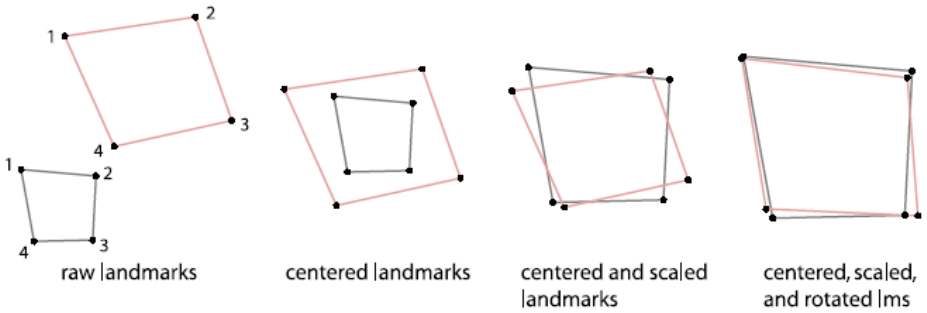

Source: Mitteroecker and Gunz, 2009

To obtain the Procrustes shape coordinates and determine the dissimilarities in shape between different landmark configurations, we calculate the Procrustes distance or Euclidean distance of the sets of Procrustes shape coordinates using partial Procrustes fitting.

The coordinates are standardized by subtracting the centroid from each landmark, translating them to the coordinate origin, and to remove absolute size differences, each coordinate is divided by the specimen's Centroid Size, scaling each specimen. For orientation, all specimens are rotated to align with the first specimen in the dataset. A mean shape is then computed by averaging the superimposed homologous coordinates, and each specimen's fit is optimized to this calculated mean shape (Mitteroecker & Gunz, 2009). Some parts of the face may show more variability compared to others, particularly those furthest from the centroid of the shape.

2.4. Statistical analysis

2.4.1. Principal Components Analysis (PCA)

The next step was exported some models of what the face shape looks like at different points in the PC space, rendered in 3D using Blender. The data of eigenvalues, Procrustes distance and mean centroid of each landmark and specimen, were statistically analyzed using an α-level of 0.05 as the threshold to indicate significance for all tests. Standard descriptive statistics were obtained, and Pearson's Chi-square tests were run on categorical variables.

In geometric morphometrics, shape variables all have the same units, allowing analyses to be based on the covariance matrix and utilizing a well-defined Procrustes metric. Multivariate methods that preserve this metric, such as principal component analysis (PCA), multivariate regression, and partial least squares, can be visualized as shapes or shape deformations in the original specimens' geometry.

The shape configuration differences are then evaluated using PCA, which shows the independent linear correlations of geometric features, reduces a large set of variables to a few dimensions that capture most of the data's variation. It is computed by performing an eigen decomposition of the sample covariance matrix and involves a rigid rotation of the data that maintains the Procrustes distances among specimens. The principal component scores are the projections of the shapes onto the low-dimensional space, like eigenvectors.

Initially, all the landmark files were loaded, and the data created was saved as a tab-delimited text file to fit the required format for Rstudio ®v.4.3.2, and with SliceMorph, we also obtained a mean shape and variance plot, which helps detect switched or mistaken landmarks, as a large variance might indicate an error.

We generated lollipop vectors indicating the direction in which each landmark is moving. Additionally, we obtained a PCA scatter plot and a 3D model visualization. For this, we loaded a reference model face that was close to the mean shape, allowing visualization of the different shapes across the principal components in the

morpho space. We also loaded the landmark set of this face, resulting in two models: one of the mean shapes and the second showing how the shape changes in the positive and negative directions of the principal components. These models were then exported.

Morphological differences between male and female adults were demonstrated through principal component analyses by assigning to each specimen the sex and reflect it in the plot.

Finally, to visualize how the face deforms along the three principal components, deformation vectors were used. This involves observing how the *landmarks* change from the mean shape toward the extremes of each principal component

2.4.2. Allometric regression

This method is used to assess to the influence of a single factor such as age or sex. This regression of shape on the logarithm of Centroid Size is the best measure if allometry, because is not sensitive to the number of dependent shape variables, so it shows the shape deformation.

An adjusted R-squared statistical analyze was realized to measure and represents the proportion of variance explained by a model, adjusting the number of predictors or independent variables to prevent overfitting. Contracting de allometric (CSize) against the PCscores. The closer is to 1, better this model explains the variance in the dependent variable.

2.5. Errors and validation

The configurations employed to localize landmarks can differ in identification precision, and this represent a problem in assessing the repeatability. To ensure that the results are reproducible, we need accurate means of identifying error due to observer differences; even the same observer will vary subtly. This variation should

be quantified and evaluated to assess its impact on the data being interpreted and improve the validity of the results (Von Cramon-Taubadel et al., 2007; Webster & Sheets, 2010).

In this investigation, evaluating the effect of discrepancy data between two observer is complicated due to the time, resources and availability. For that reason, we are not going to test it. However, the potential intra-observer variability comes with the definition and/or identification of the points, quality of measured material, and the environment. So, to reduce this error, a total of ten specimens were randomly selected as a representative part of the sample, and following the same procedure, landmarks were plotted on each, in three different trial sessions. Each session was performed every week (7 days), each time at the same period of the day, to try to emulate, as closely as possible, the working conditions.

The PCA analysis of the GPA coordinates for 10 individuals, each with 3 repetitions of landmark placements (Figure9), demonstrates consistent results across repetitions, with overlapping configurations for each individual but not between different ones. This consistency confirms the accuracy of the landmark digitization process and shows that the distribution of the sample is primarily driven by the morphological variation, ensuring the method's reliability in landmark placement and correcting any previous errors in the analysis.

We do not observe significant issues with intraspecific error; however, some minor deformation in the fossils has caused certain landmarks to be noticeably distorted. These landmarks capture these patterns of deformation, which can affect the overall analysis. Despite this, the accuracy of the landmark placement remains strong, and these distortions are primarily due to the preservation state of the fossils rather than errors in the digitization process.

Figure 9. PCA analysis of the repeated landmark configurations of the 10 individuals

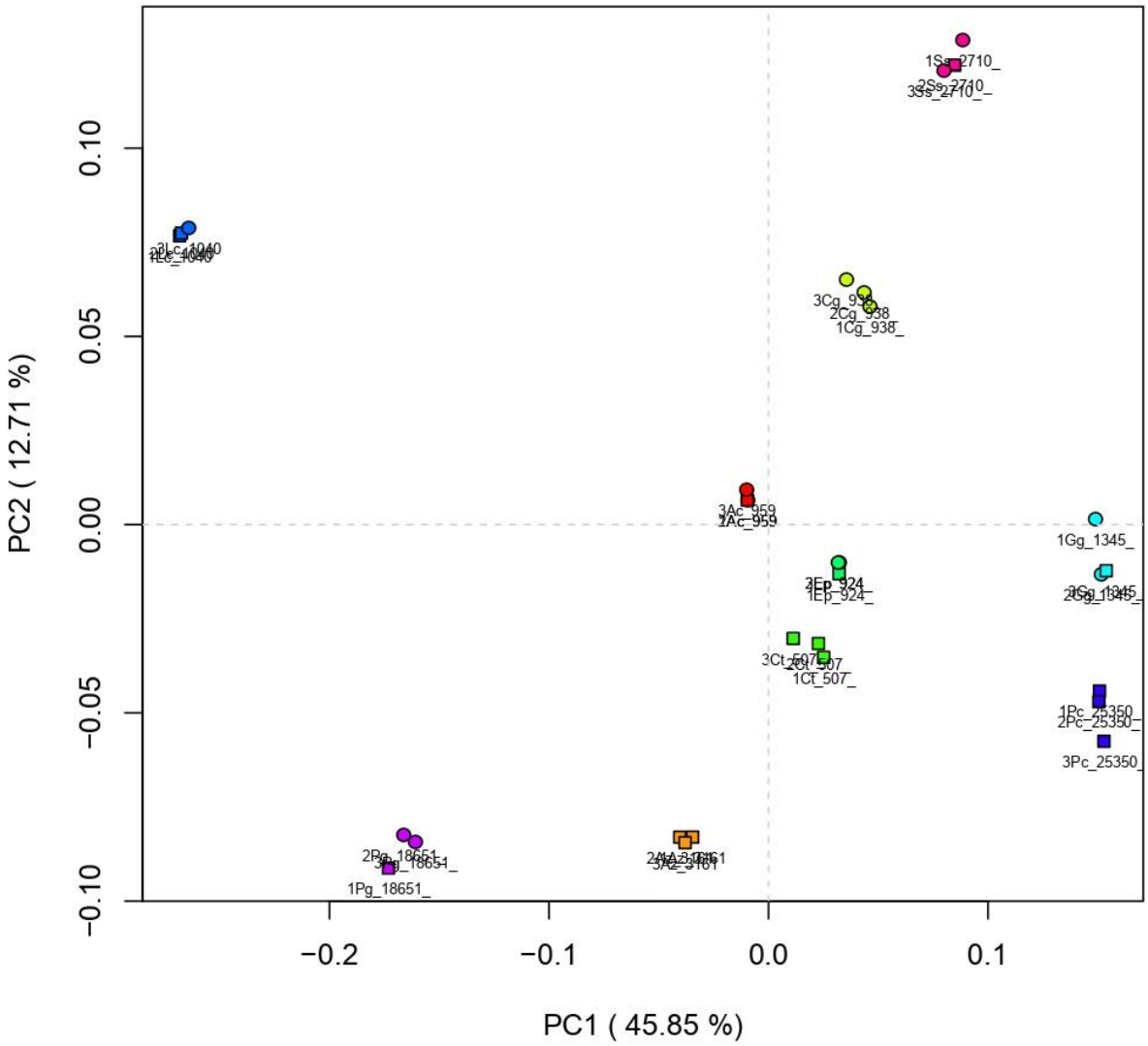

The preservation of the specimen played a lesser part, considering that the material is well-preserved and almost complete. Only †*Aegyptopithecus zeuxis* (2803) present some damage in the lateral right aspect of orbital ridge and the zygomatic, and we eliminate one specimen (5401), because is very fragmented and damage, so it requires a more complete reconstruction. In this case and of †*Parapithecus grangeri* (18651), †*Afropithecus turkanensis* (At_16999), †*Rhinocolobus turkanensis* (Rt_1885) and †*Theropithecus oswaldi* (To_60609) the

damage parts, orbit o zygomatic, were completed by mirroring the contrary part that is preserved in the software 3d blender.

In this case, the intact part was first divided, then mirrored, and finally joined with the cranium using the best-fit method. This approach helps to reconstruct missing structures and landmarks, thereby enhancing the accuracy of the analysis.

The only instance where we did not use the mirroring technique was with †*Turkanapithecus kalakolensis* (Tk_092403) due to damage in both orbits.

CHAPTER III: RESULT

This chapter presents the results of the analysis, beginning with a discussion of specific issues and unique characteristics that may have influenced the analytical framework. In Section 3.2, the results of the geometric morphometric analysis are discussed in general terms, focusing on the Generalized Procrustes Analysis (GPA).

At this stage, we examine the specific vectors of shape change, illustrating the features of variation in the facial shape, alongside the Principal Component Analysis (PCA) results, which are addressed in the following section.

Finally, the chapter concludes with the outcomes of the error test in section 3.4. In general, this chapter highlights the observed differences in the facial configurations of both extant and fossil primates, treating them separately.

3.1. Data collection and sample preparation

When working with two types of sources for the study, 3D models (in *.ply* and *.stl* formats) and 2D tomographic slices, and different repositories, each with distinct methodologies for image acquisition, as well as considering the deformation and damage in fossils, the risk of obtaining incorrect alignments increases. For this reason, in this section, we list the specific characteristics of each specimen that could potentially affect the results, in this way we avoid to eliminated them from the analysis.

Regarding extant primates, the Kyoto repository provides 2D images in *.TIFF* format, from which 3D models were constructed. A small part of this sample was obtained from the Smithsonian Institution, with 3D models were already reconstructed and could not be modified. Generally, this sample is in good condition, with the face complete and free from deformation. There are a few cases where specific features need to be mentioned, listed below:

1) *Cecocebus torquatus* (Ct_507): This is a juvenile male in which the third molars have not yet erupted, potentially affecting the actual position of the maxillary tuberosity and, as a juvenile, the overall facial configuration.

2) *Ateles geoffroyi* (Ag_551): The right third molar was erupting at the time of death.

3) *Alouatta seniculus* (As_963): The right orbit is deformed in the upper lateral part, with a notch giving a squared configuration to that area of the orbit.

For the fossils obtained from Morphosource, four were provided as 3D models and two (Az_3161 and Pg_18651) as 2D images. In an initial analysis, these last two showed an incorrect size difference due to an error in pixel spacing values, which was corrected.

1) *A. zeuxis* 85785: A juvenile individual with slight distortion (supero-inferior compression) in the right orbit and a poorly preserved nasal cavity edge.

2) *A. zeuxis* 2803: The left side of the right orbit and zygomatic arch were reconstructed by mirroring. In general, there is deformation that could affect the flatness of the 3D model.

3) *A. zeuxis* 8794: The zygomatic arch is incomplete, which could affect the analysis.

4) *P. grangeri* 18651: This specimen has compression deformation in the upper lateral corner of the orbit, as well as general lateral-medial compression in the left orbit. The missing left zygomatic arch was reconstructed by mirroring.

5) *P. catalaunicus*: The model used is a recent reconstruction due to the highly fragmented condition of the face.

Finally, for the fossils obtained from African Fossil we obtain 3D models. The left zygomatic arch of †*T. turkanensis* and the right zygomatic arch of †*R. turkanensis* were reconstructed by mirroring. In these cases, the orbital edge was also missing; however, since no landmarks were intended to be placed in this area, its reconstruction was omitted.

The right zygomatic arch of †*T. oswaldi* was also mirrored; however, this side suffers from deformation, slightly displacing the right edge of the face posteriorly,

which affected the reconstruction. Finally, in †*T. kalakolensis*, a small fragment of the orbital edge is missing in both orbits, and the right one shows slight deformation.

3.2. General Procrustes Analysis (GPA)

Through the GPA analysis, the average facial shape was obtained, allowing for the observation of deformation vectors that reflect the magnitude and direction of variation for each landmark relative to this mean. Additionally, the variation of each specimen along the main components of variation was analyzed, which will be discussed in the next section.

The Procrustes distance was also calculated to quantify the differences in facial shape between the landmark configurations of each individual. Shorter distances indicate greater similarity to the mean shape, while larger distances reflect more significant differences from this average (Table8).

The first four specimens closer to the mean shape are the male of *Macaca mulatta* (Mm_1160), the female of *Nasalis larvatus* (Nl_3734), the male of *Cercopithecus campbelli* (Cca_1073) and the male of *Alouatta seniculus* (As_963). The extreme distance between females and males of *M. mulatta* and *C. campbelli,* can be explained by an important sexual dimorphism.

In another hand, the farthest one from the mean shape are the male of *Mandrillus sphinx* (Ms_1021), the male of *Papio hamadryas* (Ph_402), the female of *A. seniculus* (As_965) and the female of *P. hamadryas* (Ph_424).

We first performed a GPA using only the extant primates including the outgroup (lemurs) and finally other analysis only with the fossils, to observe the differences and potential impacts on the resulting PCA, and how it affects the weight of each Principal Component. We visualized the variance of each landmark on a spherical graph using the sphere variance plot in 3D Slicer (Figure10), this helped identify errors in landmark placement. For the extant primates the most variables points were the zygomatic arch, maxillary flexion, infraorbital foramen, and maxillary tuberosity.

Table 8. Procrustes distance to the mean shape of the face

Sample_name	Proc.dist.	centroid
Mm_1160	0.116	179.514
Nl_3734	0.120	161.828
Cca_1073	0.121	143.224
As_963	0.127	176.409
Tgr_2366	0.128	141.407
Ll_349	0.130	154.362
Pb_946	0.132	163.439
Ag_551	0.136	152.789
Ll_542	0.137	149.562
Tk_16950	0.140	203.594
Nl_1422	0.142	201.249
Mf_1455	0.144	154.413
Mf_1157	0.144	185.755
Ep_967	0.145	169.250
Mfu_1184	0.149	190.066
Ac_961	0.149	175.784
Cg_938	0.150	182.423
Tgr_3077	0.150	148.582
Gg_2525	0.151	343.503
Mo_8519	0.151	106.839
Ca_957	0.152	148.697
Ag_540	0.154	152.493
Ct_735	0.154	166.382
Ct_507	0.155	175.540
Ca_1067	0.156	134.532
Gg_1345	0.157	387.881
Cc_302627	0.157	132.344
Cg_939	0.162	157.455
Hh_8342	0.162	158.347
Hh_1126	0.167	169.596
Az_2803	0.170	147.789
Az_3161	0.176	125.070
Nc_5422	0.176	170.941
Hl_7755	0.178	157.121
Mfu_1182	0.179	208.995
Az_8794	0.182	3661.968
Mo_8534	0.182	102.152
Ss_2710	0.184	168.474
Pc_25350	0.184	267.137
Cc_302626	0.186	137.091
Hl_7752	0.191	159.332
Ss_1719	0.198	176.155

Pm_1055	0.201	152.609
Pt_12	0.201	292.524
Pm_1057	0.202	145.490
Pt_515	0.202	305.180
Pa_1343	0.206	273.629
At_16999	0.209	295.869
Nc_4649	0.214	160.680
Az_8578	0.217	106.051
To_60609	0.228	194.838
Pb_941	0.231	158.111
Rt_1485	0.233	229.048
Cca_1070	0.247	124.836
Tg_1028	0.271	228.530
Ms_070	0.283	216.344
Ac_959	0.287	155.197
Pg_18651	0.288	100.332
Pa_796s	0.292	337.770
Tg_447	0.334	264.184
Ep_924	0.354	197.019
Mm_1463	0.366	188.361
Ph_424	0.374	245.823
As_965	0.377	148.416
Ph_402	0.383	290.241
Ms_1021	0.437	391.865

Figure 10. Landmark Variance Plot sphere type. Right side represent the landmarks variance in the sample of extant primates and the left side represent the ones in the fossil sample, the larger the spheres, the greater variability is represented, this is also reflected with the change in color.

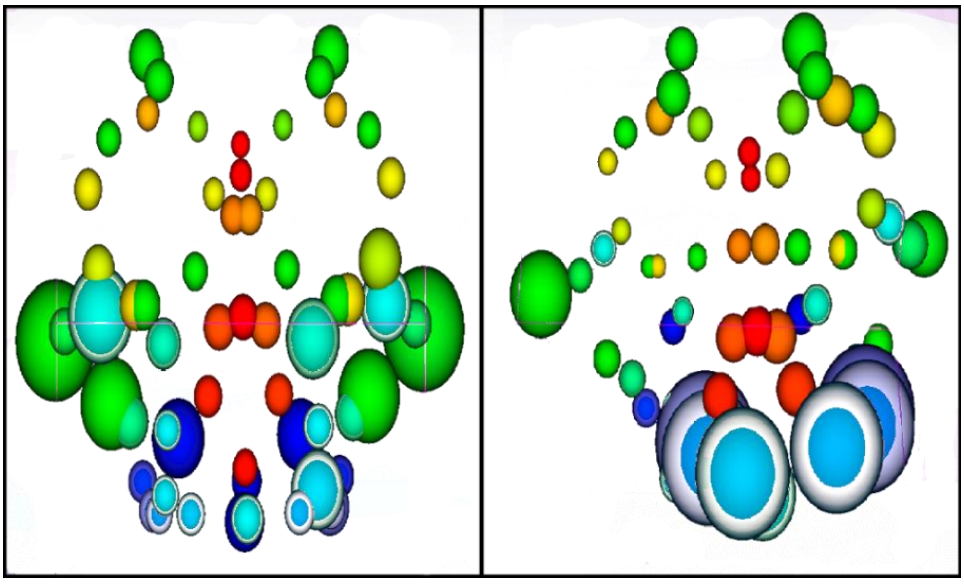

the same analysis was conducted solely on the fossils, the zygion remained a variable region, but landmarks placed on the alveolar part of the dentition and the lower part of the nasal fossa also showed high variability. These variations correspond to slight deformations in some fossils (primarily in the zygomatic bone) and missing areas, mainly from the frontal part of the snout, affecting the nasal fossa. Based on this information, a new analysis was planned, excluding the following landmarks from the entire sample: the pairs of zygomaxillare, zygion, jugale, canine jugum and alveolar I2, and the singles Incisive foramen, orale and prosthion. The new configuration is composed of 48 landmarks, with a mean shape (Figure11).

Figure 11. Mean shape of the set of 48 landmarks

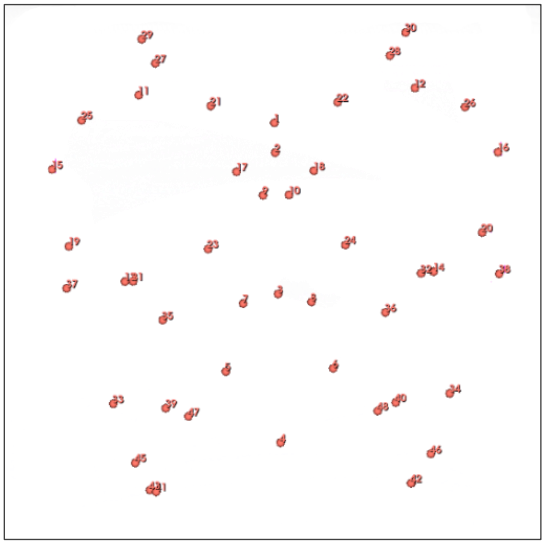

3.3. Principal Component Analysis (PCA)

The PCA analysis was performed on Procrustes residuals from all the 66 individuals of the sample, that in the graphs were labeled according to the division by sex and color-coded based on their species affiliation. The analysis utilized a combined configuration of landmarks from the face and the results provide insights into the morphological variability among the groups and identify the variables contributing most significantly to the observed differences. The relationships between the three first components and their allometric relationships were discussed.

The first Principal Component Analysis (PCA) was conducted exclusively with the sample of extant primates, revealing that the percentage of variation is primarily concentrated in the first three components: PC1-26.99%, PC2-14.79%, and PC3-11.21%, explaining a total of 52.99% of the variation.

A homogeneous dispersion is observed from the negative to the positive values along the first principal component that capture the maximum variance in the data. In the negative extreme, we find the colobine *Presbytis melalophos*, and in the positive extreme, the male *Mandrillus sphinx*. Within the negative values of this component, there is a strong clustering, which includes the subfamily Colobinae as well as the four genera of the family Hylobatidae. On the positive side, the dispersion is broader but generally groups the subfamily Cercopithecinae, apart from the species *Miopithecus ogouensis*, which is positioned in the negative values of PC1 but in the positive extreme of PC2.

Analyzing facial morphology, negative values of PC1 indicate a shorter and wider face, with a retracted maxilla but retaining slight prognathism in the alveolar area. The orbits maintain their height but wider, resulting in generally larger orbits. Positive values of this PC correspond to a more elongated face, with balanced proportions between the orbital region and the maxilla. The nasal fossa is long and narrow, and there is a prognathism that increase gradually, and is not focus on the alveolar part (Figure12).

Variation in PC2 relates to the lateral projection of the zygomatic bones. Negative values show compression, reducing the maxillary flexion (Rm and Lm) and giving the orbits a more vertical position. In contrast, positive values indicate greater lateral-posterior projection of the zygomatic bones (Figure13).

As for the Hominidae family, it is placed in the positive values, forming a cluster near the intermediate values. In contrast, the Platyrrhine have a similar distribution but in negative values.

Figure 12. 3D model of the facial morphological changes on positive and negatives values on PC1

PC1	Min.	Max.
Frontal	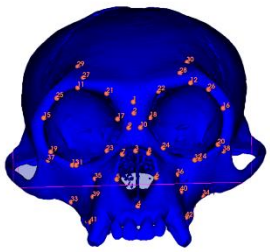	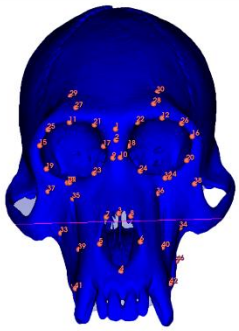
Lateral		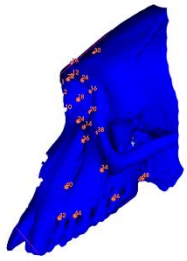

Figure 13. 3D model of the facial morphological changes on positive and negatives values on PC2

PC2	Min.	Max.
Frontal	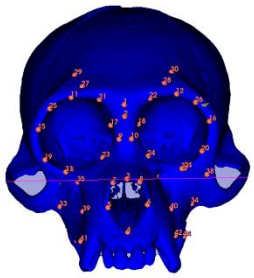	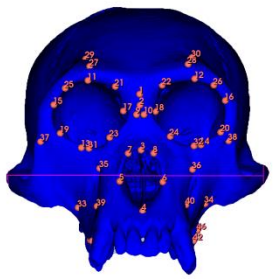
Lateral	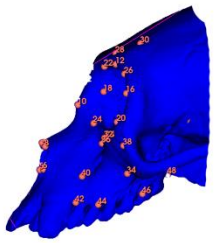	

Regarding the second component, a generally linear grouping is observed, with the exception of five individuals: the two previously mentioned *M. ogouensis* found in the positive extreme, along with the male *Ateles geoffroyi*, while in the negative extreme are the males of *Alouatta caraya* and *A. seniculus*. To this group, we could add a female *Macaca mulatta*, although it does not deviate much from the main group.

In general, the Platyrrhines are placed in positive values on PC1 and PC2, displaying a face with a wider mid-region, short and broad nasal bones, but with a greater distance between the premaxilla and orbits, a canine fossa closer to the alveolar plane, and more robust supraorbital arches (Figure14).

These species that deviated from the mean were reevaluated to check for any issues with the placement of the landmarks. After confirming that this was not the case, it was decided to remove these specimens from further analyses. With this new adjustment, the two *Alouatta* females moved further from the mean, leading to the decision to remove this species entirely. Although they are not analyzed further, we believe their position outside the mean is important and may be due to a morphology very different from the other primates or the sexual dimorphism of these species, a topic revisited in the discussion. Even though we excluded these individuals, we graphically present the sex differences in the case of the atelids (Figure15) and the differences among the other macaque species in the case of Mm_1463 (Appendix1).

Figure 14. Plot of the PC1 and PC2 of all extant primates with the set of 61 landmarks, showing the change of the facial shape along the axis

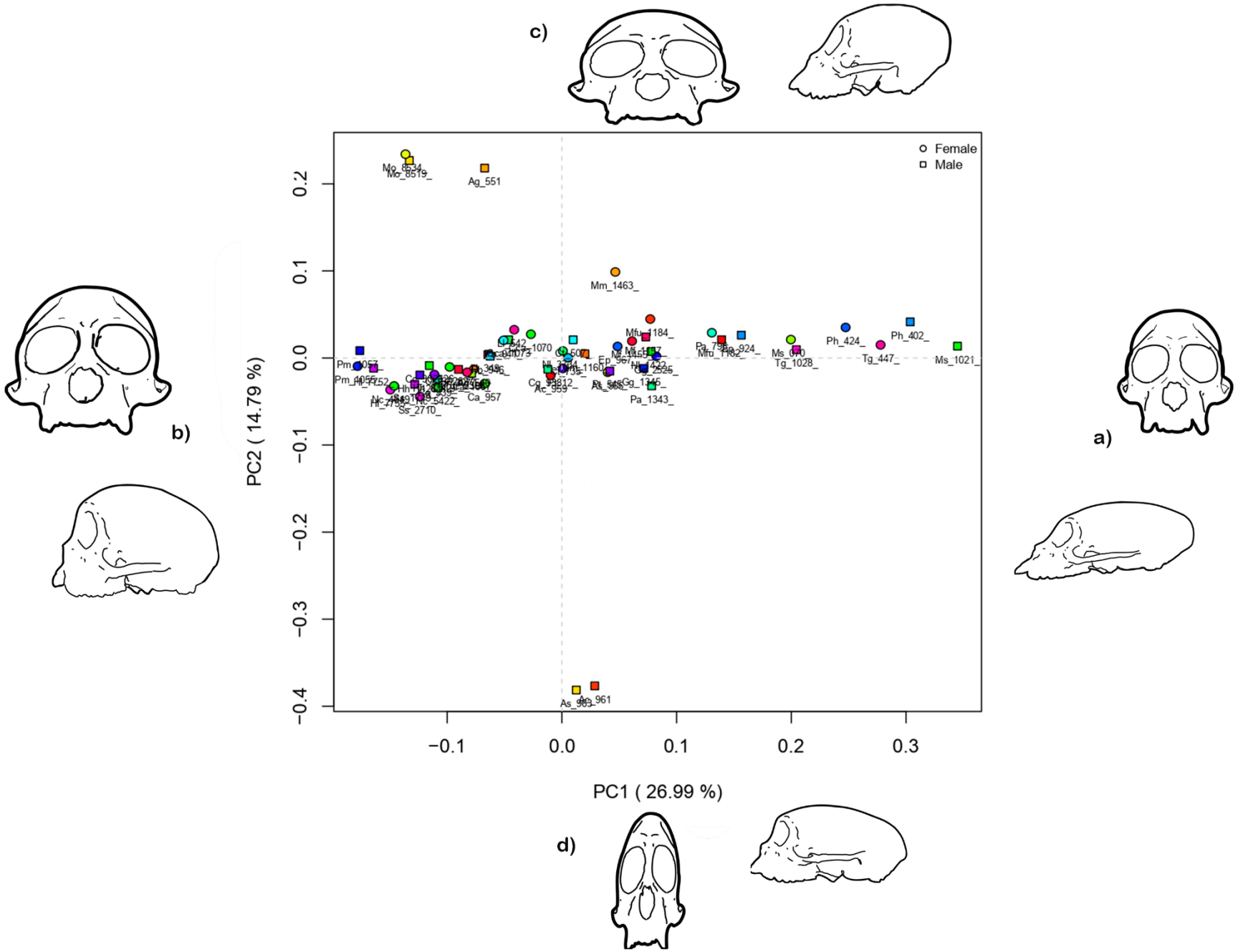

The remaining seven analyzed species of this parvorder are more clearly separated from the hylobatids when the number of landmarks is reduced (48), and this also reduces the previously observed deviation in howler and spider monkeys, except for the female *Alouatta seniculus*, which remains at the extreme positive end of PC2. These species exhibit the most variability among platyrrhines, while the three remaining species—*Cebus apella*, *Cacajao calvus*, and *Lagothrix lagotricha*—show greater homogeneity. Of these specimens, *C. apella* demonstrates sexual dimorphism, with males and females separating more distinctly than in the other two species. *L. lagotricha* is the species that comes closest to the boundary between the positive and negative values of PC2.

The outliers are grouped in the positive extreme of PC3, while the remaining individuals are generally placed in negative values, apart from *Ag_540*, *Cc_302627*, *Mf_1157*, *Mfu_1182*, *Ms_070*, *Ph_402*, and *Ms_1021*. Negative values of PC3 correspond to a latero-inferior projection of maxillary flexion, while positive values indicate a more medial and superior retraction (Appendix2)

The final analysis of this sample involved comparing PC1 and PC2 with the logarithm of Centroid Size (logCsize). Taking the logarithm helps normalize the data, which is particularly useful in cases like this, where the sizes of primates vary greatly. This comparison reveals how the primary and secondary variations (PC1 and PC2) correlate with changes in size. The results show that smaller individuals tend to cluster together along the PC1 axis, as do larger ones, but in this case, the difference between sexes is more noticeable. Specifically, apes tend to cluster near the middle, indicating the importance of their size. The greatest distance observed was between the male and female *Mandrillus sphinx*, highlighting significant sexual dimorphism in this species.

The remaining colobines are grouped with the remaining Old-World monkeys in relatively homogeneous cluster. As mentioned earlier, in the first principal component (PC1), they are found near zero on the negative side, positioned between the two families of Hominoids. They show greater differentiation in PC2,

falling within positive values, which generally places them at the same level as other cercopithecoids.

Figure 15. Facial difference between male and females of some atelids

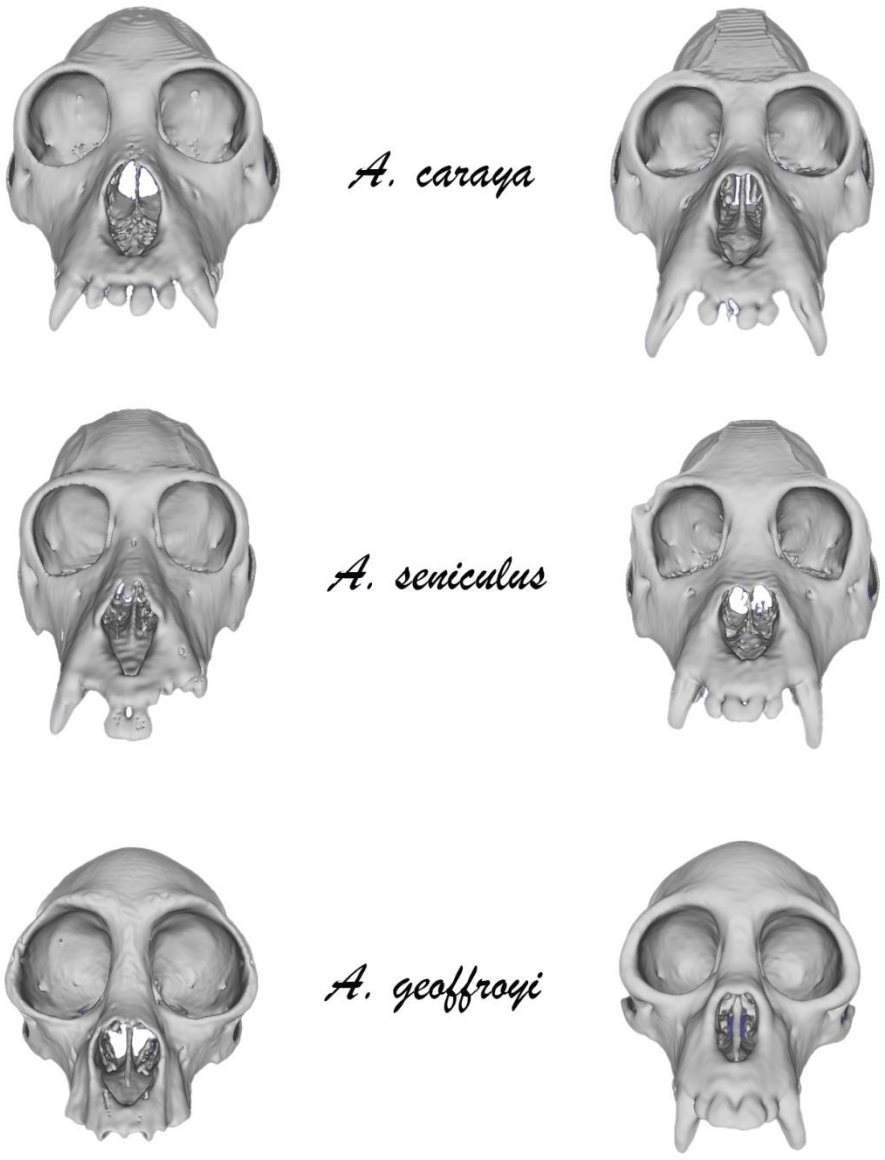

On the left side were the females of each species, with the males on the right. We can see with the naked eye that there is a significant difference in the shape of the orbits and the width of the maxilla. In the spider monkey, the larger orbits and nasal fossa are more evident in the female.

To calculate this, an adjusted R-squared plot was analyzed. In this case when we contrast de allometric with PC1, the adjusted R-squared is of 0.2121 (Appendix3) and 0.196, in the analysis with all the landmarks and in the second set of 48 landmark, respectively.

This graph shows a deviation of Az_8794, an after checking we can correct one error of the size of the document, we delated this specimen, obtaining a new adjusted R-squared of 0.43 (Figure16). Which means that about 43% of the variance in PC1 can be explained by the size of each specie. Therefore, the plot below shows a weak allometric relation between the size and PCscore.

Subsequently, when adding the external group of *Lemur catta*, the same type of distribution was observed, with a minimal change in the variance of each component: PC1-25.23%, PC2-14.02%, and PC3-11.07%. However, the outlier individuals positioned themselves in the opposite extremes, meaning those previously on the positive side of PC2 shifted to negative values. Similarly, the lemurs slightly separated from the main group towards the positive values.

This first analysis was conducted to verify if the data followed a normal distribution. After identifying some individuals that were outliers, two additional analyses were carried out. In one analysis, the fossil sample was added without any changes, and in the other analysis, the individuals with significant deviations were removed. Both analyses were performed because the deviations observed could be due to important factors or simply to errors in the CT-scan formats analyzed. To avoid losing information, we conducted both analyses to determine if there were any significant differences.

Figure 16. Regression line showing allometric effect

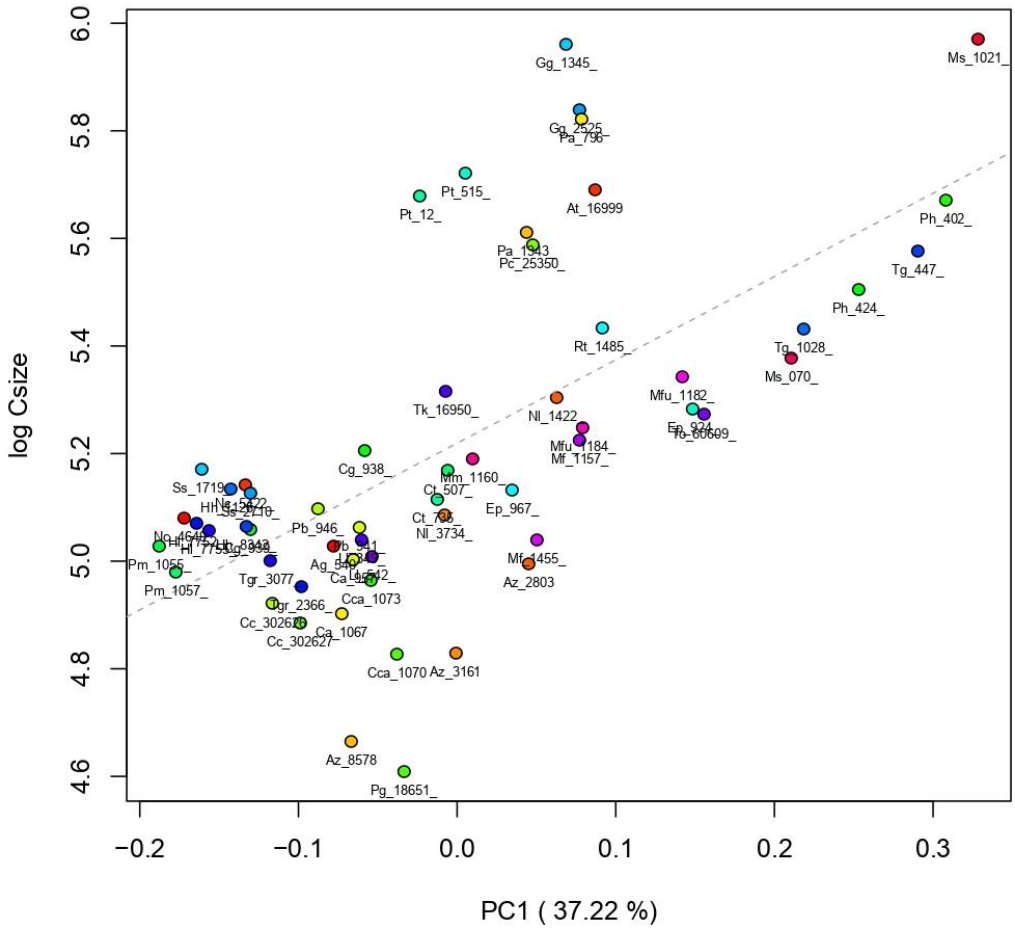

When incorporating the fossils, it was observed that the modern individuals maintained the same grouping, though with a slight decrease in the variance explained by each component, with the first three components accumulating 44.36% with 22.35%, 12.03% and 9.98% respectively. †*Aegyptopithecus* are distributed around the central region in three of the four quadrants. Az_2803 a male with the face in excellent preservation condition, is the only individual placed in positive PC1 values; while Az_8578 (female) and Az_8794 (male) have negative values in components 1 and 2. Lastly, Az_3161, belonging to a probable juvenile male, is also positioned in negative PC1 values, but unlike the others, it has positive values in PC2 (Figure17).

Figure 17. Plot of PC1 and PC2 of all primate the sample removing the outliers

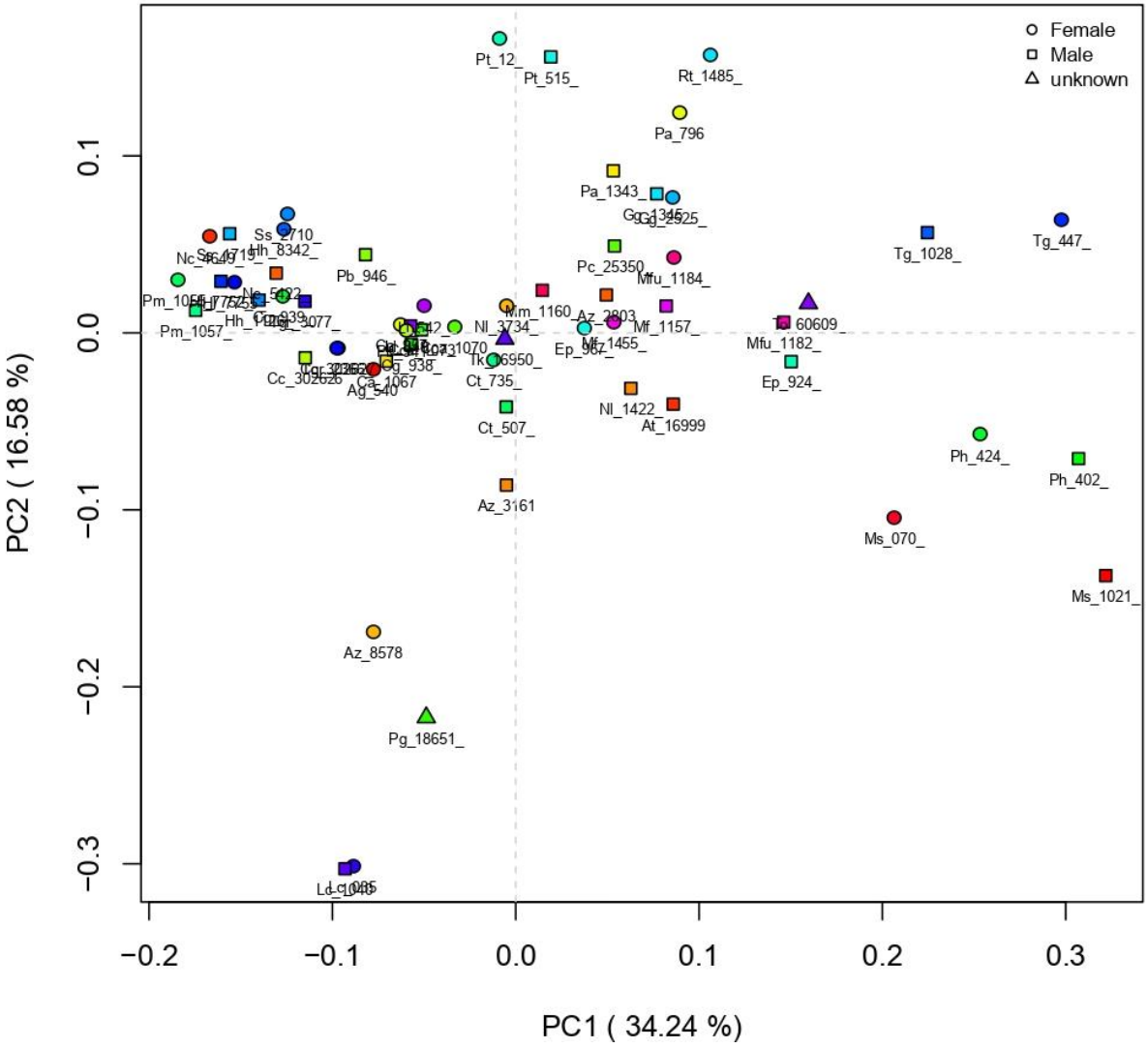

Despite this variation, they consistently show a pattern of being the species closest to the central point on PC1 and having the most positive values on PC2. Alongside this group is also the fossil of †*P. grangeri*, whose position as a stem catarrhine aligns with that of the other individuals.

The other Oligocene primate, †*Parapithecus grangeri*, is close to †*Aegyptopithecus* specimen (Az_3161). As for the three Miocene primates, †*Afropithecus turkanensis* groups with the Cercopithecines near the great apes, while †*Pierolapithecus catalaunicus* approaches the hominoid group with slightly more negative values in PC2. Finally, †*Turkanapithecus kalakolensis* is the only one with negative PC1 values and groups with species from various families: *Cercopithecus campbelli, Lagothrix lagotricha*, and *Piliocolobus badius*.

Concerning the Plio-Pleistocene primates, †*Rhinocolobus turkanensis* behaves like †*Afropithecus turkanensis*, grouping among cercopithecoids and hominoids. However, †*Theropithecus oswaldi* does not show the expected results as it distances itself from *T. gelada* and groups with Oligocene fossils and some members of the platyrrhines. PC3 provides greater separation between great apes and cercopithecoids.

When comparing the results with body size, significant variation is observed in the previously mentioned outliers, as well as in the female of †*A. zeuxis,* (Az_8578) which is positioned at the extreme. Additionally, the importance of size is noted in chimpanzees, gorillas, orangutans, and the Miocene and Plio-Pleistocene primate fossils. Nevertheless, while the first seem to be due to an error in the file, the Miocene and Plio-Pleistocene fossil could be due to a size pattern.

To better visualize the effect of size on the fossils, the sample was analyzed by excluding all other primates. Unlike the previous analysis, in PC1, the female †*A. zeuxis* aligns with the group, while specimen Az_8794 shows a strong size effect, separating from the main group and positioning at the upper extreme. This pattern persists in PC2 and PC3 (Figure18 and Figure19).

Removing outlier individuals from the analysis resulted in greater homogeneity, with lemurs positioned at the positive end of PC2 and the †*A. zeuxis* fossil, †*P. grangeri*, and the female *A. seniculus* placed between these and the rest of the primates in the sample. In PC1, a homogeneous distribution is maintained. The same overall configuration is observed when the full sample is analyzed, but with increased weight for each component: 27.44% for the first, 12.31% for the second, and 8.45% for the third.

Using the new configuration of 48 landmarks, the data distribution remains similar to the previous ones, highlighting lemurs as an outgroup, positioned in the negative values of PC1 and positive values of PC2. Due to their role as an outgroup, they were removed to better visualize the grouping of the other primates. In this way, cercopithecoids and great apes are again grouped, along with the fossils of †*T. oswaldi*, in the positive values of PC1, while colobines,

hylobatids, and platyrrhines are in the negative values of PC1, grouped near the mean and in the positive values of PC2.

Figure 18. Plot of PC2 and PC3 of all the primate sample removing outliers

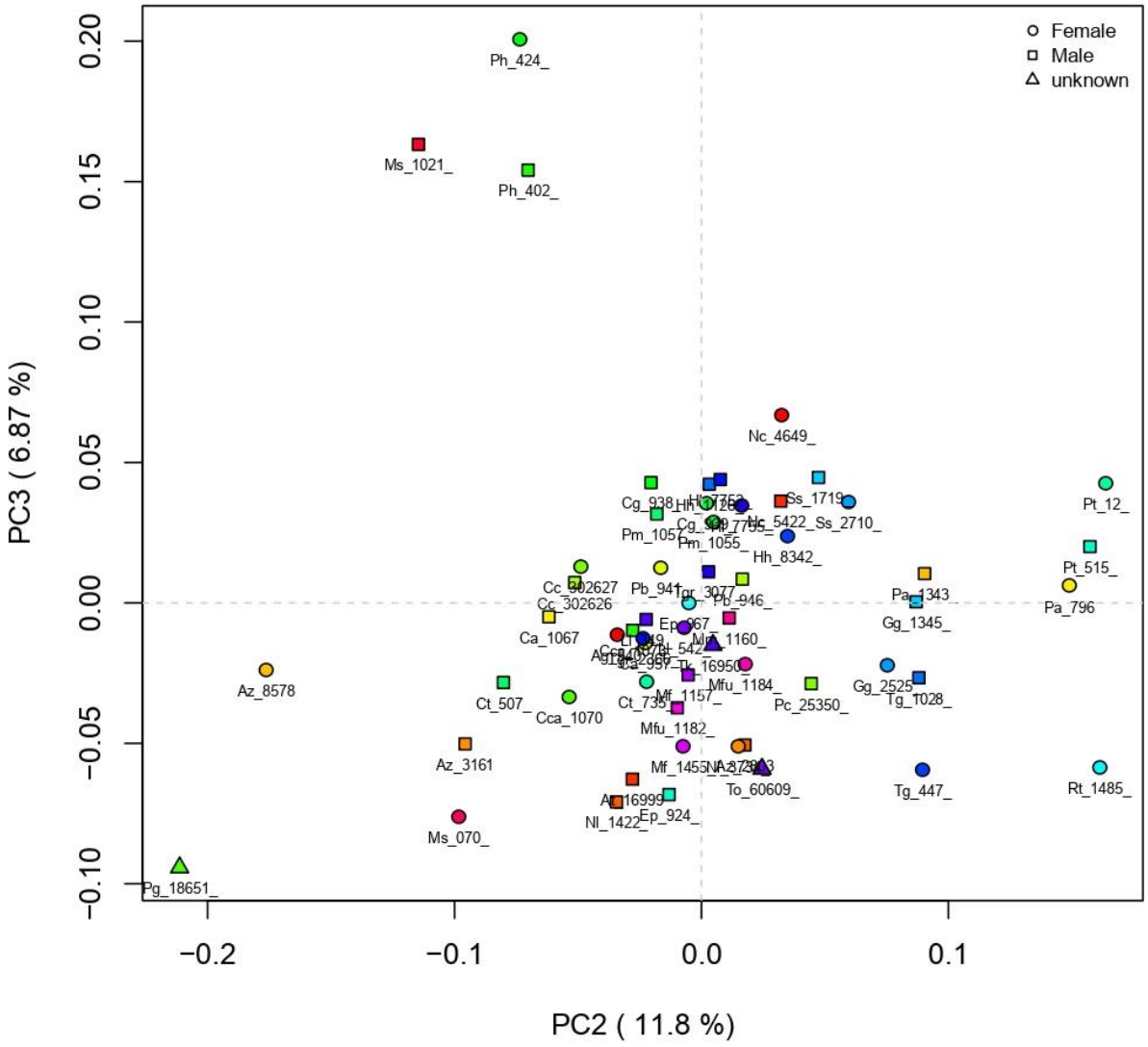

Colobines and hylobatids are found more toward the negative extreme of PC1 and at the beginning of the negative values of PC2. The great apes are situated in negative values for both PC1 and PC2, with the latter representing the extreme values that differentiate them from the cercopithecoids. It is noteworthy that †*R. turkanensis* (female) is close to the female *Pongo abelii*, while †*P. catalaunicus* is positioned near the midpoint between cercopithecoids and gorillas.

Figure 19. 3D model of the facial morphological changes on positive and negatives values on PC3

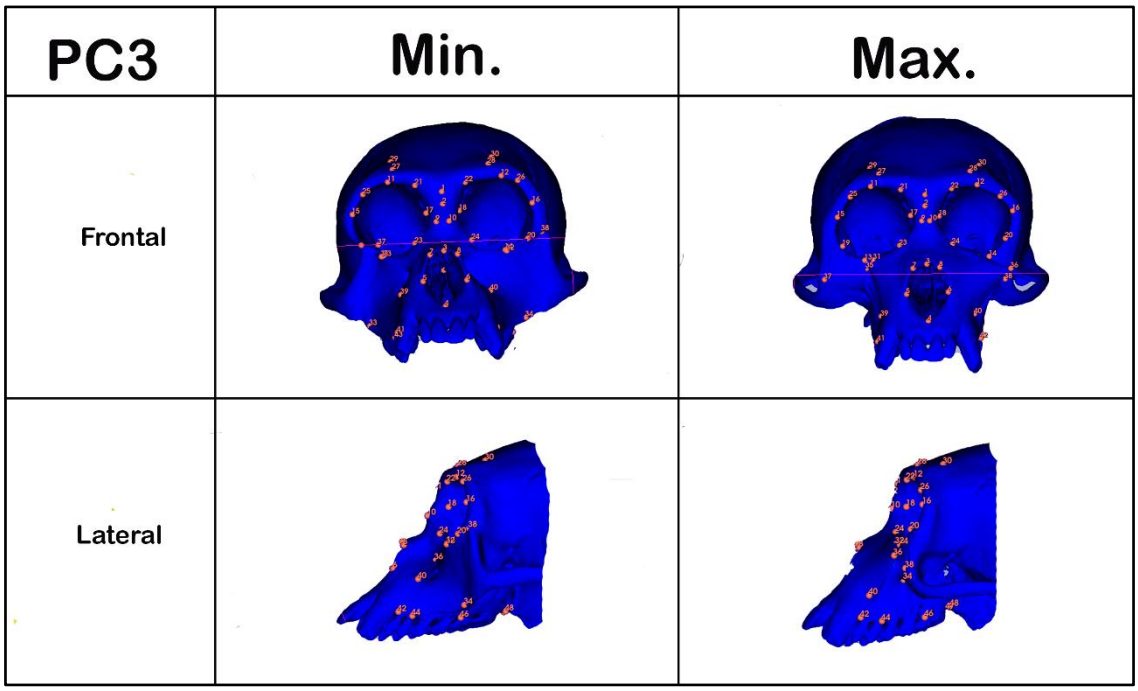

Regarding the Oligocene fossils, they seem to cluster in intermediate values of PC1, like chimpanzees, though they separate in PC2, representing the positive extremes. It is important to highlight that the distribution of the four †*A. zeuxis* individuals is quite varied: Az_8794 and Az_3161 approach a male *Cercocebus torquatus*, while Az_2803 is the only individual located on the negative axis of PC2, close to female patas monkeys and macaques. The female is close to †*P. grangeri* and the female *A. seniculus* at the extreme of the positive values of PC2. Meanwhile, PC3 separates *Papio hamadryas*, the male *Mandrillus sphinx*, and the female *Macaca mulatta* at the positive extreme. With this reduction of landmarks, the total variance explained by the first three components is 32.28%, 11.03%, and 8.13%, respectively.

The negative values of PC1 indicate an increase in the orbits, mainly in their width, causing the temporal lines to flex downward, approaching the orbits. The nasal bones shorten, with the rhinion closer to the nasion, shortening the length of the nasal fossa while maintaining its width. Similarly, the canine fossa is closer to the infraorbital foramen, resulting in a shortening of the zygomaticomaxillary area and a reduction in maxillary prognathism.

Figure 20. Plot of PC1 and PC2 of all the primate sample with the set of 48 landmarks

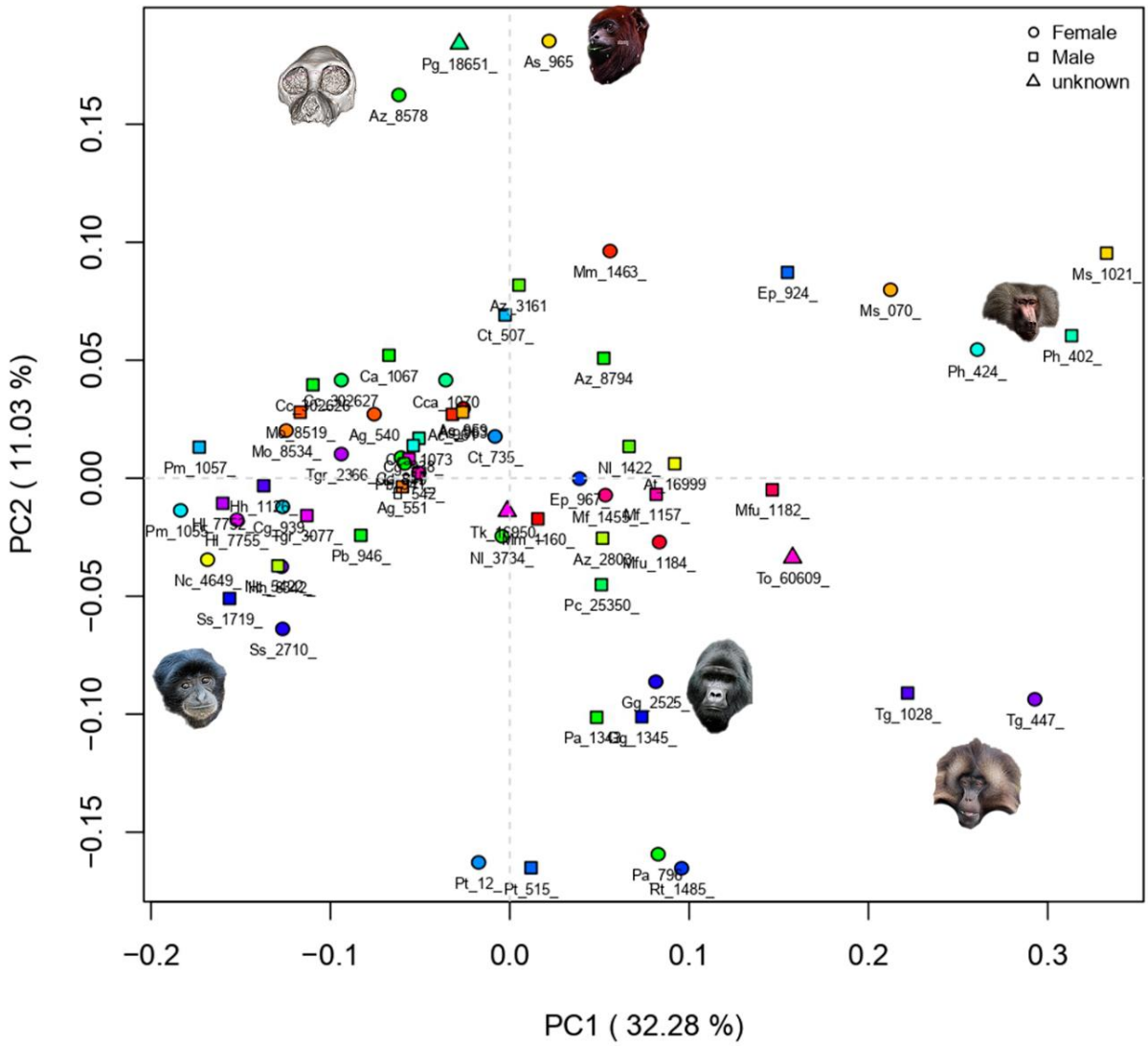

On the other hand, the positive values of PC1 show greater prognathism, a more elongated face, with reduced orbits and elongated nasal bones and nasal fossa. The temporal lines are closer together. Regarding the values of PC2, the negative values indicate greater prognathism in the nasal area, projecting the rhinion forward, while the maxillary tuberosity moves posterior-superiorly, also causing the orbits to project forward in the medial part and to recede in the lateral part. The positive values of PC2 show the opposite pattern.

In the case of PC3, the positive values reveal changes in the facial foramina and the flexion of the maxilla. The infraorbital foramen is positioned more laterally, widening the upper part of the maxilla, while the zygomaticofacial

foramen descends, moving away from the orbits, and the maxillary flexion constricts more medially.

3.4. Error and validation

The preservation of the specimen played a lesser part, considering that the material is well-preserved and almost complete. Only one fossil of †*A. zeuxis* (2803) present some damage in the lateral right aspect of orbital ridge and the zygomatic, and we eliminate one specimen (5401), because is very fragmented and damage, so it requires a more complete reconstruction.

In this case and of †*P. granger* (18651) †*A. turkanensis* (KNMWK16999), †*R. turkanensis* (1885) and †*T. oswaldi* (60609) the damage parts, orbit o zygomatic, were completed by mirroring the contrary part that is preserved in the software 3d blender.

The intact part was first divided, then mirrored, and finally joined with the cranium using the best-fit method. This approach helps to reconstruct missing structures and landmarks, thereby enhancing the accuracy of the analysis.

The only instance where we did not use the mirroring technique was with †*T. kalakolensis* (092403) due to damage in both orbits.

CHAPTER IV: DISCUSSION

In this section, we discuss the findings of our research, which aimed to describe and analyze the facial morphology of primates to address each of our objectives. First, we present the general morphology of each species analyzed, comparing them with the fossil samples to shed light on key aspects of primate evolution, the split in some individuals by their sex.

After establishing a baseline for primate facial morphology, we focus on the phylogenetic position of fossil primates from the Oligocene and Miocene, particularly †*Aegyptopithecus zeuxis*. Offering a new insight into the evolutionary history and morphological diversity of early catarrhines and the variation within this group, to understand its role in the evolutionary divergence of Hominoidea and Cercopithecoidea.

The following discussion is divided by families because the results generally showed a grouping of individuals according to the family to which they belong.

4.1. Facial Morphology of extant and fossil primates

In terms of distance from the mean shape, the individuals closest to it are three cercopithecoids (one belonging to Cercopithecinae and two to Colobinae) and one platyrrhine (Alouattidae). This proximity may reflect the plesiomorphies shared by these groups before the divergence between platyrrhines and haplorrhines (Arenson et al., 2022).

To understand this further, the ecology of these primates should be studied in more depth, as they exhibit sexual dimorphism and generally live in social groups composed of one male and multiple females. Except for macaques, these are arboreal species. Notably, the species that deviate the most from this mean shape are those that are more terrestrial and have a more omnivorous diet. The influence of locomotion and diet on facial morphological changes should be investigated further to better understand their roles.

4.1.1. Platyrrines: New Wold Monkeys

Platyrrhines retain several primitive characteristics that have been lost or modified in Old World catarrhines (three premolars, tympanic ring fused to the wall of the auditory bulla without forming a tube). It is important to consider one of their unique features in the pterion region, where the parietal and zygomatic bones meet, separating the frontal bone from the sphenoid. There is a possible relation of the grouping and their locomotion (J. G. Fleagle, 2013; J. Fleagle & Kay, 1994). On the negative side of PC1, it seems that arboreal primates are grouped together (New World monkeys, siamangs and gibbons), and in PC2 a distinction of quadrupedal arboreal primates with suspension (Platyrrhines, positive values) and brachiators (Hylobatids, negative values).

By analyzing species from the three distinct clades, pitheciids, atelids, and cebids (Figure21), we can explain the morphological heterogeneity of this infraorder through the heterogeneity of their ecological behaviors. The sample in this study includes the largest species from each clade: the uakaris (*Cacajao*) are the largest pitheciids, spider monkeys are the largest atelids (with this clade being the largest overall), and the capuchin monkey is relatively robust among cebids. Their diets range from specialization in hard-shelled fruits (*Cacajao*), to folivore (*Alouatta*), pulp (*Lagothrix*), and omnivore (*Cebus*) (Gingerich, 1977; M. F. Tejedor & Bosco, 2016; M. Tejedor & Novo, 2016).

Capuchins, medium-sized sexually dimorphic primates, show morphological differences, with each sex at opposite ends of the group. Their “slow” life history, long lactation periods, long interbirth intervals, and a long lifespan (J. G. Fleagle, 2013), should also be analyzed, as this development can impact facial morphology.

C. apella and *L. lagotricha* are closely related to colobines: *Colobus guereza* and *Piliocolobus badius*. This is intriguing because Cebus has been suggested to retain primitive platyrrhine and anthropoid morphology (Campbell et al., 2021; J. G. Fleagle, 2013; J. Fleagle & Kay, 1994), which is confirmed by encompassing the entire facial variability of the group (being at the extremes). According to our study, these primitive characteristics suggest a short face, broad

in the midsection, with large orbits, wide and rounded nasal apertures, greater interorbital space, shortened maxilla, and more projected zygomatic bones.

We can also confirm that pitheciids are the sister taxon to atelids and cebids, with their most negative position on PC2. Among atelids, Alouatta is the sister taxon to the other genera (*Ateles* and *Lagothrix*), indicating a greater divergence from both(Hartwig & Rosenberger, 2006; M. Tejedor & Novo, 2016).

The marked difference in howler monkeys may be due to their characteristics, as they are the most phylogenetically distinct genus, with several subfamilies. Additionally, they are distinguished by having a relatively small cranial capacity, lack of cranial flexion, and significant sexual dimorphism (J. G. Fleagle, 2013), especially in the hyoid, which in turn affects jaw size and may alter facial morphology.

Figure 21. Skulls of several extant Platyrrhines. *Fleagle (2013)*

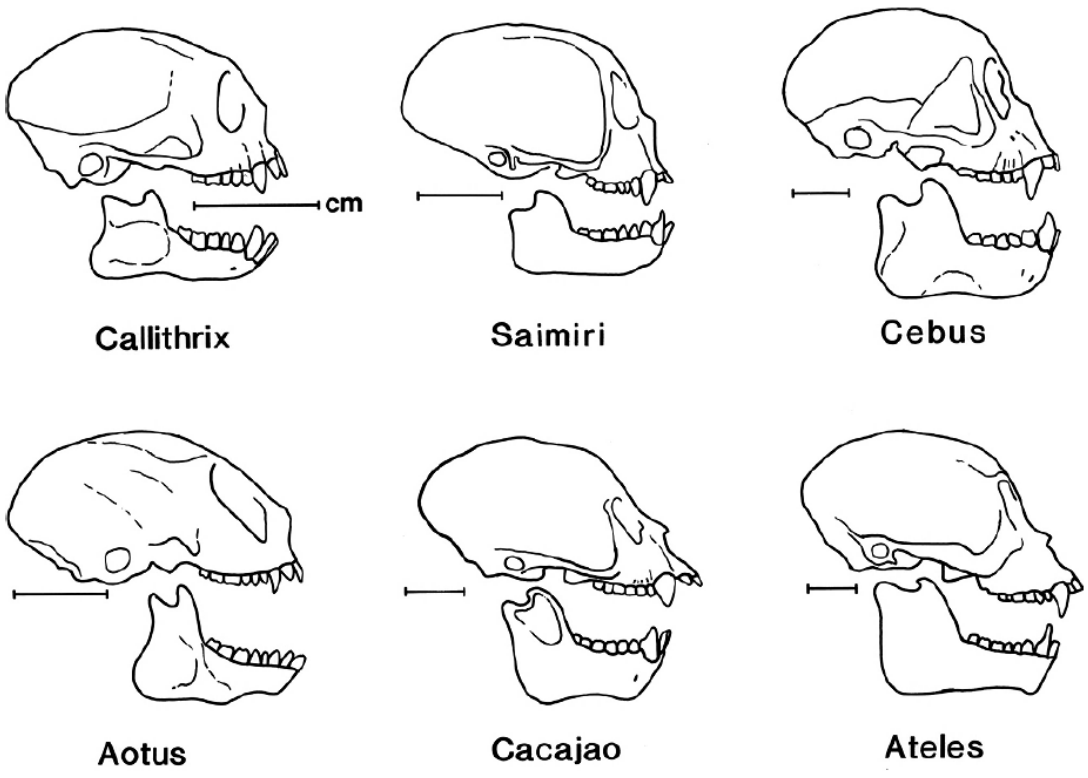

Moreover, platyrrhines typically have dichromatic color vision, with trichromatic color vision present only in some females. In *Alouatta*, trichromatic color vision is found in all or nearly all individuals, like catarrhines (Singleton, 2013).

In spider monkeys, it is notable that males and females are virtually identical in size, so the separation in the analysis of the two sexes points to sexual differences based on shape, even though the size is the same.

The large separation between males and females of *Alouatta* and *Ateles* contradicts studies on the range of sexual dimorphism (Clutton-Brock & Harvey, 1977), where in the case of spider monkeys (*Ateles*), no significant difference is observed, and in howler monkeys (*Alouatta*), the size difference is typically 25-30% larger in males compared to females. In this case, however, the difference seems to far exceed that seen in other well-known dimorphic primates, such as the hamadryas baboon (95%), orangutans (86%), or gorillas (72%). However, previous studies are based on a comparison of individual weights (Appendix4).

Our study indicates that there is a significantly distinct morphology between males and females in these atelids, in terms of form, far greater than that seen in gorillas. This contrasts with the expectation that species with greater size dimorphism also exhibit greater facial form dimorphism. Finally, this leads us to focus on the anatomical parts that are varying within the species beyond the expected range of variability. We observe that while the orbits remain relatively homogeneous across large primate groups, in this case, they show the greatest variability

4.1.2. Catarrhines: Old Word Monkeys

Catarrhines are characterized by numerous anatomical specializations that set them apart from the more primitive platyrrhines. The snout is frequently long and prominent, a feature that is especially marked, such as baboons and great apes (visible in positive values of PC1).

Of the living catarrhines, the Old-World monkeys are the more taxonomically diverse and numerically successful. Our analysis reflects the two

separate subfamilies: the cercopithecines or cheek-pouch monkeys (fruit eaters), and the colobines, or leaf-eating monkey's structures (Figure22), Many of their differences are related to basic dietary adaptations, and in the cranial anatomy (J. G. Fleagle, 2013; Pugh et al., 2023a).

Figure 22. Characteristic features of the colobines and cercopithecines. *Fleagle (2013)*

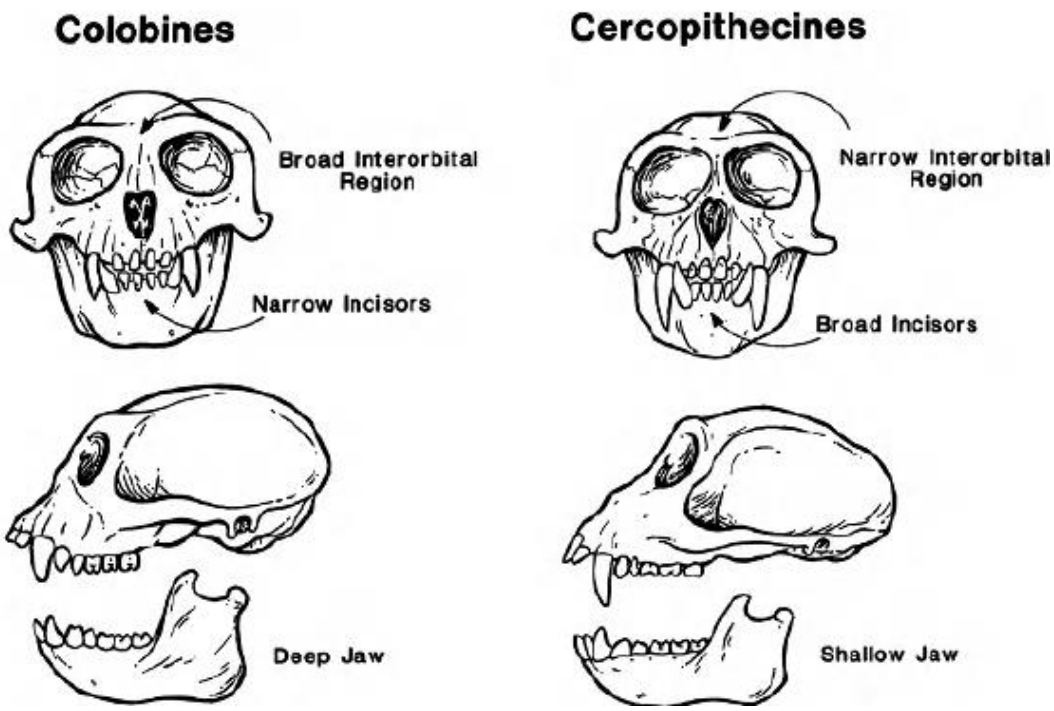

A) Cercopithecoidea

Cercopithecines have a narrow interorbital region, longer snout and shallower mandibles than do colobines (E. Simons, 1987). In our analysis, we also distinguished between the two clades of cercopithecines: the larger papionins (macaques, mangabeys, mandrills, geladas, and baboons) and the smaller cercopithecines. In the case of mangabeys, molecular phylogeny indicates that the more terrestrial, *Cercocebus* are closely related to mandrills, instead of the arboreal mangabeys (*Lophocebus)*, that are closer to baboons and geladas (J. G. Fleagle, 2013). This is partially supported by the relationship between *Cercocebus* and mandrills however, baboons are also grouped with them,

contrary to expectations. It would be interesting to include *Lophocebus* to see how they group.

The allometric trajectories of *Mandrillus* and *Papio* differ significantly from the trajectory of these two mangabeys and from *Macaca*. If macaques represent the primitive condition, like Collar and O´higgins (2001) suggests, the facial similarities between *Mandrillus* and *Papio* are homoplasy derived from different trajectories, while the similarities between *Cercocebus* and *Lophocebus* are plesiomorphic (Figure23).

Within the Papionini tribe, the division is reinforced by the very prognathic and tall face with a narrow nasal fossa found in three species: Mandrillus sphinx, Papio hamadryas, and Theropithecus gelada. We observe a tilted nasal fossa, more projected at the nasospinale point, which contributes to an elongated prognathism. This gives the appearance of an inclined prognathism that grows progressively.

The grouping of these three species reflects the similarities historically observed in their taxonomy and classification, as Mandrills and geladas were initially classified within the genus Papio. Although some evidence suggests they might still be similar enough to be included in Papio, particularly given their similarity in multilevel social structures with one-male, multi-female “harem” groups as the primary social unit (Mittermeier et al., 2013).

No direct behavioral comparisons were made in this research. However, the close relationship between mandrills, baboons, and geladas is evident in their morphological similarities, such as the significant sexual dimorphism (Figure24), which makes the females and males of this group more clearly distinguishable than in other species (Clutton-Brock & Harvey, 1977). The extreme position of the M. sphinx male can be explained by the prominent swellings along each side of the upper snout (J. G. Fleagle, 2013; Gommery et al., 2023).

Baboons differ from drills and mandrills in having a narrower nasal region, with wide nasal openings that point directly forward and a longer tail. The northeastern species *P. hamadryas* has a slightly upturned nose tip, or snub-nosed appearance. However, they differ in the specific focus of this general

prognathism in the snout. The separation between them seems to be due to the exact position of the nasal fossa, where the widest part, represented by the alar points, is in the lower half in geladas and mandrills, while in baboons, it is in the upper half.

Theropithecus gelada, also known as the gelada baboon or "bleeding heart" baboon, is restricted to a small mountainous region in Ethiopia at high altitudes. Their snout is shorter from front to back, ending in a rounded shape, approaching chimpanzee-like morphology, and higher than the muzzle of Papio species (J. G. Fleagle, 2013; D. A. Getahun et al., 2023). The round end can explain the proximity of great apes in our results. The nasal openings are less forward-facing, somewhat triangular, and tilted upward.

Figure 23. Molecular phylogeni of cercopitecines. *Fleagle (2013)*

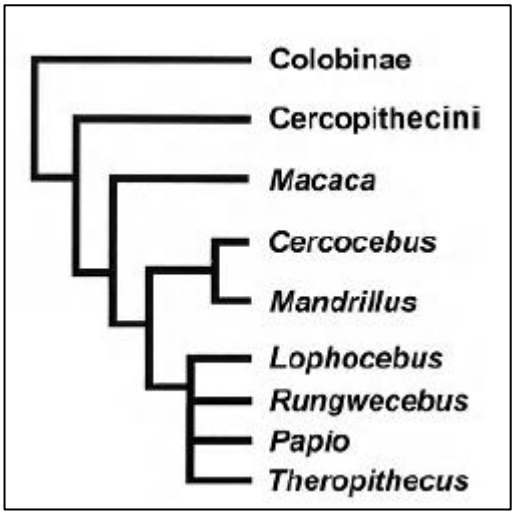

The *Theropithecus* genus diverged from a papionin ancestry soon after 4.5 Ma (D. Getahun et al., 2023). †T. oswaldi, know from later Plio-Pleistocene groups with the fossils of its own lineage only when we analyze the configuration of 48 landmarks. However, when 61 landmarks are considered, this fossil shows closer affinities to colobines and hylobatids. It is assumed that this discrepancy arises because, in the first configuration, the zygomatic bone explained a large portion of the variance. However, in this specimen, the right zygomatic bone was missing and had to be reconstructed, which significantly affected its placement.

The last members of the Papionini tribe, the genus Macaca, are the most common and geographically widespread of all primate genera, adapting to a wide variety of environments. Their internasal septum is often very narrow, and their nasal openings project downward and somewhat laterally, with a protruding muzzle that positions them between larger cercopithecines and hominins (Li et al., 2009). We corroborate these characteristics, and their closer proximity to

great apes suggests a reduction in this feature compared to mandrills and baboons.

The eyes are positioned closer together, with the orbitale and zygoorbitale points projected more laterally, giving a wider shape to the lower orbital border, which is projected slightly forward, yet maintaining an almost vertical orientation of the orbital aperture. This frontality represents an apomorphy, contrasting with the less vertical configuration present in strepsirrhines (Singleton, 2013).

Figure 24. Comparison of the phenotypical (upper) and craniofacial (down) sexual dimorphism in male (left) and female of *M. sphinx*.

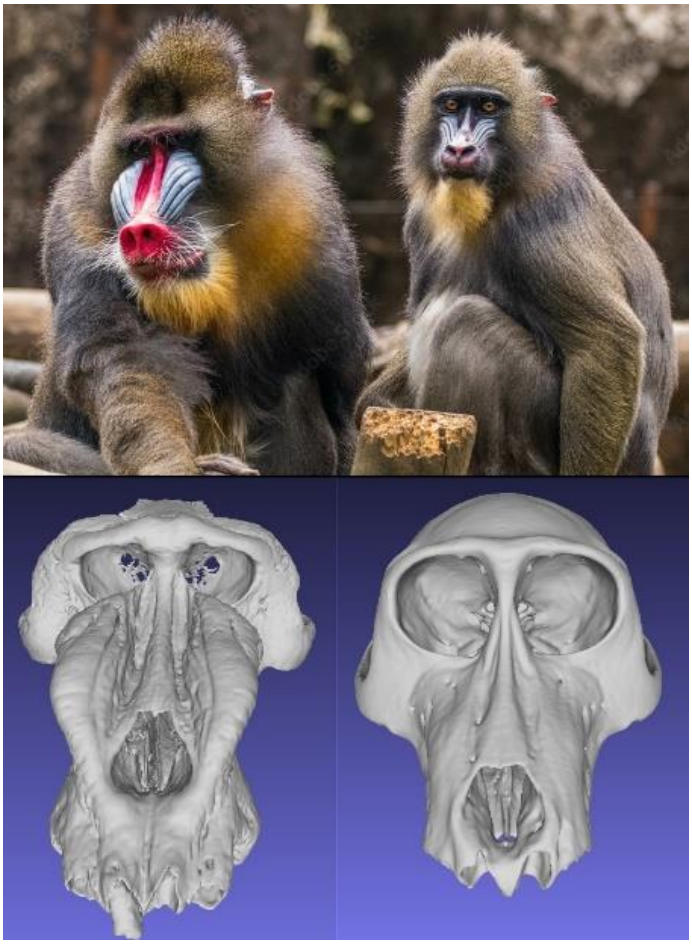

In contrast to females, male macaques have larger brow ridges, possibly explaining why the female *M. mulatta* is positioned with increasingly negative values, related to the less prominent brow ridge. Within this group, the proximity of individuals belonging to *M. fascicularis* (crab-eating macaque) is notable, due to their lower sexual dimorphism compared to the other species.

Focusing now on the other tribe of the Cercopithecinae, the Cercopithecini, the relationships among guenons, vervets, and grivets, patas monkeys (*Erythrocebus*), and talapoin monkeys (*Miopithecus*) have long been an area of confusion (Arenson et al., 2022).

There are at least 19 guenon species, but their relationships are complex and almost certainly reflect a history of hybridization (J. Xing et al., 2007). Here

we only have *C. campbelli* (more arboreal guenons, *Cercopithecus*) as a representative member, which limits our ability to confirm their position as a paraphyletic taxon, with the relatively terrestrial species more closely related to vervets and patas monkeys than to other guenons (Cardini & Elton, 2008; Sargis et al., 2008).

The talapoin monkey (*Miopithecus*) is the smallest Old-World monkey and the smallest living catarrhine. Their relatively large head, large eyes, and short snout align with the theory suggesting that talapoins are neotenic guenons, as this morphology is also present in young animals (Shea, 1992), the size and also their basal differentiation for the arboreal guenons , can explain their distance of other species of their group, providing a support to the proposal of a single evolutionary transition from a arboreal to terrestrial locomotion in the tribe Cercopithecini , and this also con affect their facial morphology. Corroborating that the Talapoin is a highly divergent taxon (Cardini & Elton, 2008; J. Xing et al., 2007).

This species also experiences displacement due to the reduction of landmarks (of the zygomatic and alveolar parts), shifting from being an outlier to grouping with hylobatids and platyrrhines. Allometric analyses show that size influences their positioning on PC2, reflecting that this species shares neotenic features with hylobatids and some colobines, being separated only by size.

Erythrocebus patas (patas monkey) is a close relative of the vervets and has extreme specializations for life on open grasslands, a characteristic that may explain their proximity to the larger cercopithecines, which also have a more terrestrial mode of locomotion.

All this show that guenon skulls appear to be more evolutionarily conserved compared to their sister group, the papionins, patron sees in the face too. Explained by cardini and collaborators (2008), possible for the largely terrestrial, open-habitat papionins developing more pronounced hard tissue features, resulting in greater variation in skull morphology. In contrast, the primarily arboreal guenons may have relied more on soft tissue traits that might have been more beneficial in the low-light conditions of forests.

B) Colobus

The other subfamily of Old-World monkeys is the colobines, or leaf-eating monkeys, found in Africa and Asia. Generally, living colobine monkeys are more arboreal, better leapers, folivorous, and their infants mature much faster than those of cercopithecines.

The *Colobinae* are characterized by short faces, a narrow interorbital septum, long and narrow nasal bones, a moderately prognathic snout, tall infraorbital facial height, and a long premaxilla with relatively broad central incisors (B. R. Benefit & Mccrossin, 1991a).

However, the genetic and phylogenetic relationships within and between them are very complex. Like the relationships among cercopithecines, they likely reflect a complex history of hybridization (Roos, 2022; Wang et al., 2015). This complexity, in our research, is more evident in colobines because they are distributed in a mixed group with the two tribes, Colobini and Presbytini. In cercopithecines, a similar situation is visible with some species overlapping between different tribes, such as *C. torquatus* or *C. campbelli*, but in general, the large groups can be better differentiated.

Despite this overlap, it is possible to distinguish the two major groups of colobines: an internal group corresponding to the African colobine monkeys (Colobini) and a larger group comprising the Asian colobines (Presbytini).

Regarding the African colobus species analyzed, *Colobus guereza*, or black-and-white colobus monkeys, are the largest, quite robust, and exhibit considerable sexual dimorphism in size. They move more frequently by quadrupedal walking and bounding. *Piliocolobus badius* (Red colobus) is sympatric with the former species. Red colobus monkeys are smaller than black-and-white colobus, with broader incisors, more gracile skulls, and less sexual size dimorphism (J. G. Fleagle, 2013).

Research on the relationship between ontogeny and allometry (Kozakowski, 2013) shows that the ontogenetic trajectory of *Colobus*, which exhibits increases in orbital width, midfacial size, facial prognathism, pre-

maxillary length and width, and nasal aperture width relative to length, is consistent across all hominoid taxa. This trajectory is highly conserved in the Catarrhini, indicating that *Colobus* has a common catarrhine pattern of growth, where the adult forms are characterized by increased post-orbital constriction and an airorhynch facial profile. In Kozakowski's study, *Colobus* is used as an outgroup to analyze the Hominoidea family. In this research, its close relationship with other colobines allows us to assume that the colobine facial pattern is primitive, preserved in hominoids but not in the large cercopithecines (Kozakowski, 2013).

Figure 25. Face of *Presbytis melalphos* (Sumatran lagur) compared with the cranium. *(Rudloff, 2013)*

As for the Asian colobines, they have reached their greatest diversity and abundance due to climatic and sea level fluctuations during the Pleistocene in Southeast Asia. Our results also highlight the ongoing debate regarding their phylogeny and systematics due to their evolutionary history, likely involving varying degrees of hybridization among taxa (Roos, 2022; Wang et al., 2015). This is evidenced by the close clustering of this group, showing that all clades share a wide and short face, a retracted maxilla with minimal alveolar prognathism, and wider orbits. However, when focusing on the reduced set of landmarks, the separation between tribes and even species becomes apparent, even in the genera *Trachypithecus*, *Nasalis*, and *Presbytis*.

In this group, the disparity presented by *Presbytis melalophos*, or the black-crested Sumatran langur (Figure25), stands out when compared to the literature. The literature mentions that this species is distinguished from other Presbytis species by having long nasal bones, underdeveloped or absent

superciliary arches, and prominent, elongated nasal bones (Roos, 2022). However, this elongation is not reflected in the average nose shape among the negative values of the PCA (Figure14).

Instead, these values show a closer proximity between the nasion and rhinion, resulting in shorter nasal bones. What is noticeable, however, is the prominence of the nasal bones, as the rhinion points more superiorly.

But our result is consistent with the general description of the species as having globular-shaped heads, short snouts, nasal openings positioned close together but widely separated from the upper lip, and very short noses (Meijaard & Groves, 2004).

Our results align with molecular studies, which separate Nasalis larvatus (proboscis monkey), another genus of Asian colobines, into a distinct clade. This separation is also reflected in facial morphology, as this species is the most divergent from all other colobines, even approaching macaques and/or great apes. Additionally, it is evident that *N. larvatus* exhibits the greatest sexual dimorphism among colobines. The position of the female, indicating a smaller interorbital space, as well as shorter and longer nasal bones along with a longer nasal fossa, could be explained by the role of the pendulous nose, as females have a smaller one.

†*Rhinocolobus turkanensis* from our sample, this species, which lived in East Africa between 3 and 1.5 Ma, contrary to expectations, this fossil does not group with its modern relatives but instead clusters with the great apes, particularly with the female *Pongo* (Arenson et al., 2022; B. R. Benefit & Mccrossin, 1991b). While this specimen is larger than current colobines, it does not group with the great apes when considering allometric differentiation, indicating that size is not the factor explaining this difference. A possible explanation is that †*Rhinocolobus* has been classified among the colobines due to similar postcranial skeletal characteristics (Arenson et al., 2022), but in our research the face show difference, for example compared to its modern relatives, it has a notably shorter nose.

C) Lesser ape

The hylobatids are anatomically the most primitive of living apes, retaining many plesiomorphic (ancestral) catarrhine features alongside a highly derived postcranial skeleton adapted for suspensory locomotion (J. G. Fleagle, 2013). This is evident in our result with a homogeneous group formed with the four genera for this study: *Hylobates lar*, *Nomascus concolor*, *Hoolock leuconedys* (commonly known as gibbons), and *Symphalangus syndactylus* (the siamang).

This highlights the ongoing challenges in resolving the controversy surrounding the number of species and subspecies, particularly given their distinctive karyotype, which exhibits heavily reshuffled chromosomes(Gilbert et al., 2020; Kozakowski, 2013), adding that their contiguous population geographically diverged more rapidly than their close relatives, the great apes (Pugh, 2020). In our study the closeness with other species of platyrrhines (*C. calvus*, *C. apella*, and *A. geoffroyi*) and colobines (*C. guereza*), can be a reflect of the degree of morphological similarity across these families, probably for this fast divergent, with few times to change in big scale the morphology of this group.

Unlike the other family of hominoids, the Hominidae, hylobatids are smaller in size, with short snouts and shallow faces, large orbits with protruding rims, and a wide interorbital distance. Due to a lack of fossil evidence (Gilbert et al., 2020), it is difficult to determine which exactly traits are the ancestral.

We can see other features in gibbons that differ from other catarrhines of similar body mass by having longer gestation periods, a later age at first reproduction, and a relatively large brain (Kozakowski, 2013).

Also, we confirm the difference that separate the siamang from the members of the closely related genus *Hylobates*, principally by great robustness, facial length in siamangs, followed by *Nomascus concolor* and *Hoolock leuconedys*. Like that siamangs and *N. concolor* gibbons represent the earliest distinct lineages (Haimoff et al., 1982).

In the case of *Symphalangus*, the face has a markedly more airorhynch (Figure26), oriented more dorsally, leading to a projecting pre-maxilla and a more

superiorly oriented upper face. This condition is present in great apes and, additionally, in primates with enlarged laryngeal sacs, such as howler monkeys and orangutans (Kozakowski, 2013). This relation is difficult to appreciate in the analysis, because we cannot measure the effect of the sacs directly in the face orientation.

Phylogenetic and morphological analyses ((Haimoff et al., 1982; Israfil et al., 2011)) have demonstrated that Symphalangus is the most basal taxon of the Hylobatidae, followed by a rapid radiation with significant incidents of hybridization, which contributed to their highly uniform morphology, as seen in our study, with more separtion for the other species.

Figure 26. Angular orientation of the face with airorhynchy and klinorhynchy configuration. *Singleton (2013)*

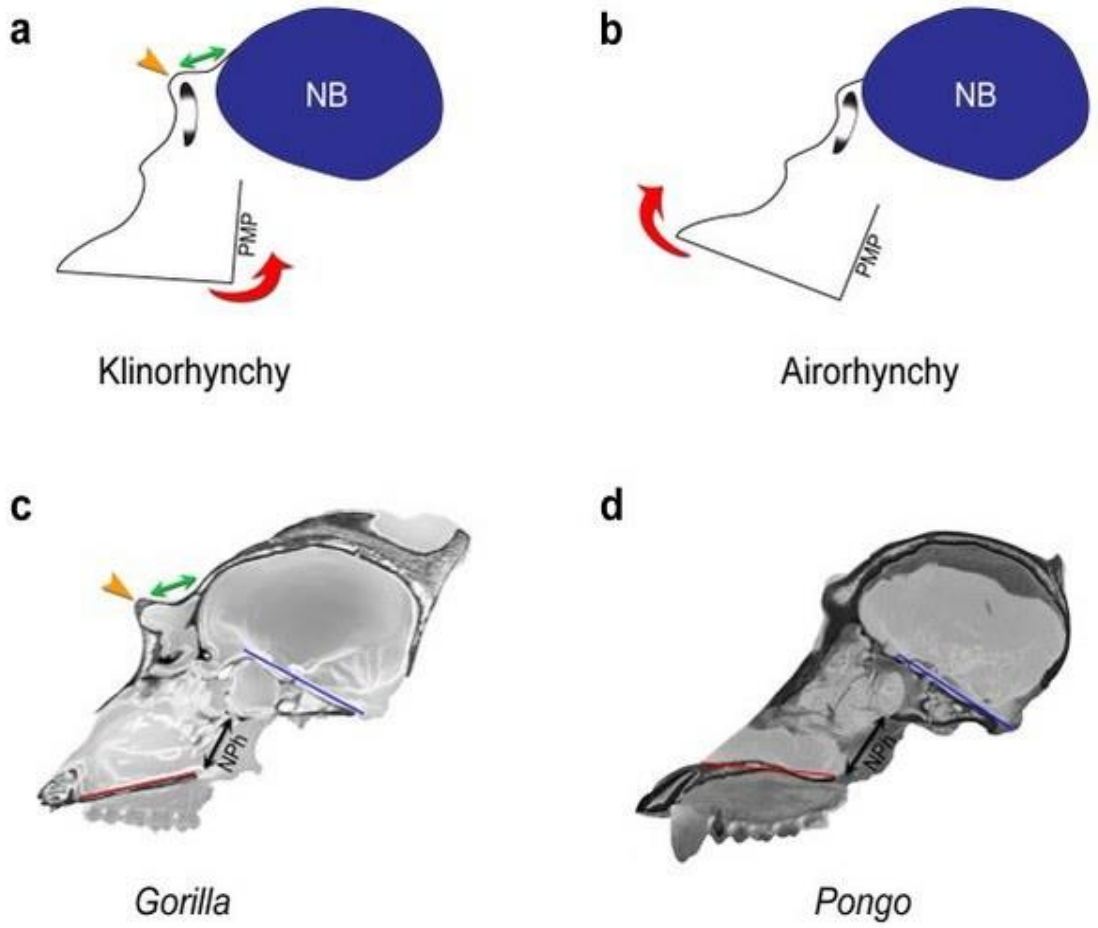

This orientation of the face, by himself is evident in the positive values of PC1, showing a gradual reduction from colobines to lesser apes and great apes (in negative values), progressing to a fully klinorhynch orientation in other cercopithecoids. This configuration is also reflected in PC2, specifically in the orbital orientation, with less fronted orbits in the positive values and more fronted orbits in the negative values (Singleton, 2013). This explains why *Pongo abelii* and *S. syndactylus* appear slightly farther apart in the lower part of the PCA plot relative to other members of their respective families. It also accounts for the outliers in the negative values, corresponding to the males of the two analyzed *Alouatta* species, further corroborating the dorsal facial orientation due to the presence of laryngeal sacs.

A) Great apes

The family Hominidae, share facial synapomorphies such as high face, high zygomatic root, pyriform nasal aperture widest at the base, deep palate, and nasals that project slightly anteriorly beneath the level of the lower orbital rims, same pattern present in †*Pierolapithecus* (Moyà-Solà et al., 2009), which explain the grouping of this taxa.

In this group the differences in craniofacial morphology can be explained by several factors, like the large size of most hominoids, the large brain size, greater flexibility of social interactions or the considerable extended lifespan. In this last point the intraspecific differences are explained in the relative extension or truncation of ontogenetic trajectories (Collard & O'higgins, 2001). The shape changes are more extensive in gorillas that exhibit craniofacial shapes like-chimpanzees, as well as a larger size at any stage of growth, with these shape differences being independent of size. Contrary to chimps, both *P. pygmaeus* and *G. gorilla* exhibited significantly greater shape and size differences between males and females (Kozakowski, 2013).

The nasoalveolar morphology in hominoids shows a range of primitive and derived traits, and some of this creates a differentiation between orangutans and African apes. *Pongo* has highly derived features, such as taller orbits, smooth nasal region, and a very elongated subnasal clivus, as well as the anteriorly

oriented zygomatics (Pugh et al., 2023a). In this context, orangutans are positioned somewhat farther towards the negative values of PC2.

In contrast, gorillas and chimps have wider orbits, a stepped nasal floor, a moderately to very elongated subnasal clivus, a pronounced supraorbital torus, a long premaxilla that overlaps the hard palate, with a well-defined incisive canal and a laterally sloping zygomatic region (Pugh et al., 2023a).

Pongo and *Gorilla* showed significantly higher shape and size differences relative to females, with the first exhibiting the highest amount of static allometry in the face, whereas gorillas in the complete cranium, consequence of a later onset of maturation relative to females, called “bimaturism” (Atmoko & van Hooff, 2009; Shea, 1986).

We do not observe the pattern of greater sexual dimorphism in gorillas among the great apes (Clutton-Brock & Harvey, 1977). Although it is argued that in gorillas and chimpanzees, dimorphism is present both in form and size (Cobb & O’Higgins, 2007), it has been observed that size plays a greater role in interspecific variation of facial differences(Fernández-Montraveta & Moya-Laraño, 2007; E. Simons, 1987). Our study seems to highlight this difference, although facial dimorphism values in chimpanzees surpass those of gorillas.

Chimpanzees exhibit dimorphism similar to that of orangutans, which contradicts the idea of a closer relationship between orangutans and gorillas ((J. Fleagle et al., 1980; Shea, 1986). *Pan* shows greater sexual dimorphism in the width of the interorbital space and the zygomatic region (Cobb & O’Higgins, 2007; Fernández-Montraveta & Moya-Laraño, 2007).

Primitive taxa, such as the stem hominoids from the Proconsulidae family: †*Afropithecus*[5], †*Turkanapithecus*, and †*Proconsul*, share some of these features like the wide incisive fossa; but other like the no-stepped nasal floor is share with orangutans, and in general resemble more extant cercopithecines, whose facial profiles are marked by pronounced alveolar and midfacial prognathism, with the glabella positioned posteriorly to the nasion and rhinion.

[5] Occasionally regarded as a stem hominid or stem catarrhine (Pugh, 2020)

Instead, Miocene primates, such as the dryopithecine †*Hispanopithecus*, †*Ouranopithecus*, †*Ankarapithecus*, and †*Sivapithecus*, exhibit morphology with a short, high premaxilla projecting posteriorly, closest to the extant great apes. Also characterized by a pronounced alveolar prognathism, with the rhinion and nasion positioned posteriorly relative to the glabella, resulting in the midfacial concavity typical of this group (Moyà-Solà et al., 2009; Pérez de Los Ríos et al., 2012; Susanna et al., 2014).

This information is corroborated here by †*A. turkanensis*, which clusters between cercopithecines and great apes, displaying positive values. A similar intermediate range is partially observed in †*T. kakolensis*. In the case of †*Afropithecus*, the affinities lie with baboons and mandrills, whereas in †*T. kakolensis*, they are more aligned with the subfamily Colobinae. The difference can be explained by the width of nasal region that in cercopithecines is narrow (PC1 positive) and in colobines is wide (PC1 negative).

The fossil closest to great apes is †*P. catalaunicus*, which is nearest to gorillas, as indicated by its relatively wide orbits. The low midfacial prognathism, orbits situated above the nasal aperture, and relatively tall midfaces are derived features consistent with a stem hominid position. This characteristic is also present in other catarrhines, such as *Papio* and *Macaca*, which have longer muzzles and taller faces (Arenson et al., 2022; J. Xing et al., 2007). However, there are several differences between †*Pierolapithecus* and great apes, like a shorter subnasal, while the moderately elongated clivus in †*Afropithecus* is likely convergent with hominids (Leakey et al., 1991; E. Simons, 1987). Another distinct feature is the relatively shorter height of the face, despite the clear elongation of the midface, a broad interorbital pillar, a premaxilla that does not overlap the palate, a short subnasal clivus, a laterally sloping zygomatic region, and a more vertically oriented frontal squama (Pugh et al., 2023a).

4.4. Oligocene stem-catarrhines: †*Aegyptopithecus*

The divergence between hominoids and cercopithecoids is estimated to have occurred in the late Paleogene, approximately 25–23 million years ago. However, genomic studies have suggested an earlier divergence, between 34.5 and 29.2

million years ago, which nearly coincides with the entire temporal range of Propliopithecoids (Stevens et al., 2013; Zalmout et al., 2010).

In this scenario †*Aegyptopithecus (Figure27)*, may have played a more direct role in the evolution of later crown catarrhines, as its cranial morphology closely resembles this ancestral morphotype. This hypothesis is supported by the observation that many traits present in †*Aegyptopithecus*, such as midfacial projection and long nasals, are retained in early Miocene apes, most notably in †*Afropithecus*, †*Morotopithecus*, and †*Proconsul* (Zalmout et al., 2010).

The facial anatomy of †*Aegyptopithecus* does not possess any autapomorphic traits that would exclude it from the catarrhines. This aligns with the predominant view of researchers over the past two decades (B. Benefit & McCrossin, 1997; B. R. Benefit & Mccrossin, 1991b; E. Simons, 1987). Although it has not been easily placed within any of the current catarrhine groups, it is evident that †*A. zeuxis* is neither a modern ape nor a cercopithecoid (Simons, 1987). Nonetheless, it remains within Hominoidea, implying that cercopithecoid monkeys must have evolved from a hominoid ancestor (Von Cramon-Taubadel et al., 2007). This is further corroborated by its position among these groups, revealing that its unspecialized facial morphology is evident.

Figure 27. Artistic rendering of *Aegyptopithecus*. *(Goldberg, 2024)*

Despite its similarity in size to species such as *Cebus*, *Alouatta*, *Hylobates*, *Presbytis* or †*Pliopithecus*, but †*Aegyptopithecus* has a more robust face, resembling that of the great apes (Ankel-Simons, 2007). The fact that *Aegyptopithecus* is not found alongside this species suggests that despite maintaining a similar size, the differences in facial structure are not explained by allometric factors but rather by a change in morphological structure. Sharing some features with this group such as small, elliptical orbits, deep faces, temporal crests, broad lacrimals, wide zygomatic bones, forward-facing orbits, and an interorbital septum—plesiomorphic characteristics shared by Hominoidea (Simons, 1987) and *Afropithecus*. Another similarity with *Pongo* and other Old-World monkeys is the size of the zygomaticofacial foramen.

The nasal bones are long, and among monkeys, only baboons have a comparable size. The orbits are smaller than in any other cercopithecoid, but their frontal orientation is significant. Cladistic analysis predicts that archaic catarrhines likely had short snouts. In the case of †*Aegyptopithecus*, its face is shorter compared to baboons or †*Afropithecus*, but longer than that of other anthropoids (Leakey et al., 1991; Mccabe, 2017; E. Simons, 1987).

Regarding †*Afropithecus*, the differences seem to be more related to size than to shape (Leakey et al., 1991), sharing more features than †*A. turkanensis* than with her contemporary †*Proconsul*. Relation visible in this study.

In this case, the variation among the four individuals is greater than that observed in any of the other species. The broad range of intraspecific variation has been confirmed (Simons, 1987). It should also be noted that the sample consists of two male adults, one male subadults, and one female adult (Figure28). For this reason, we might expect this sample to show more variance due to the wider age range represented.

However, the males' features have been accorded phylogenetic significance in catarrhine systematics (well-developed rostrum, elongate sagittal crest, and frontal trigon). Characteristic that in the crania of female lack. And the dispersion in our sample possibly follows this unique pattern of craniofacial sexual dimorphism that may have characterized advanced stem and basal crown

catarrhines (J. Fleagle et al., 1980; E. Simons, 2001; E. Simons & Kay, 1983; E. L. Simons et al., 2007). Regardless, extreme differences in the size of male and female *Aegyptopithecus* clearly led to striking differences in craniofacial morphology.

Figure 28. Cranial remains of *Aegyptopithecus zeuxis.* A)Female cranium (CGM85785), B) male cranium (CGM40237) with unassociated mandible; rostrals views of C)DPC2803, D)DPC3161, and E)CG,42842. F-J) 3D reconstruction of CGM85785. (Seiffert, et.al. 2012).

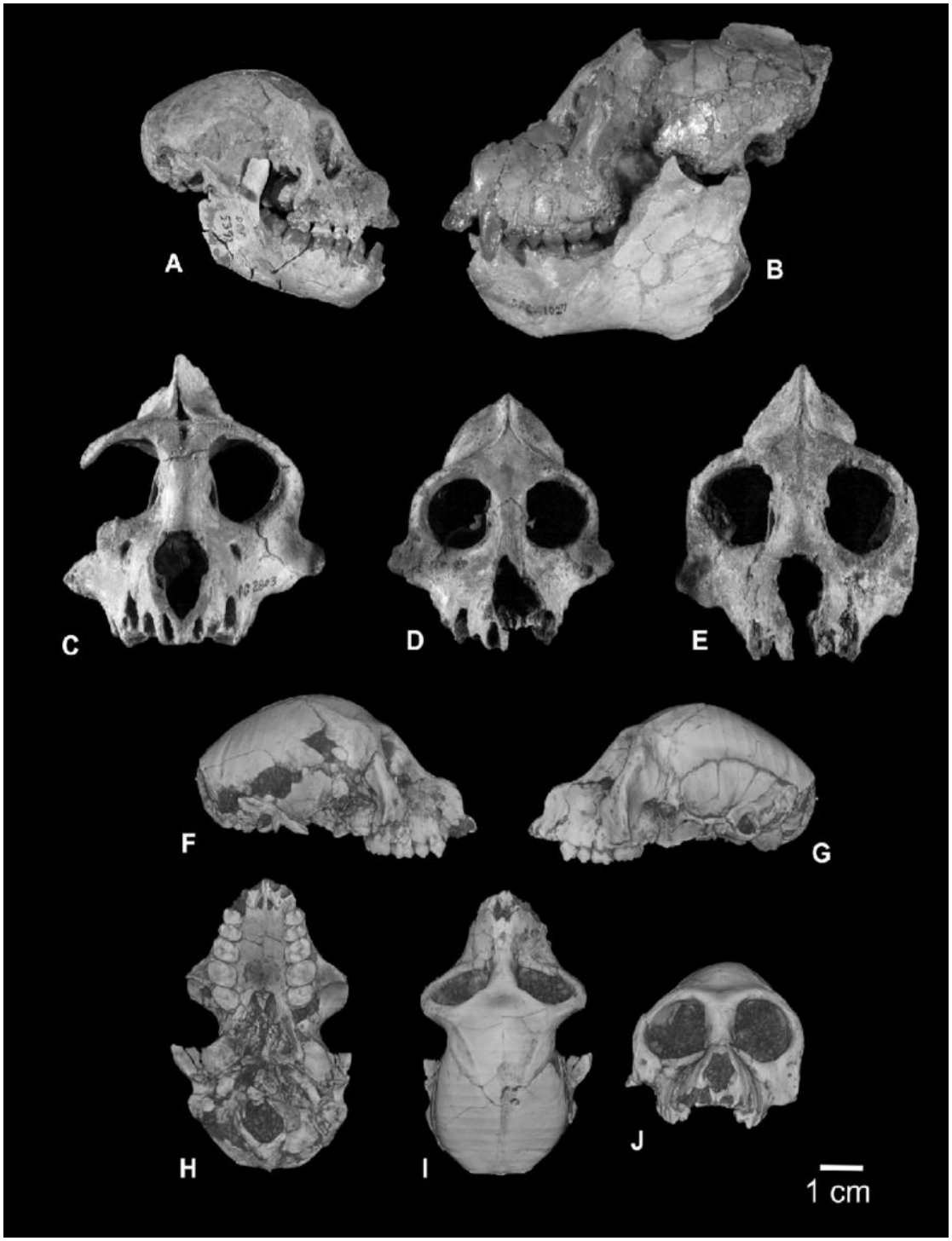

Compared with *†P. grangeri* and all other early anthropoids, the lacrimal bone and foramen lie within the orbit. We corroborate the closeness of the two oligocene primates, with a differentiation that can be for the nasal bones longer in *†A. zeuxis (R. Kay et al., 1981; E. L. Simons et al., 2007)*. In the case of *†P. grangeri,* studies in molar anatomy, suggest that parapithecids are in or near the ancestry Old-world monkeys, been not related with modern apes, and the characteristics that these two groups share must evolve in parallel, such as the loss of P_2 (E. Simons & Kay, 1983). †*Parapithecus* represent an early stage in Anthropoid evolution before the reduction of olfactory system (Bush et al., 2004).

The plesiomorphies of †*Aegyptopithecus,* were identified in papionins, and in a lesser degree in hominids in having long, lower crania with prognathic faces, but in specific for hominoids is suggest an ancestor of larger-bodied, greater ape-like (Pugh et al., 2023b). This reflex a nearest cluster of †*Aegyptopithecus,* with the Old-world monkeys than with Hominoids, like in our results.

In this context, it is of particular interest to further analyze the position of the fossil in relation to cercopithecoids. Revisiting the craniofacial polarity exhibited by colobines in relation to other cercopithecids, with a shorter face, a pattern like that seen in hylobatids compared to great apes, suggests that these families, along with Colobinae, are often considered representative of the primitive facial configurations, orthognathic (straightness of the facial profile), in Cercopithecoidea and Hominoidea, respectively.

This assumption is based on the principle that similarities between non-sister taxa are likely to be conserved. However, this view is challenged by Benefit and McCrossin (1997), who argue that certain species, such as †*Aegyptopithecus* or †*Afropithecus*, exhibit a facial morphology markedly different from the Colobus-like face.

These primates display plesiomorphic characteristics, including a moderately long muzzle and midfacial region, a long and anteriorly positioned premaxilla, broad upper central incisors, a narrow, inferiorly V-shaped nasal aperture of moderate height, and a deep cheek region relative to facial height. Some of these plesiomorphic traits are also present in extant cercopithecines,

such as *Macaca* and *Cercopithecus*. This explains the close relationship between †*Aegyptopithecus* and the subfamily Cercopithecinae. Our findings support the classification of †Aegyptopithecus as a stem-catarrhine, and suggest that colobines (as in the case of *Cebus*, previously discussed) may possess facial characteristics that predate the divergence between platyrrhines and catarrhines

The hypothesis was partially corroborated, with †*A. turkanensis* being more closely related to the different species of macaques. However, this relationship is less evident in †*A. zeuxis* and *C. cambelli*, which are positioned between the groups of Cercopithecinae and Colobinae, with a slight tendency towards being closer to the latter group.

The upper surface of the nasals is concave ventrally in †*Aegyptopithecus* whereas in †*Parapithecus* this surface in profile is flat with a slight upturn distally. Because of these relationships the rostrum of †*Parapithecus* rides higher between the orbits than in †*Aegyptopithecus* so that the orbital opening is directed somewhat more upward and less frontally oriented. The large zygomaticofacial or malar foramen resembles that of platyrrhines whereas the jugal and parietal bones being separated by an alisphenoid-frontal contact is seen in catarrhines (E. Simons, 2001).

At last, we can say that sexual dimorphism in the cranium demonstrates some pattern variation among ape species, aligning with the idea that the neurocranium exhibits less dimorphism than the face (Pugh et al., 2023).

Since some of the shape changes along PC1 appear to be related to overall size, with smaller taxa (e.g., platyrrhines and hylobatids) on the negative end of PC1 and larger taxa (e.g., great apes and Mandrillus) on the positive end, we evaluated the relationship between overall face shape (PC1 scores) and centroid size (CS), this plot effectively separates extant groups, with a clear difference in face size between extant great apes and other extant anthropoids, except for Papio, Theropithecus, and Mandrillus, which fall within the great ape range (Figure29.).

Colobus guereza and *Piliocolobus* are similar between sexes, whereas in the case of *Nasalis larvatus*, the male is positioned in the negative values of PC1,

and in *Trachypithecus germaini*, the male falls within the negative values of PC2, indicating sexual dimorphism. *T. germaini* is the species that deviates the most from the general group.

Males of the great ape taxa exhibited wider faces, superiorly oriented temporal lines, increased cranial robusticity, elongated crania, and nuchal and sagittal cresting. However, the degree varied among the taxa, in the study of shows that Hylobatids exhibit the lowest amount of static allometry and *Colobus* the highest.

Figure 29. Plot of PC1 against Csize of all the sample removing outlier

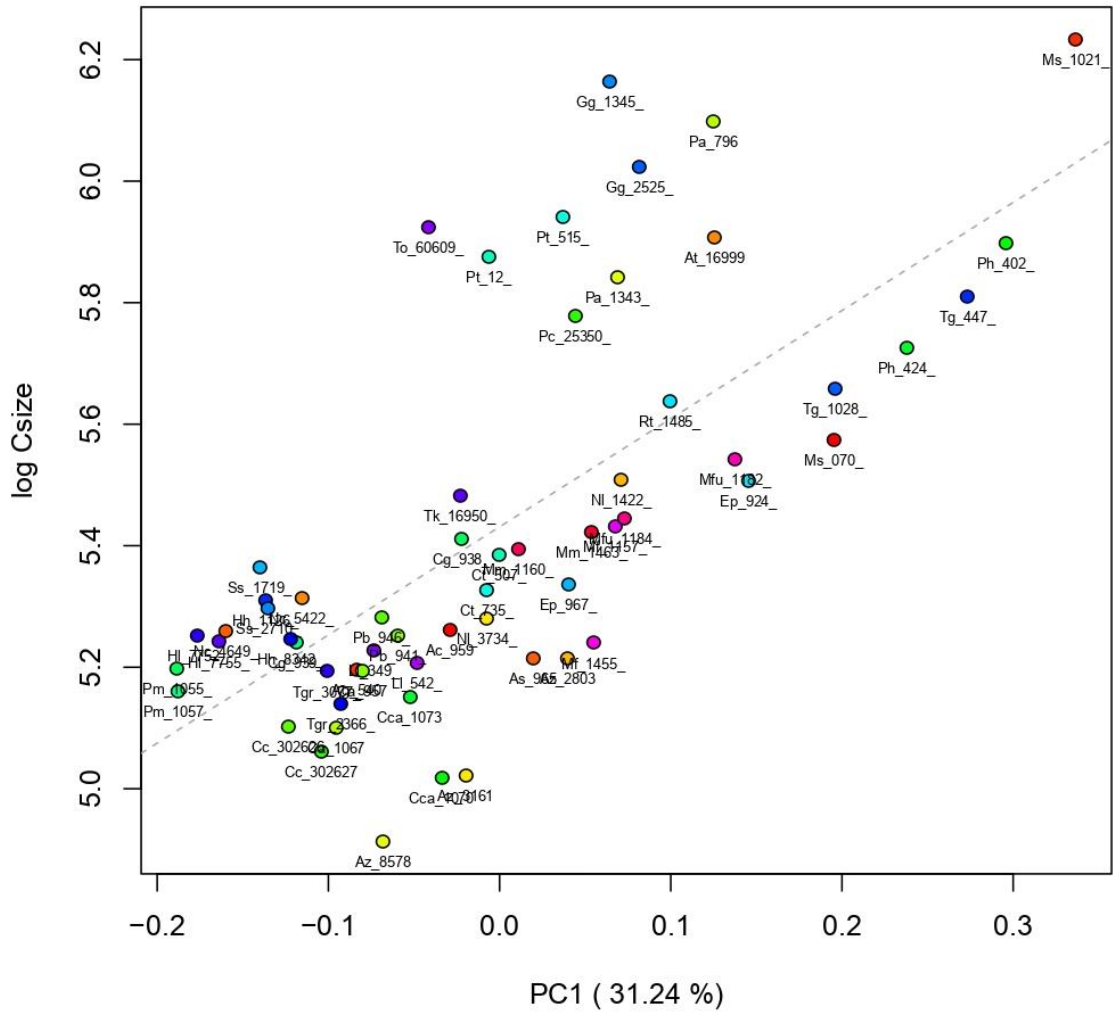

Finally, is important that we considerate Cardini and collaborator (Cardini et al., 2021; Cardini & Polly, 2020) caution that PCA can exaggerate or create differences between groups, especially with small sample sizes and many variables. They suggest that studies should include 25–40 specimens per group

for accurate results, particularly in sexually dimorphic species. However, in fields like paleoanthropology, sample sizes are often limited, which increases the risk of error.

Our analysis of modern primates, which follow similar evolutionary patterns, highlights the need for caution with small samples. Future research should focus on increasing sample sizes to verify findings. Additionally, primate studies may require larger samples due to greater susceptibility to sampling error, as demonstrated by the variability observed in howler monkeys in our study. Accurate species identification depends on balancing within-group variability and between-group differences.

CONCLUSIONS

The results of this study provide important insights into questions concerning the facial shape variation observed in primates. This study specifies a primate facial morphology and its evolutionary implications across a wide range of extant and extinct species. By integrating data from PCA analysis and extensive morphological descriptions, we have been able to discern key patterns and relationships.

The research had the main aim of describe and analyze the facial morphology of †*Aegyptopithecus zeuxis*, with a focus on exhibiting the key features that align this species with the evolutionary traits shared by both Hominoidea and Cercopithecoidea, corroborating its positions as a stem-catarrhine. To achieve this goal, the specific aims focus on documenting and analyzing primates' facial morphology, and examinate the variation to understand which factors like sexual dimorphism are behind their shape. Thirdly, compare the facial morphology within all species, and fossils, to understand their relation in the divergence of Hominoidea and Cercopithecoidea.

A critical finding from our research is the clear distinction between the facial morphologies of different primate families, particularly within the cercopithecoids and hominoids. The PCA results illustrate how the extreme positive and negative values of PC1 capture the divergent evolutionary trajectories among these groups. For instance, within the cercopithecoids, species such as Mandrillus sphinx and Papio hamadryas, with their elongated and prognathic facial structures, contrast sharply with colobines like Presbytis melalophos, which exhibit a short, wide face with retracted maxilla. This contrast not only highlights the diversity within cercopithecoids but also emphasizes the distinct adaptive paths these species have taken, influenced by their ecological niches and social structures.

The placement of the fossil species †*Rhinocolobus turkanensis* in proximity to great apes rather than its modern colobine relatives is particularly intriguing. This unexpected clustering suggests that †*Rhinocolobus* may have

retained certain primitive features or evolved unique craniofacial traits that align more closely with great apes, despite its classification within the colobines. This finding prompts a reevaluation of the evolutionary relationships within this group.

Furthermore, our analysis of the Hominidae family, reveals that many craniofacial differences within this group can be attributed to variations in allometric growth trajectories. The study confirms that species such as *Pongo abelii* and *Gorilla gorilla* exhibit significant sexual dimorphism, in the size of the face but also in the shape, so this dimorphism cannot be explained like a simple increase of size.

The study also highlights the presence of both primitive and derived traits in the nasoalveolar region among hominoids, which serve to differentiate orangutans from African apes. Pongo, for example, exhibits highly derived features such as taller orbits and a smooth nasal region, while gorillas and chimps display a more pronounced supraorbital torus and a longer premaxilla. These morphological variations reflect the divergent evolutionary paths within the Hominidae family, shaped by factors such as diet, social behavior, and ecological pressures.

Our research further explores the craniofacial traits of stem hominoids and their evolutionary significance. The Miocene fossils confirm their status in the superfamily Hominoidea and at the same time show that there is a distinctive face that separates the family Proconsulidae, with †*Afropithecus* and †*Turkanapithecus* cluster a little farther from great apes, while Pierolapithecus confirm not only the closer relation in the Hominidae family, also the specific relation with gorillas.

The inclusion of †*Aegyptopithecus*, a stem catarrhine from the Oligocene, in our analysis further enriches our understanding of primate evolution. The cranial morphology of †*Aegyptopithecus*, with its midfacial projection and long nasals, closely resembles that of early Miocene apes, suggesting that these traits were conserved well into the hominoid lineage. This finding supports the hypothesis that Aegyptopithecus may have played a direct role in the evolution

of later crown catarrhines, with a facial morphological that conservates features present in modern catarrhines and hominoids.

Finally, our study underscores the complexity of sexual dimorphism in primate craniofacial morphology. While size dimorphism plays a significant role in shaping facial structures, our analysis shows that shape does not always correlate directly with size. For example, species like *Nasalis larvatus* and *Miopithecus ogouensis* demonstrate that similar face sizes can exhibit distinct shapes, and vice versa.

This complexity highlights the need for a subtle approach when interpreting the evolutionary significance of facial morphology in primates. The broad distribution of †*A. zeuxis* indicates significant variability that cannot be only attributed to sexual dimorphism or age-related changes, because even the two adult males present significance shape differences that are not evidenced in the macroscopy analysis. So, we corroborate the position of this taxon like a stem-catarrhine, but we discover that the intraspecific variability is greater, and other studies are needed to understand this diversity in the posterior morphology of primates, including our own species. However, these analyses are limited by small sample sizes, which, combined with likely close phylogenetic relationships, complicate the evaluation of intra- vs. interspecific variation variation.

These findings contribute to a deeper understanding of primate evolution and offer valuable insights for future studies aimed at unraveling the intricate history of our closest relatives.

However, to gain a broader perspective and considering the challenges encountered during this research, we believe it is essential to conduct future analyses. One of the main points is to increase the sample size of current primates, both in terms of the number of individuals per species and the number of males and females within each species.

In addition, it is important to expand studies of sexual dimorphism beyond the species that are commonly analyzed, such as the great apes, recognizing the need to create formulas or indices that do not solely focus on size differences. Complementing this with ethological and ecological studies is crucial, as these

can help us understand the influence of these factors on the structuring of facial morphology. Similarly, we must analyze the impact of the landmarks used in this study and their significance in defining phylogenetic traits.

Through this research, we were also able to confirm that the face is an important component that provides valuable data on species differences. However, our initial mapping served to highlight areas of interest that require further, separate study, as they show significant variability within certain primate tribes or families, such as the orbital region and the mid-face. Therefore, we recommend conducting focused studies to better understand the variable landmarks in these anatomical areas.

Lastly, it is necessary to develop a standardized protocol for processing 3D images, especially when reconstructions are required or when parameters must be applied to correct any deformation.

BIBLIOGRAPHY

3D Slicer image computing platform | 3D Slicer. (n.d.). Retrieved August 24, 2024, from https://www.slicer.org/

Adams, D. C., & Otárola-Castillo, E. (2013). Geomorph: An r package for the collection and analysis of geometric morphometric shape data. *Methods in Ecology and Evolution*, *4*(4), 393–399. https://doi.org/10.1111/2041-210X.12035

Alba, D., Bouchet, F., Fortuny, J., Robles, J. M., Galindo, J., Luján, À. H., Moyà-Solà, S., & Zanolli, C. (2024). New remains of the Miocene great ape Anoiapithecus brevirostris from Abocador de Can Mata. *Journal of Human Evolution*, *188*. https://doi.org/10.1016/j.jhevol.2024.103497

Alba, D. M., Urciuoli, A., Hammond, A. S., Almécija, S., Rook, L., Zanolli, C., & Alba, D. M. (2024). Miocene ape evolution: Where does Oreopithecus fit in? *Bollettino Della Società Paleontologica Italiana*, *63*(2), 153–182. https://doi.org/10.4435/BSPI.2024.01

Andrews, P. (1992). Evolution and environment in the Hominoidea. *Nature*, *360*, 641–646.

Ankel-Simons, F. (2007). *Primate Anatomy: An Introduction* (F. Ankel-Simons, Ed.; Third edition). ELSIEVER. www.bookaid.org

Ankel-Simons, F., Fleagle, J., & Chatrath, P. (1998). Femoral anatomy of Aegyptopithecus zeuxis, an early oligocene anthropoid. In *American Journal of Physical Anthropology* (Vol. 106, Issue 4, pp. 413–424). https://doi.org/10.1002/(SICI)1096-8644(199808)106:4<413::AID-AJPA1>3.0.CO;2-K

Arenson, J. L., Harrison, T., Sargis, E. J., Taboada, H. G., & Gilbert, C. C. (2022). A new species of fossil guenon (Cercopithecini, Cercopithecidae) from the Early Pleistocene Lower Ngaloba Beds, Laetoli, Tanzania. *Journal of Human Evolution*, *163*. https://doi.org/10.1016/j.jhevol.2021.103136

Arnal, M., Kramarz, A. G., Vucetich, M. G., Frailey, C. D., & Campbell, K. E. (2020). New Palaeogene caviomorphs (Rodentia, Hystricognathi) from Santa Rosa, Peru: systematics, biochronology, biogeography and early evolutionary trends. *Papers in Palaeontology*, *6*(2), 193–216. https://doi.org/10.1002/spp2.1264

Asher, R. J. (1998). Morphological diversity of anatomical strepsirrhinism and the evolution of the lemuriform toothcomb. *American Journal of Physical Anthropology*, *105*(3), 355–367. https://doi.org/10.1002/(SICI)1096-8644(199803)105:3<355::AID-AJPA5>3.0.CO;2-Q

Atmoko, S. U., & van Hooff, J. A. R. A. M. (2009). Alternative male reproductive strategies: male bimaturism in orangutans. *Sexual Selection in Primates*, 196–207. https://doi.org/10.1017/CBO9780511542459.013

Beard, K. C., Coster, P., Salem, M., Chaimanee, Y., & Jaeger, J. J. (2016). A new species of Apidium (Anthropoidea, Parapithecidae) from the Sirt Basin, central Libya: First record of Oligocene primates from Libya. *Journal of Human Evolution*, *90*, 29–37. https://doi.org/10.1016/j.jhevol.2015.08.010

Benefit, B., & McCrossin, M. (1997). Earliest known Old World monkey skull. *Nature*, *388*, 368–371.

Benefit, B. R., & Mccrossin, M. L. (1991a). Ancestral facial morphology of Old World higher primates. *Proceedings of the National Academy of Sciences of*

the United States of America, *88*(12), 5267–5271. https://doi.org/10.1073/pnas.88.12.5267

Benefit, B. R., & Mccrossin, M. L. (1991b). Ancestral facial morphology of Old World higher primates. *Proceedings of the National Academy of Sciences of the United States of America*, *88*(12), 5267–5271. https://doi.org/10.1073/pnas.88.12.5267

Bernardi, M., & Couette, S. (2017). Eocene Paleoecology of Adapis parisiensis (Primate, Adapidae): From Inner Ear to Lifestyle. *Anatomical Record*, *300*(9), 1576–1588. https://doi.org/10.1002/ar.23609

Bloch, J., & Boyer, D. (2003). Response to Comment on "Grasping Primate Origins." *Science*, *300*(5620), 741–741. https://doi.org/10.1126/SCIENCE.1082060

Bocherens, H., Schrenk, F., Chaimanee, Y., Kullmer, O., Pushkina, D., & Jaeger, J.-J. (2015). *Flexibility of diet and habitat in Pleistocene South Asian mammals: Implications for the fate of the giant fossil ape Gigantopithecus*. https://doi.org/10.1016/j.quaint.2015.11.059

Bonnefille, R. (2010). Cenozoic vegetation, climate changes and hominid evolution in tropical Africa. *Global and Planetary Change*, *72*(4), 390–411. https://doi.org/10.1016/j.gloplacha.2010.01.015

Bookstein, F. (1991). *Morphometric tools for landmarks data* (First). Cambridge University Press.

Bush, E., Simons, E., Dubowitz, D., & Allman, J. (2004). Endocranial Volume and Optic Foramen Size in Parapithecus grangeri. In C. Ross & R. Kay (Eds.), *Anthropoids origin, developments in Primatology*. Springer.

Campbell, K., O'sullivan, P., Fleagle, J., De Vries, D., & Seiffert, E. (2021). An Early Oligocene age for the oldest known monkeys and rodents of South America. *PNAS*, *118*, 1–8. https://doi.org/10.1073/pnas.2105956118/-/DCSupplemental

Cardini, A., & Elton, S. (2008). Variation in guenon skulls (I): species divergence, ecological and genetic differences. *Journal of Human Evolution*, *54*(5), 615–637. https://doi.org/10.1016/J.JHEVOL.2007.09.022

Cardini, A., Elton, S., Kovarovic, K., Strand-Viđarsdóttir, U., & Polly, D. (2021). On the Misidentification of Species: Sampling Error in Primates and Other Mammals Using Geometric Morphometrics in More Than 4000 Individuals. *Evolutionary Biology*, *48*(2), 190–220. https://doi.org/10.1007/s11692-021-09531-3

Cardini, A., & Polly, P. D. (2020). Cross-validated Between Group PCA Scatterplots: A Solution to Spurious Group Separation? *Evolutionary Biology*, *47*(1), 85–95. https://doi.org/10.1007/s11692-020-09494-x

Cartmill, M. (2018). Primate origins. *The International Encyclopedia of Biological Anthropology*, 1–14. https://doi.org/10.1002/9781118584538.IEBA0403

Chester, S. G. B., Bloch, J. I., Boyer, D. M., & Clemens, W. A. (2015). Oldest known euarchontan tarsals and affinities of Paleocene Purgatorius to primates. *Proceedings of the National Academy of Sciences of the United States of America*, *112*(5), 1487–1492. https://doi.org/10.1073/pnas.1421707112

Clutton-Brock, T., & Harvey, P. (1977). Primate ecology and social organization. *Journal of Zoology*, *183*(1), 1–39. https://doi.org/10.1111/j.1469-7998.1977.tb04171.x

Cobb, S. N., & O'Higgins, P. (2007). The ontogeny of sexual dimorphism in the facial skeleton of the African apes. *Journal of Human Evolution*, *53*(2), 176–190. https://doi.org/10.1016/J.JHEVOL.2007.03.006

Collard, M., & O'higgins, P. (2001). Ontogeny and homoplasy in the papionin monkey face. *Evolution & Develpment*, *3*(5), 322–331.

Conroy, G. (1976). Hallucial tarsometatarsal joint in an Oligocene anthropoid Aegyptopithecus zeuxis. *Nature*, *262*.

deMenocal, P. B. (2004). African climate change and faunal evolution during the Pliocene-Pleistocene. *Earth and Planetary Science Letters*, *220*(1–2), 3–24. https://doi.org/10.1016/S0012-821X(04)00003-2

Fedorov, A., Beichel, R., Kalpathy-Cramer, J., Finet, J., Fillion-Robin, J.-C., Pujol, S., Bauer, C., Jennings, D., Fennessy, F., Sonka, M., Buatti, J., Aylward, S., Miller, J. V, Pieper, S., & Kikinis, R. (2012a). 3D Slicer as an Image Computing Platform for the Quantitative Imaging Network. *Magn Reson Imaging*, *30*(9), 1323–1341. https://doi.org/10.1016/j.mri.2012.05.001

Fedorov, A., Beichel, R., Kalpathy-Cramer, J., Finet, J., Fillion-Robin, J.-C., Pujol, S., Bauer, C., Jennings, D., Fennessy, F., Sonka, M., Buatti, J., Aylward, S., Miller, J. V, Pieper, S., & Kikinis, R. (2012b). 3D Slicer as an Image Computing Platform for the Quantitative Imaging Network. *Magn Reson Imaging*, *30*(9), 1323–1341. https://doi.org/10.1016/j.mri.2012.05.001

Fernández-Montraveta, F., & Moya-Laraño, J. (2007). Sex-specific plasticity of growth and maturation size in a spider: implications for sexual size dimorphism. *Journal Evol. Biol.*, *20*, 1689–1699. https://doi.org/10.1111/j.1420-9101.2007.01399.x

Fleagle, J. G. (2013). *Primate Adaptation and Evolution* (Third edition). Elsevier.

Fleagle, J., & Kay, R. (1994). *Anthropoid Origins*. Springer.

Fleagle, J., Kay, R., & Simons, E. (1980). Sexual dimorphism in early anthropoids. *Nature*, *287*, 328–330.

Fleagle, J., & Simons, E. (1982). The humerus of Aegyptopithecus zeuxis: A primitive anthropoid. *American Journal of Physical Anthropology*, *59*(2), 175–193. https://doi.org/10.1002/ajpa.1330590207

Geology, S., & Program, P. (2005). New apes fill the gap. In *National Science Foundation* (Vol. 4201). www.pnas.orgcgidoi10.1073pnas.0710109105

Getahun, D. A., Delson, E., & Seyoum, C. M. (2023). A review of Theropithecus oswaldi with the proposal of a new subspecies. *Journal of Human Evolution*, *180*. https://doi.org/10.1016/j.jhevol.2023.103373

Getahun, D., Delson, E., & Seyoum, C. (2023). A review of Theropithecus oswaldi with the proposal of a new subspecies. *Journal of Human Evolution*, *180*. https://doi.org/10.1016/J.JHEVOL.2023.103373

Gilbert, C. C., Ortiz, A., Pugh, K. D., Campisano, C. J., Patel, B. A., Singh, N. P., Fleagle, J. G., & Patnaik, R. (2020). New Middle Miocene Ape (Primates: Hylobatidae) from Ramnagar, India fills major gaps in the hominoid fossil record: New Middle Miocene Ape from Ramnagar. *Proceedings of the Royal Society B: Biological Sciences*, *287*(1934). https://doi.org/10.1098/rspb.2020.1655

Gingerich, P. D. (1977). Correlation of Tooth Size and Body Size in Living Hominoid Primates, with a Note on Relative Brain Size in Aegyptopithecus and Proconsul. *American Journal of Physical Anthropology*, 395–398.

Godinot, M. (1998). A summary of adapiform systematics and phylogeny. In *Folia Primatologica* (Vol. 69, Issue SUPPL. 1, pp. 218–249). S. Karger AG. https://doi.org/10.1159/000052715

Godinot, M. (2006). Lemuriform origins as viewed from the fossil record. In *Folia Primatologica* (Vol. 77, Issue 6, pp. 446–464). https://doi.org/10.1159/000095391

Goldberg, K. (2024). *Oligocene Primates – ANTH 161: Introduction to Biological Anthropology*. https://anth161.goldberg.uofsccreate.org/station-4-oligocene-primates/

Gommery, D., Kgasi, L., Vilakazi, N., Sénégas, F., Pickford, M., Kuhn, B., Schnyder, J., & Pois, V. (2023). First in situ middle Pliocene cercopithecoid fossils from the Palaeokarst System of Bolt's Farm (South Africa). *Geodiversitas*, *45*, 163–195. http://sciencepress.mnhn.fr

Gower, J. C. (1975). Generalized Procrustes Analysis. *Psychometrika*, *40*(1), 33–51.

Haimoff, E., Chivers, D., Gittins, P., & Whitten, T. (1982). A Phylogeny of Gibbons (Hylobates spp.) Based on Morphological and Behavioural Characters. *Folia Primatol.*, *39*, 213–237.

Hartwig, W. C., & Rosenberger, A. L. (2006). New World Monkeys. In *Encyclopedia of Life Sciences*. Wiley. https://doi.org/10.1038/npg.els.0004201

Israfil, H., Zehr, S. M., Mootnick, A. R., Ruvolo, M., & Steiper, M. E. (2011). Unresolved molecular phylogenies of gibbons and siamangs (Family: Hylobatidae) based on mitochondrial, Y-linked, and X-linked loci indicate a rapid Miocene radiation or sudden vicariance event. *Molecular Phylogenetics and Evolution*, *58*(3), 447–455. https://doi.org/10.1016/J.YMPEV.2010.11.005

Kay, R. F., Ross, C., & Williams, B. A. (1997). Anthropoid Origins. *Science*, *275*, 797–804. http://www.sciencemag.org

Kay, R., Fleagle, J., & Simons, E. (1981). A revision of the Oligocene apes of the Fayum Province, Egypt. *American Journal of Physical Anthropology*, *55*(3), 293–322. https://doi.org/10.1002/ajpa.1330550305

Kozakowski, S. (2013). *3D Geometric Morphometric Analysis of Hylobatid Cranial Ontogeny: Implications for Interpreting the Evolutionary History of Hominoid Cranial Growth*. University of Toronto.

Kunimatsu, Y., Nakatsukasa, M., Sawada, Y., Sakai, T., Hyodo, M., Hyodo, H., Itaya, T., Nakaya, H., Saegusa, H., Mazurier, A., Saneyoshi, M., Tsujikawa, H., Yamamoto, A., & Mbua, E. (2007). *A new Late Miocene great ape from Kenya and its implications for the origins of African great apes and humans*. www.pnas.orgcgidoi10.1073pnas.0706190104

Kuykendall, K. L., Mahoney, C. J., & Conroy, G. C. (1992). Probit and survival analysis of tooth emergence ages in a mixed-longitudinal sample of chimpanzees (Pan troglodytes). *American Journal of Physical Anthropology*, *89*(3), 379–399. https://doi.org/10.1002/ajpa.1330890310

Leakey, M., Leakey, R., Richtsmeier, J., Simons, E., & Walker, A. (1991). Similarieties in Aegyptopithecus and Afropithecus Facial Morphology. *Folia Primato*, *56*, 65–85.

Lewis, R. J., Kirk, E. C., & Gosselin-Ildari, A. D. (2023). Evolutionary Patterns of Intersexual Power. *Animals*, *13*(23). https://doi.org/10.3390/ani13233695

Li, J., Han, K., Xing, J., Kim, H.-S., Rogers, J., Ryder, O. A., Disotell, T., Yue, B., & Batzer, M. A. (2009). Phylogeny of the macaques (Cercopithecidae: Macaca) based on Alu elements. *Gene*, *448*(2), 242–249. https://doi.org/10.1016/j.gene.2009.05.013

Maddison, W. P., Donoghue, M. J., & Maddison, D. R. (1984). Outgroup analysis and parsimony. *Systematic Biology*, *33*(1), 83–103. https://doi.org/10.1093/sysbio/33.1.83

McBrearty, S., & Jablonski, N. G. (2005). First fossil chimpanzee. *Nature*, *437*(7055), 105–108. https://doi.org/10.1038/nature04008

Mccabe, S. C. J. (2017). Aegyptopithecus. In A. Fuentes (Ed.), *The International Encyclopedia of Primatology* (Vol. 1, pp. 9–10).

Meijaard, E. A., & Groves, C. P. (2004). THE BIOGEOGRAPHICAL EVOLUTION AND PHYLOGENY OF THE GENUS PRESBYTIS. *Primate Report*, *68*, 71–90.

Mittermeier, R., Rylands, A., & Wilson, D. (2013). Mandrillus sphinx (Linnaeus, 1758). In R. Mittermeier, A. Rylands, & D. Wilson (Eds.), *Handbook of the Mammals of the World* (Lynx Edicions, Vol. 3, pp. 550–775). Lynx Edicions.

Mitteroecker, P., & Gunz, P. (2009). Advances in Geometric morphometrics. *Evolutionary Biology*, *36*(2), 235–247. https://doi.org/10.1007/s11692-009-9055-x

Morse, P. E., Pampush, J. D., & Kay, R. F. (2023). Dental topography of the Oligocene anthropoids Aegyptopithecus zeuxis and Apidium phiomense: Paleodietary insights from analysis of wear series. *Journal of Human Evolution*, *180*. https://doi.org/10.1016/j.jhevol.2023.103387

Moyà-Solà, S., Alba, D. M., Almécija, S., Casanovas-Vilar, I., Köhler, M., De Esteban-Trivigno, S., Robles, J. M., Galindo, J., & Fortuny, J. (2009). A unique Middle Miocene European hominoid and the origins of the great ape and human clade. *Proceedings of the National Academy of Sciences of the United States of America*, *106*(24), 9601–9606. https://doi.org/10.1073/pnas.0811730106

Neaux, D., Guy, F., Gilissen, E., Coudyzer, W., Vignaud, P., & Ducrocq, S. (2013). Facial Orientation and Facial Shape in Extant Great Apes: A Geometric Morphometric Analysis of Covariation. *PLoS ONE*, *8*(2). https://doi.org/10.1371/journal.pone.0057026

Novo, N. M., Tejedor, M. F., González-Ruiz, L. R., Fleagle, J. G., Brandoni, D., & Krause, M. (2021). Primate diversity in the early miocene pinturas formation, Southern Patagonia, Argentina. *Anais Da Academia Brasileira de Ciencias*, *93*. https://doi.org/10.1590/0001-3765202120201218

Paddock, K., Zeigler, L., Harvey, B., Prufrock, K. A., Liptak, J. M., Ficorilli, C. M., Hogg, R. T., Bonar, C. J., Evans, S., Williams, L., Vinyard, C. J., DeLeon, V. B., & Smith, T. D. (2020). Comparative dental anatomy in newborn primates: Cusp mineralization. *Anatomical Record*, *303*(9), 2415–2475. https://doi.org/10.1002/ar.24326

Pérez de Los Ríos, M., Moyà-Solà, S., & Alba, D. M. (2012). The nasal and paranasal architecture of the Middle Miocene ape Pierolapithecus catalaunicus (primates: Hominidae): Phylogenetic implications. *Journal of Human Evolution*, *63*(3), 497–506. https://doi.org/10.1016/j.jhevol.2012.05.012

Posit team. (2024). *RStudio: Integrated Development Environment for R.* (4.3.2). Posit Software, PBC.

Post, N. W., Gilbert, C. C., Pugh, K. D., & Mongle, C. S. (2023). Implications of outgroup selection in the phylogenetic inference of hominoids and fossil hominins. *Journal of Human Evolution*, *184*. https://doi.org/10.1016/j.jhevol.2023.103437

Preuss, T. M. (2007). Evolutionary Specializations of Primate Brain Systems. In M. Ravosa & M. Dagosto (Eds.), *Primates Origins: Adaptations and Evolution* (pp. 625–675).

Pugh, K. D. (2020). *The Phylogenetic Relationships of Middle-Late Miocene Apes: The Phylogenetic Relationships of Middle-Late Miocene Apes: Implications for Early Human Evolution Implications for Early Human Evolution*. https://academicworks.cuny.edu

Pugh, K. D., Catalano, S. A., de los Ríos, M. P., Fortuny, J., Shearer, B. M., Gazabón, A. V., Hammond, A. S., Moyà-Solà, S., Alba, D. M., & Almécija, S. (2023a). The reconstructed cranium of Pierolapithecus and the evolution of the great ape face. *Proceedings of the National Academy of Sciences of the United States of America*, *120*(44). https://doi.org/10.1073/pnas.2218778120

Pugh, K. D., Catalano, S. A., de los Ríos, M. P., Fortuny, J., Shearer, B. M., Gazabón, A. V., Hammond, A. S., Moyà-Solà, S., Alba, D. M., & Almécija, S. (2023b). The reconstructed cranium of Pierolapithecus and the evolution of the great ape face. *Proceedings of the National Academy of Sciences of the United States of America*, *120*(44). https://doi.org/10.1073/pnas.2218778120

Roos, C. (2022). Taxonomic Classification of Colobine Monkeys. *The Colobines*, 3–12. https://doi.org/10.1017/9781108347150.003

Ross, C. F., & Martin, R. D. (2007). The Role of Vision in the Origin and Evolution of Primates. In *Evolution of Nervous Systems* (Vol. 4, pp. 59–78). Elsevier Inc. https://doi.org/10.1016/B0-12-370878-8/00001-X

Rossie, J. (2005). Anatomy of the nasal cavity and paranasal sinuses in Aegyptopithecus and early miocene African catarrhines. *American Journal of Physical Anthropology*, *126*(3), 250–267. https://doi.org/10.1002/ajpa.20139

Rossie, J. B., & Smith, T. D. (2007). Ontogeny of the nasolacrimal duct in primates: Functional and phylogenetic implications. *Journal of Anatomy*, *210*(2), 195–208. https://doi.org/10.1111/j.1469-7580.2006.00682.x

Rudloff, K. (2013). *Presbytis melalophos mitrata (Grey Sumatran Surili)*. BioLib.Cz. https://www.biolib.cz/en/image/id275029/

Sargis, E. J., Terranova, C. J., & Gebo, D. L. (2008). Evolutionary morphology of the guenon postcranium and its taxonomic implications. *Vertebrate Paleobiology and Paleoanthropology*, *9781402069963*, 361–372. https://doi.org/10.1007/978-1-4020-6997-0_16

Shea, B. T. (1986). Ontogenetic approaches to sexual dimorphism in anthropoids. *Human Evolution*, *1*(2), 97–110. https://doi.org/10.1007/BF02437489

Shea, B. T. (1992). Ontogenetic scaling of skeletal proportions in the talapoin monkey. *Journal of Human Evolution*, *23*(3), 283–307. https://doi.org/10.1016/S0047-2484(05)80004-1

Shook, B., Nelson, K., Aguilera, K., & Braff, L. (2024, February). *Explorations: an open invitation to biological anthropology*. LibreTexts. https://socialsci.libretexts.org/Bookshelves/Anthropology/Biological_Anthropology/EXPLORATIONS%3A__An_Open_Invitation_to_Biological__Anthropology_1e/08%3A_Primate_Evolution/8.03%3A_The_Origin_of_Primates

Silcox, M. (2001). *A Phylogenetic analysis of Plesiadapiformes and their relationship toEuprimates and other Archontans*. Johns Hopkins University.

Simons, E. (1987). New faces of Aegyptopithecus. *JournalofHumanEvolution*, *16*, 273–289.

Simons, E. (2001). The cranium of Parapithecus grangeri, an Egyptian Oligocene anthropoidean primate. *PNAS*, *98*, 7892–7897. www.pnas.orgcgidoi10.1073pnas.051003398

Simons, E., & Kay, R. (1983). Qatrania, new basal anthropoid primate from the Fayum, Oligocene of Egypt. *Nature*, *304*.

Simons, E. L., Seiffert, E. R., Ryan, T. M., & Attia, Y. (2007). A remarkable female cranium of the early Oligocene anthropoid Aegyptopithecus zeuxis (Catarrhini, Propliopithecidae). *Proceedings of the National Academy of Sciences of the United States of America*, *104*(21), 8731–8736. https://doi.org/10.1073/pnas.0703129104

Simons, E., & Rasmussen, T. (1989). Cranial morphology of Aegyptopithecus and Tarsius and the question of the tarsier-anthropoidean clade. *American Journal of Physical Anthropology*, *79*(1), 1–23. https://doi.org/10.1002/ajpa.1330790103

Simpson, G. G. (1933). The "Plagiaulacoid" Type of Mammalian Dentition: A Study of Convergence. *Journal of Mammalogy*, *14*(2), 97–107. https://doi.org/10.2307/1374012

Singleton, M. (2013). Primate Cranial Diversity. *Nature*. https://www.nature.com/scitable/knowledge/library/primate-cranial-diversity-108207646/

Slice, D. E. (2007). Geometric Morphometrics. *Annual Review of Anthropology*, *36*, 261–281. https://doi.org/10.1146/annurev.anthro.34.081804.120613

Smith, B. H., & Boesch, C. (2011). Mortality and the magnitude of the "wild effect" in chimpanzee tooth emergence. *Journal of Human Evolution*, *60*(1), 34–46. https://doi.org/10.1016/j.jhevol.2010.08.006

Springer, M. S., Meredith, R. W., Gatesy, J., Emerling, C. A., Park, J., Rabosky, D. L., Stadler, T., Steiner, C., Ryder, O. A., Janečka, J. E., Fisher, C. A., & Murphy, W. J. (2012). Macroevolutionary Dynamics and Historical Biogeography of Primate Diversification Inferred from a Species Supermatrix. *PLoS ONE*, *7*(11). https://doi.org/10.1371/journal.pone.0049521

Stevens, N. J., & Heesy, C. P. (2006). Malagasy primate origins: Phylogenies, fossils, and biogeographic reconstructions. *Folia Primatologica*, *77*(6), 419–433. https://doi.org/10.1159/000095389

Stevens, N. J., Seiffert, E. R., O'Connor, P. M., Roberts, E. M., Schmitz, M. D., Krause, C., Gorscak, E., Ngasala, S., Hieronymus, T. L., & Temu, J. (2013). Palaeontological evidence for an Oligocene divergence between Old World monkeys and apes. *Nature*, *497*(7451), 611–614. https://doi.org/10.1038/nature12161

Susanna, I., Alba, D. M., Almécija, S., & Moyà-Solà, S. (2014). The vertebral remains of the late Miocene great ape Hispanopithecus laietanus from Can Llobateres 2 (Vallès-Penedès Basin, NE Iberian Peninsula). *Journal of Human Evolution*, *73*, 15–34. https://doi.org/10.1016/j.jhevol.2014.05.009

Sussman, R. W. (1991). Primate origins and the evolution of angiosperms. In *American Journal of Primatology* (Vol. 23, Issue 4, pp. 209–223). https://doi.org/10.1002/ajp.1350230402

Sussman, R. W., Tab Rasmussen, D., & Raven, P. H. (2013). Rethinking Primate Origins Again. In *American Journal of Primatology* (Vol. 75, Issue 2, pp. 95–106). https://doi.org/10.1002/ajp.22096

Tabuce, R., Marivaux, L., Lebrun, R., Adaci, M., Bensalah, M., Fabre, P. H., Fara, E., Rodrigues, H. G., Hautier, L., Jaeger, J. J., Lazzari, V., Mebrouk, F., Peigné, S., Sudre, J., Tafforeau, P., Valentin, X., & Mahboubi, M. (2009). Anthropoid versus strepsirhine status of the African Eocene primates Algeripithecus and Azibius: Craniodental evidence. *Proceedings of the Royal Society B: Biological Sciences*, *276*(1676), 4087–4094. https://doi.org/10.1098/rspb.2009.1339

Tejedor, M. F., & Bosco, J. (2016). CAPÍTULO 13. EVOLUCIÓN DE LOS PRIMATES: DESDE SU ORÍGEN HASTA LOS PRIMEROS REGISTROS DE HOMININOS. In L. Madrigal & R. Gonzáles (Eds.), *Introducción a la Antropología Biológica* (pp. 360–417).

Tejedor, M., & Novo, N. (2016). Evolución y paleobiogeografía de los primates platirrinos. In F. Agnolin, G. Lio, F. Brissón, N. Chimento, & F. Novas (Eds.), *Historia evolutiva y paleobiogeográfica de los vertebrados de América del Sur* (Vol. 6, pp. 386–393). MACN.

Von Cramon-Taubadel, N., Frazier, B. C., & Lahr, M. M. (2007). The problem of assessing landmark error in geometric morphometrics: Theory, methods, and modifications. *American Journal of Physical Anthropology*, *134*(1), 24–35. https://doi.org/10.1002/ajpa.20616

Wang, B., Zhou, X., Shi, F., Liu, Z., Roos, C., Garber, P. A., Li, M., & Pan, H. (2015). Full-length Numt analysis provides evidence for hybridization between the Asian colobine genera Trachypithecus and Semnopithecus. *American Journal of Primatology*, *77*(8), 901–910. https://doi.org/10.1002/AJP.22419

Webster, M., & Sheets, D. (2010). A practical introduction to landmark-based geometric morphometrics. *Quantitative Methods in Paleobiology*, *16*, 163–188.

Xing, J., Wang, H., Zhang, Y., Ray, D. A., Tosi, A., Disotell, T., & Batzer, M. (2007). A mobile element-based evolutionary history of guenons (tribe Cercopithecini). *BMC Biology*, *5*. https://doi.org/10.1186/1741-7007-5-5

Xing, S., Gibbon, V., Clarke, R., & Liu, W. (2013). Geometric morphometric analyses of orbit shape in Asian, African, and European human populations. *Anthropological Science*, *121*(1), 1–11. https://doi.org/10.1537/ase.120803

Zalmout, I. S., Sanders, W. J., MacLatchy, L. M., Gunnell, G. F., Al-Mufarreh, Y. A., Ali, M. A., Nasser, A. A. H., Al-Masari, A. M., Al-Sobhi, S. A., Nadhra, A. O., Matari, A. H., Wilson, J. A., & Gingerich, P. D. (2010). New oligocene primate from Saudi Arabia and the divergence of apes and old world monkeys. *Nature*, *466*(7304), 360–364. https://doi.org/10.1038/nature09094

Zelditch, M. L., & Swiderski, D. L. (2023). Effects of Procrustes Superimposition and Semilandmark Sliding on Modularity and Integration: An Investigation Using Simulations of Biological Data. *Evolutionary Biology*, *50*(2), 147–169. https://doi.org/10.1007/s11692-023-09600-9

APPENDIX

A.1. Facial differences Between the female of different species of *Macaca* analyzed

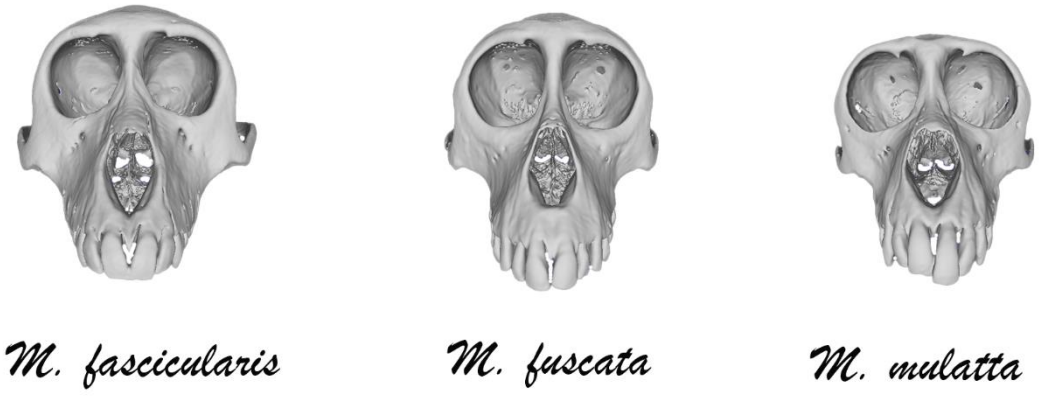

A.2. Plot of PC1 and PC2 with the sample of extant primate removing the outliers

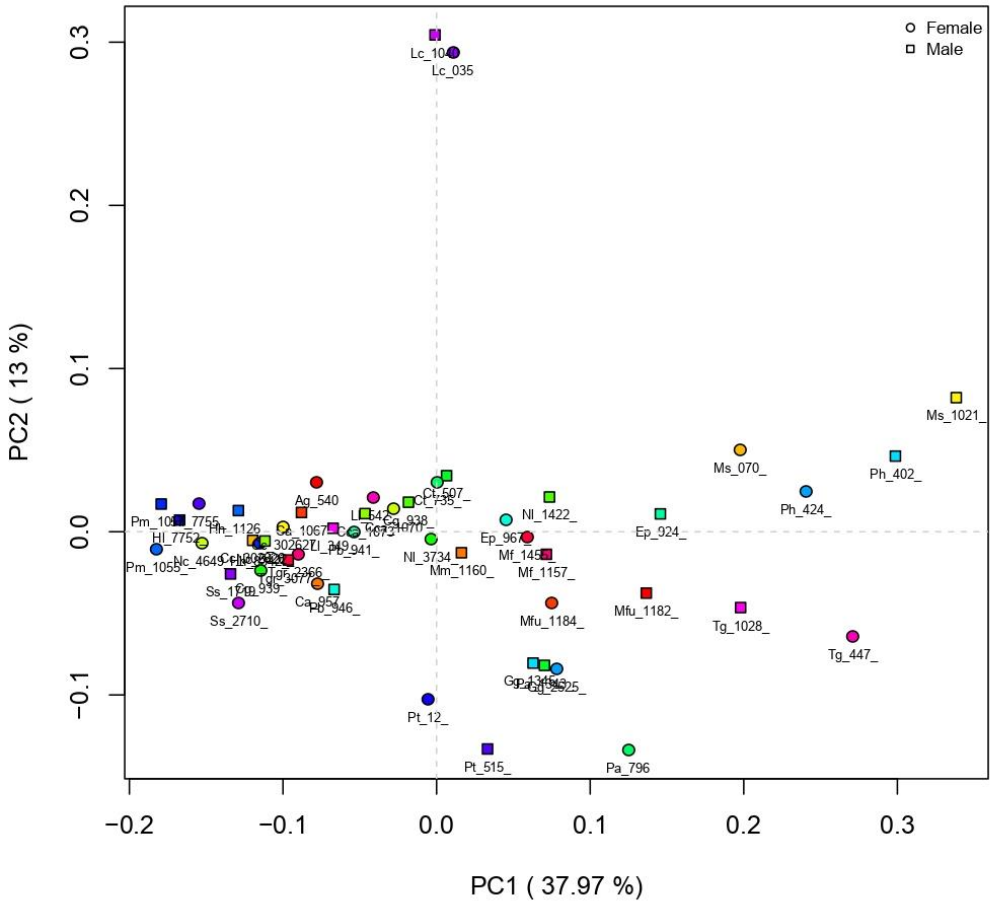

A.3. Regression line showing allometric effect and the error of Az_8794

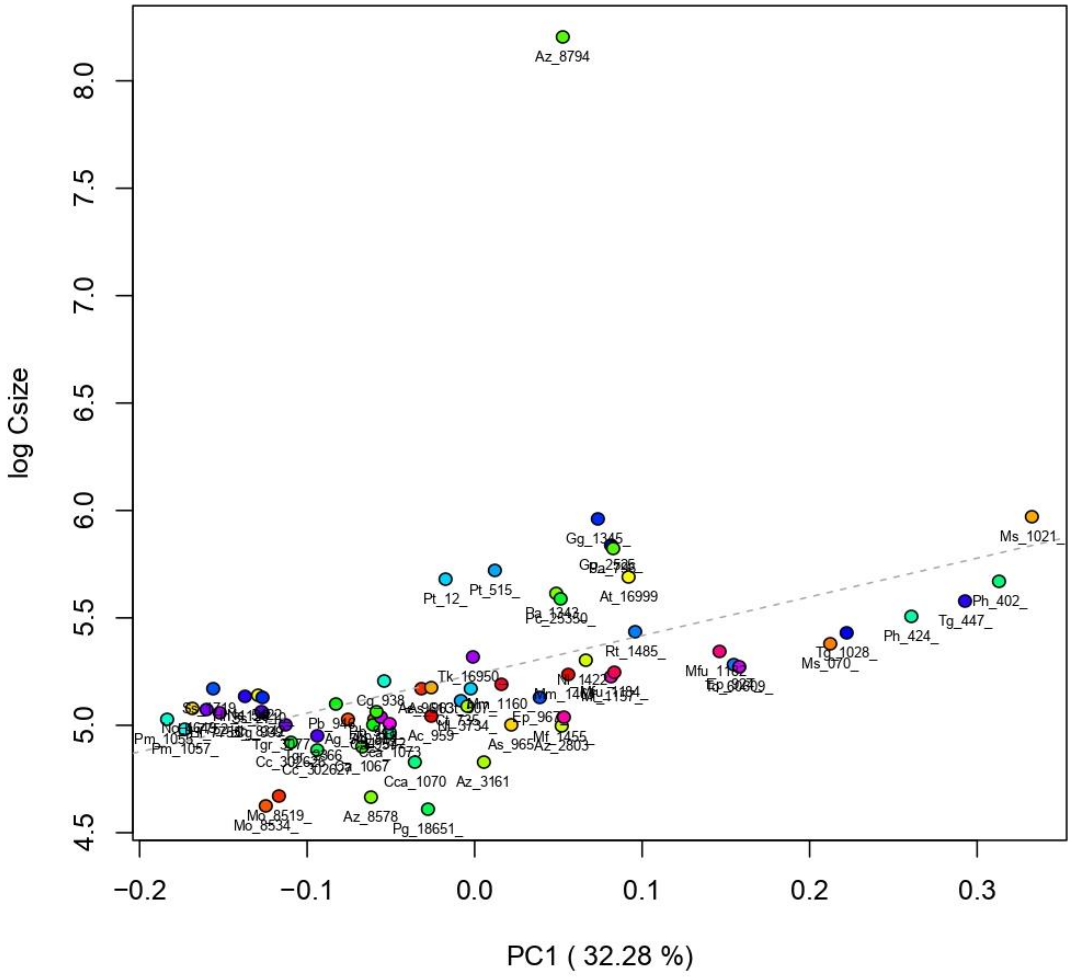

A.4. Table of some features of social organization and ecology of Primates

Species	Nocturnal/ diurnal	Arboreal/ terrestial	Diet	Sex dimorphism
Lemur catta	D	T	FR	1.16
Cebus apella	D	A	FR	1*
Alouata caraya	D	A	FO	1.26*
Alouata seniculus	D	A	FO	1.27
Ateles Geoffroyi	D	A	FR	1.07
Lagothrix lagothricha	D	A	FR	1.14
Cercopithecus campbelli	D	A	FR	1*
Miopithecus talapoin	D	T	FR	1.27
Erytrocebus patas	D	T	FR	1.79
Cercocebus torquata	D	A	FR	2*
Macaca fascicularis	D	T	FR	1.44
Macaca fuscata	D	T	FR	1.19
Macaca mulatta	D	T	FR	1.09
Papio hamadryas	D	T	FR	1.95
Mandrillus leucophaeus+	D	T	FO	1.62*
Theropithecus gelada	D	T	FO	1.51
Colobus guereza	D	A	FO	1.18
Presbytis melalophos	D	A	FO	1*
Nasalis larvatus	D	A	FO	1.77
Hylobates concolor	D	A	FR	1*
Hylobates hoolock	D	A	FR	1*
Hylobates lar	D	A	FR	1.11
Symphalangus syndactylus	D	A	FO	1*
Pongo pygmaeus+	D	A	FR	1.86
Pan troglodytes	D	A	FR	1.2
Gorilla gorilla	D	A	FO	1.72

+These specimens were used instead of *M. sphinx* and *P. abelii* (of our sample), because we don't have reference of this species. *These values are calculated from the information of the authors; they don't put the ratio because they consider there is not enough specimens of each sex. FR. Frugivorous and FO. Folivores. Source: (Clutton-Brock & Harvey, 1977)

A.5. Predicted 3D facial model for extant primates for the maximum and minimum values of PC1

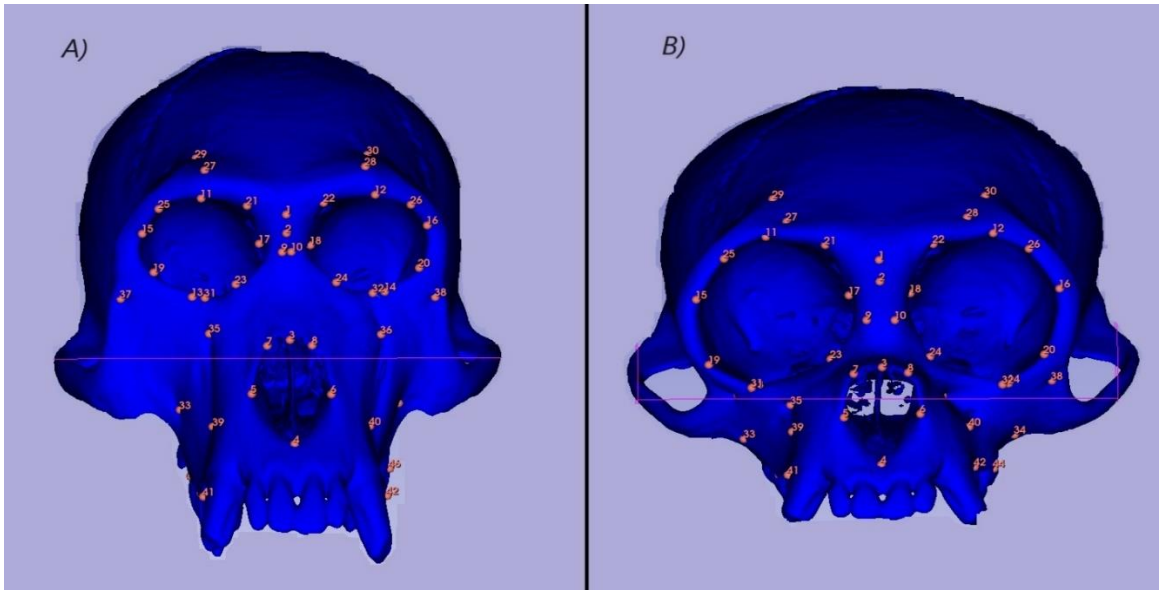

Model 3D generate with the combination of extreme values of PC1 and PC2 considering 61 landmarks in the extant primates. A) Positive values corresponding with the morphology of cercopithecoids, and B) negative values corresponding with the morphology of colobines